CHARACTERIZATION OF *let-765*/*nsh-1* AND ITS ROLE IN RAS SIGNALLING IN *Caenorhabditis elegans*

by

Carrie Leanne Simms
MSc, Simon Fraser University 2004
BSc, Simon Fraser University 1999

THESIS SUBMITTED IN PARTIAL FULFILLMENT OF
THE REQUIREMENTS FOR THE DEGREE OF

DOCTOR OF PHILOSOPHY

In the
Department of Molecular Biology and Biochemistry

SIMON FRASER UNIVERSITY

Fall 2009

APPROVAL

Name: **Carrie L. Simms**

Degree: **Doctor of Philosophy**

Title of Thesis: **Characterization of *let-765/nsh-1* and its role in RAS signalling in *Caenorhabditis elegans***

Examining Committee:

Chair: **Dr. Jack N. Chen**

Associate Professor of Molecular Biology and Biochemistry

Dr. David L. Baillie
Senior Supervisor
Professor of Molecular Biology and Biochemistry

Dr. Nicholas Harden
Supervisor
Associate Professor of Molecular Biology and Biochemistry

Dr. Nancy Hawkins
Supervisor
Assistant Professor of Molecular Biology and Biochemistry

Dr. Esther Verheyen
Supervisor
Associate Professor of Molecular Biology and Biochemistry

Dr. Bruce P. Brandhorst
Internal Examiner
Professor of Molecular Biology and Biochemistry

Dr. Paul W. Sternberg
External Examiner
Professor of Biology, HHMI Investigator
California Institute of Technology

Date Defended/Approved: November-9-2009

Declaration of
Partial Copyright Licence

ABSTRACT

The broad diversity of cell types generated during development of a multicellular organism result from cell-fate decisions. Many fate decisions are directed by the actions of signalling pathways such as the RAS/map kinase (MAPK) pathway via the transcriptional regulation of target genes. The differential expression of target genes is, in turn, responsible for the determination of cell fate. In *C. elegans*, a RAS/MAPK pathway acts downstream of the epidermal growth factor (EGF) receptor to regulate cell fates in several tissues. In particular, development of the vulva has provided an opportunity to dissect the function of RAS pathway components as well as positive and negative regulators of the pathway.

I have identified the essential gene, *let-765*, as *n*otch *s*ignalling pathway *h*omolog-1 (*nsh-1*), a DExD/H box protein. To investigate the role of *let-765* with respect to *C. elegans* development, I performed a genetic and molecular analysis of the gene. *let-765* was found to be broadly expressed throughout development and an assessment of reduction-of-function phenotypes suggests that it is likely required for RAS pathway-directed processes, including larval viability, vulval induction, and development of the male tail and posterior ectoderm. By investigating genetic interactions between the EGFR/RAS/MAPK pathway and *let-765*, I have demonstrated that it promotes RAS pathway activity and is required for vulval induction. These studies indicate that *let-765* acts upstream of the ligand and antagonizes the repressive activity of the synthetic multivulva (synMuv) genes. Specifically, LET-765 appears to positively regulate the transcription of *lin-3* EGF, which is required to specify vulval cell fates.

The variety of phenotypes generated by a loss or reduction of *let-765* function is consistent with a role for LET-765 regulating multiple processes through interactions with factors in addition to the EGFR/RAS pathway. A novel role for DExD/H box proteins in transcriptional

regulation has been proposed recently and, together with the data demonstrating a role for LET-765 in the regulation of *lin-3* transcription, I propose that LET-765 may interact with transcriptional regulatory complexes to promote gene expression. In summary, this study has provided novel insight into the control of LIN-3/EGF expression and the EGFR/RAS pathway during *C. elegans* development.

Keywords: epidermal growth factor, EGF, lin-3, RAS, DExD/H helicase, transcription, C. elegans

To my brother, Jeff

ACKNOWLEDGEMENTS

I would like to express my sincere gratitude to my senior supervisor, Dr. David Baillie, for his encouragement, support, and guidance throughout my graduate career. I would also like to thank the members of my supervisory committee, Dr. Nick Harden, Dr. Nancy Hawkins, and Dr. Esther Verheyen for their helpful advice and critical reading of the thesis and manuscript. I thank my internal examiner, Dr. Bruce Brandhorst, for his useful comments on the thesis and for taking the time to attend my defence. I extend sincere thanks to my external examiner, Dr. Paul Sternberg, for his thoughtful insight and appreciation of this work.

I would like to thank Dr. Jack Chen for his advice and critical comments during this project, and to the members of his lab for thoughtful discussions as well as for sharing equipment and reagents. I have had the opportunity to work alongside many talented students, post doctoral fellows, and technicians in the Baillie lab over the years. I appreciate the friendship and support from all members past and present, and for making it such an enjoyable place to work. I especially thank Domena Tu for saving me many, many hours at the injection scope.

A special thank you to Hani for his patience, support, and encouragement, and for his assistance with the preparation of this thesis. Finally, I thank my family for their many years of unwavering support and encouragement during my post-secondary education.

TABLE OF CONTENTS

LIST OF FIGURES

LIST OF TABLES

CHAPTER 1: INTRODUCTION

1.1 Transcriptional regulation of gene expression

The development and patterning of a multicellular organism requires the generation of cellular diversity, which is achieved by cell divisions that establish distinct cell fates. Moreover, each cell possesses unique characteristics that result from the differential regulation of gene expression. This typically involves complex networks of transcription factors and signalling pathways, but ultimately requires the collaboration of interacting proteins that assemble at a specific promoter.

Gene expression is, not surprisingly, regulated most strongly at the level of transcription. Multiple factors, including activator and repressor proteins, are required to control the initiation of RNA synthesis by RNA polymerase II. The basal transcriptional machinery includes the multisubunit polymerase together with general transcription factors (GTFs) denoted TFII–A, –B, –D, –E, –F, and –H. TFII–D is in turn composed of several subunits that include the TATA binding protein (TBP) and TBP associated factors (TAFs). The complex is critical for the formation of the initiation complex, achieved by the accumulation of GTFs and RNA polymerase II at a specific promoter (Woychik and Hampsey, 2002). TFII–D recognizes the TATA sequence along with other promoter elements and binds to the DNA, creating a nucleation site for the other GTFs and RNA pol II (Casamassimi and Napoli, 2007). The GTFs are thought to provide stability to the initiation complex and create an asymmetry within the complex responsible for unidirectional transcription. This is followed by the conformational rearrangement of the

polymerase into the active form as mediated by TFII–H in an ATP-dependent manner. Subsequent to this step, the carboxy-terminal domain (CTD) of RNA pol II is phosphorylated allowing it to enter the elongation phase of transcription Although the initiation complex can assemble independently at a promoter sequence *in vitro*, gene expression in a eukaryotic cell requires additional coactivators and gene-specific transcription factors. Namely, the Mediator complex transduces signals between sequence specific regulatory factors and the GTFs/RNA Pol II.

The Mediator complex was first identified in yeast where it was found to be required for transcription in a reconstituted complex (Myers and Kornberg, 2000). It is unable to bind to specific DNA sequences but instead interacts with RNA Pol II; an interaction between Mediator and the unphosphorylated CTD has been demonstrated (Kornberg, 2005). In addition, it promotes initiation through regulation of the CTD kinase of TFII–H. However, once elongation begins, the Mediator complex disassociates from the polymerase. The complex is comprised of greater than 20 protein subunits, which combine to form three main submodules: the head, middle, and tail. The 'head' region makes contact with RNA pol II and these proteins exhibit the greatest conservation between yeast and mammals, whereas the 'tail' domain makes contact with the gene specific regulatory factors and, not surprisingly, is less conserved (Cantin et al., 2003; Takagi and Kornberg, 2006). It has been suggested that the conserved 'core' proteins are required at most (if not all) promoters, while the more divergent subunits may regulate different subsets of genes. For example, *C. elegans* MED6, MED7, and MED10 are required for the expression of developmental-stage specific genes, but not of ubiquitously expressed genes (Kwon et al., 1999). Furthermore, some mediator

homologs in *C. elegans* exhibit mutant phenotypes that suggest a role in distinct developmental events; for instance LET-425/MED6 and SUR-2/MED23 positively regulate vulval induction and mutations in *med-6* lead to a loss of rays in the male tail (Kwon and Lee, 2001; Singh and Han, 1995). Conversely, mutations in *let-19* and *dpy-22/sop-1*, which encode MED13 and MED12 respectively, cause a multivulval phenotype and T cell lineage defects (Moghal and Sternberg, 2003; Yoda et al., 2005). The exact means by which Mediator complexes are recruited to promoters is poorly understood, but interactions with the activation domain of DNA-bound regulatory proteins have been demonstrated, posing a potential mechanism (Cantin et al., 2003).

Gene-specific activator proteins modulate transcription at target promoters by binding to regulatory sequences and recruiting the basal transcriptional machinery. Typically, they contain a DNA binding domain, which binds the recognition site, and an activation domain that recruits other activator proteins. A multitude of transcription factors have been studied and include proteins containing classes of DNA-binding domains from the homeodomain, zinc finger, basic helix turn helix (bHLH), and basic leucine zipper families (Garvie and Wolberger, 2001). Often these proteins function as homodimers or heterodimers, allowing for additional diversity at potential recognition sites. Alternatively, transcriptional repressors bind promoter sequences and can interfere with activator binding or the assembly of the initiation complex. In addition to attracting transcription factors to the promoter, gene regulatory proteins can recruit chromatin modifying enzymes to assist in making the DNA more or less accessible for the transcription machinery.

Eukaryotic chromatin is comprised of chromosomal DNA and associated proteins that are tightly packaged within the nucleus. DNA is wrapped around histone core proteins, forming nucleosomes that function to compact the DNA and restrict access by DNA interacting proteins. Chromatin modifiers, including nucleosome remodelling and histone modifying proteins, enable the transcriptional machinery to access their target promoters. The amino-terminal ends of histones can be modified to promote or repress transcriptional activity by acetylation or methylation of lysine residues respectively, and phosphorylation of serine or threonine residues. Modified histones also change the structure of the nucleosome altering the accessibility of the transcription machinery to the DNA. Histone deacetylase complexes (HDAC) and histone methyltransferases (HMT) are associated with transcriptional repression, while histone acetyltransferases (HAT) promote a transcriptionally active state. Many modifier complexes have been identified, each with different specificities for the set of histones or residues that they target (Strahl and Allis, 2000). Furthermore, modified histones create a scaffold for other modifier proteins, in order to propagate the modification, or for nucleosome remodelling proteins via specialized histone-binding domains: bromodomain, chromodomain, PHD and SANT domains interact with modified histone tails.

Although histone-DNA binding is inherently dynamic, it can also be controlled by specialized protein complexes. Nucleosome remodelers are multi-subunit complexes that utilize the energy from ATP hydrolysis to slide or transfer nucleosomes on the DNA, including SWI/SNF, ISWI, and Mi-2 (Vignali et al., 2000). They bind tightly to the histone core, and translocate the DNA to reveal sites for transcription factor binding and initiation. The catalytic subunit is similar between complexes, characterized by DNA

translocase and ATPase activities, making these components members of the SF2 family of DEAD/H box proteins, although they do not posess helicase activity (Saha et al., 2006). The complexes also contain a histone-binding domain enabling them to be localized to particular sites on the chromosome. The activity of nucleosome remodelling complexes is often mediated by sequence-specific transcription factors. Clearly, the regulation of eukaryotic transcription requires multiple levels of control and an impressive array of participants. Current and future studies relating to transcriptional regulatory networks and coactivator proteins will aid in unveiling a detailed picture of how this complex interplay takes place.

1.2 The DExD/H box helicase protein family

DExD/H – box RNA helicases are found in nearly all organisms and constitute a significant portion of the proteins encoded by their genome – about 2% of protein coding genes in yeast are helicases (Lander et al., 2001; Shiratori et al., 1999; Venter et al., 2001). This diverse family of proteins is defined by the presence of eight conserved motifs and are members of the SF2 family of RNA and DNA helicases. They utilize the energy generated by binding and hydrolysing NTPs to dissociate duplexes or displace bound proteins; however, examples of DExD/H box proteins that processively translocate along and unwind double stranded nucleic acids are rare. Proteins in this family also share a common structure that folds into two α-β RecA-like domains (Figure 1), although they are often far less conserved in overall sequence. The flanking regions of the protein are thought to confer specificity for protein interactions relating to their individual functionality (Cordin et al., 2006). RNA helicases are involved in all aspects of RNA processing and metabolism, extending to potential RNPase activity (Jankowsky et al.,

2001; Schwer, 2001). In addition, there is emerging evidence that DExD/H helicases have roles in transcriptional regulation, which are exclusive of any helicase activity, through putative interactions with activator/repressor proteins (Fuller-Pace, 2006).

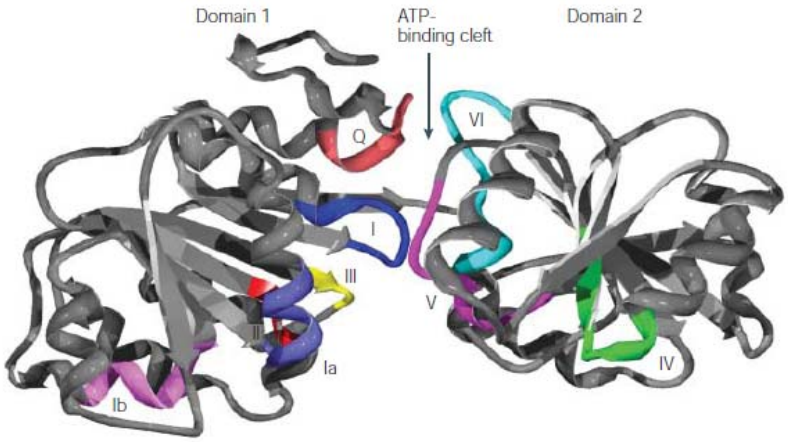

From (Rocak and Linder, 2004).

Figure 1. General structure of a DExD/H box helicase.

Of the RNA helicases that have been purified and analyzed biochemically, all possess an ATPase activity. The ability of the enzyme to hydrolyze ATP is stimulated by RNA binding, although optimal activity likely requires the association of protein binding partners or regulators (Cordin et al., 2006). In turn, the RNA binding affinity is strongest in the presence of ATP, and greatly reduced upon binding of ADP. Furthermore, while the affinity for RNA by the helicase core is generally non-specific, some RNA helicases may interact with specific RNA structures via their carboxy- and amino-terminal ends (Tsu et al., 2001).

DExD/H box proteins are differentially required in essentially all processes involving RNA. Pre-RNA splicing requires several helicase proteins, most of which are

involved in the assembly of the spliceosome. Similarly, ribosome assembly utilizes about 15 DExD/H box helicases. In both contexts, the helicase proteins are thought to unwind small duplexes between snoRNAs and rRNAs. In yeast, the Dbp5 helicase functions at the nuclear pore to promote mRNA export, perhaps by dislodging other proteins from the RNA in preparation for translation (Tseng et al., 1998). The eIF4A protein has a well characterized role in translation initiation (Rogers et al., 2002) where it is proposed to remove proteins from the mRNA and unwind duplexes at the 5'-end prior to ribosome scanning. Alternatively, the Drosophila protein Vasa, functions in translational control of mRNA in the germline (Johnstone and Lasko, 2004). Finally, helicases are also involved in mRNA decapping and decay.

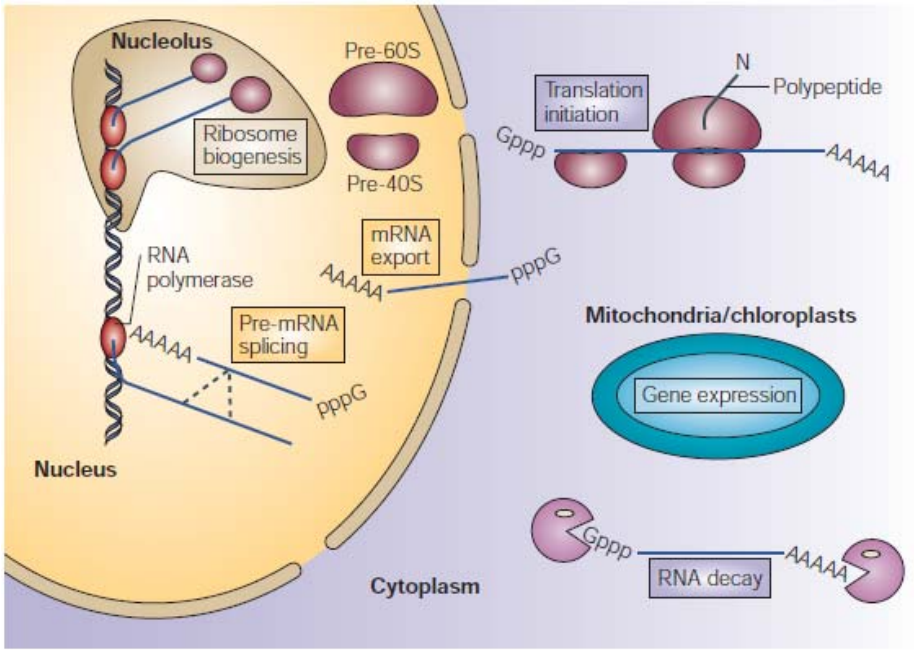

From (Rocak and Linder, 2004).

Figure 2. DExD/H box proteins are required for a multitude of RNA-dependent processes.

Several cellular functions have been attributed to DExD/H box proteins including ribosome biogenesis, pre-mRNA splicing, mRNA export, translation initiation, gene expression in organelles, and mRNA decay.

DExD/H box proteins have recently been implicated in interactions with the transcriptional machinery, revealing functional diversity beyond their enzymatic activity. The identification of proteins that act as interaction partners with DExD/H helicases during these processes will assist in elucidating mechanistic details as well as untangling how functional specificity is determined with respect to gene regulatory mechanisms.

1.3 Regulation of developmental processes by an EGFR/RAS/MAPK pathway

Signalling by receptor tyrosine kinase (RTK) pathways controls a broad range of fundamental developmental processes including cell growth and proliferation, differentiation, migration, and apoptosis (Dhillon et al., 2007). Although there exists substantial diversity in receptor-ligand interactions, they share a common mechanism of activation. Ligand binding by the extracellular domain induces receptor dimerization, resulting in autophosphorylation of tyrosine residues by the catalytic protein kinase domain. This generates sites for the interaction of SH2 (Src homology 2) and PTB (phosphotyrosine binding) domain proteins including the GRB-2 adaptor, SHP-2/protein tyrosine phosphatase, c-CBL, and GTPase activating proteins (Hubbard and Miller, 2007). Receptor activation leads to interaction with the SOS/rasGEF via SH3 domains, which stimulates guanosine triphosphate (GTP) loading of RAS. This, in turn, leads to the recruitment of Raf kinase and triggers a phosphorylation cascade involving the mitogen-activated protein kinases MEK and ERK. Activated ERK proteins can phosphorylate numerous targets including signalling molecules and cytoskeletal proteins, or enter the nucleus and stimulate transcription factors to promote downstream gene expression (Dhillon et al., 2007).

Activation of RAS/MAPK pathways by growth factors has been well characterized, in part, because of its relevance to human cancers. Approximately one third of cancers involve misregulation of ERK pathways, the most prominent being activating (or oncogenic) mutations in RAS. Most of these mutations occur in residues 12, 13, and 61 (Bos, 1989). Another common source of misregulation is the overexpression or activation of the growth factor RTKs, epidermal growth factor receptor (EGFR) or ERBB2/HER2, which is commonly seen in breast and ovarian tumours. Furthermore, excessive autocrine production of the EGF ligand, TGF-α, is proposed to cause inappropriate activation of EGFR in epithelial cancers (Downward, 2003). Studies in *C. elegans* and *Drosophila,* together with the development of mouse models, have contributed to elucidating the function and components of this and other signalling pathways. This has led to the development of kinase inhibitors, small-molecule receptor inhibitors, and antibodies against EGFR that block receptor-ligand interactions as therapeutics to treat tumour progression.

Strong evolutionary conservation of signalling pathway components allows the compilation of research from various model systems, through sequence and functional homology. *C. elegans* provides an opportunity to study the regulation and function of EGFR/RAS signalling, which has led to the identification of new regulatory proteins and lent insight into its interaction with other players in a complex network of signalling pathways. Many core pathway components were identified as a result of their role in vulval development and include LIN-3/EGF, LET-23/EGFR, SEM-5/GRB2, LET-341/SOS-1, LET-60/RAS, LIN-45/RAF, MEK-2/MEK, and SUR-1/MPK-1/MAPK (Aroian et al., 1990; Beitel et al., 1990; Chang et al., 2000; Clark et al., 1992; Hajnal et

al., 1997; Han et al., 1993; Han and Sternberg, 1990; Hill and Sternberg, 1992; Lackner et al., 1994; Sternberg and Han, 1998; Wu and Han, 1994). In addition, a conserved triplex of proteins required for baso-lateral localization of LET-23/EGFR during vulval induction has been studied (LIN-2/MAGUK and the PDZ containing proteins LIN-7 and LIN-10). LIN-7 binds to the C-terminus of the receptor and interacts with LIN-10 and membrane-bound LIN-2 (Hoskins et al., 1996; Simske et al., 1996; Stetak et al., 2006).

Additional regulators of LET-23 have been isolated based on phenotypes generated in a sensitized genetic background; GAP-1/RasGAP functions primarily in vulval development, while GAP-2 and GAP-3 are required for other RAS-dependent processes; SLI-1/c-CBL negatively regulates LET-23; and a Raf-related scaffold protein KSR-1 promotes signalling downstream of RAS in cooperation with the adaptor protein CNK-1 (Hajnal et al., 1997; Jongeward et al., 1995; Kornfeld et al., 1995; Rocheleau et al., 2005; Stetak et al., 2008; Sundaram and Han, 1995; Yoon et al., 1995). Many other regulatory proteins have been identified through screens that suppress mutations in core pathway components (see (Sundaram, 2006)). A summary of EGFR signalling in *C. elegans* is shown in Figure 3.

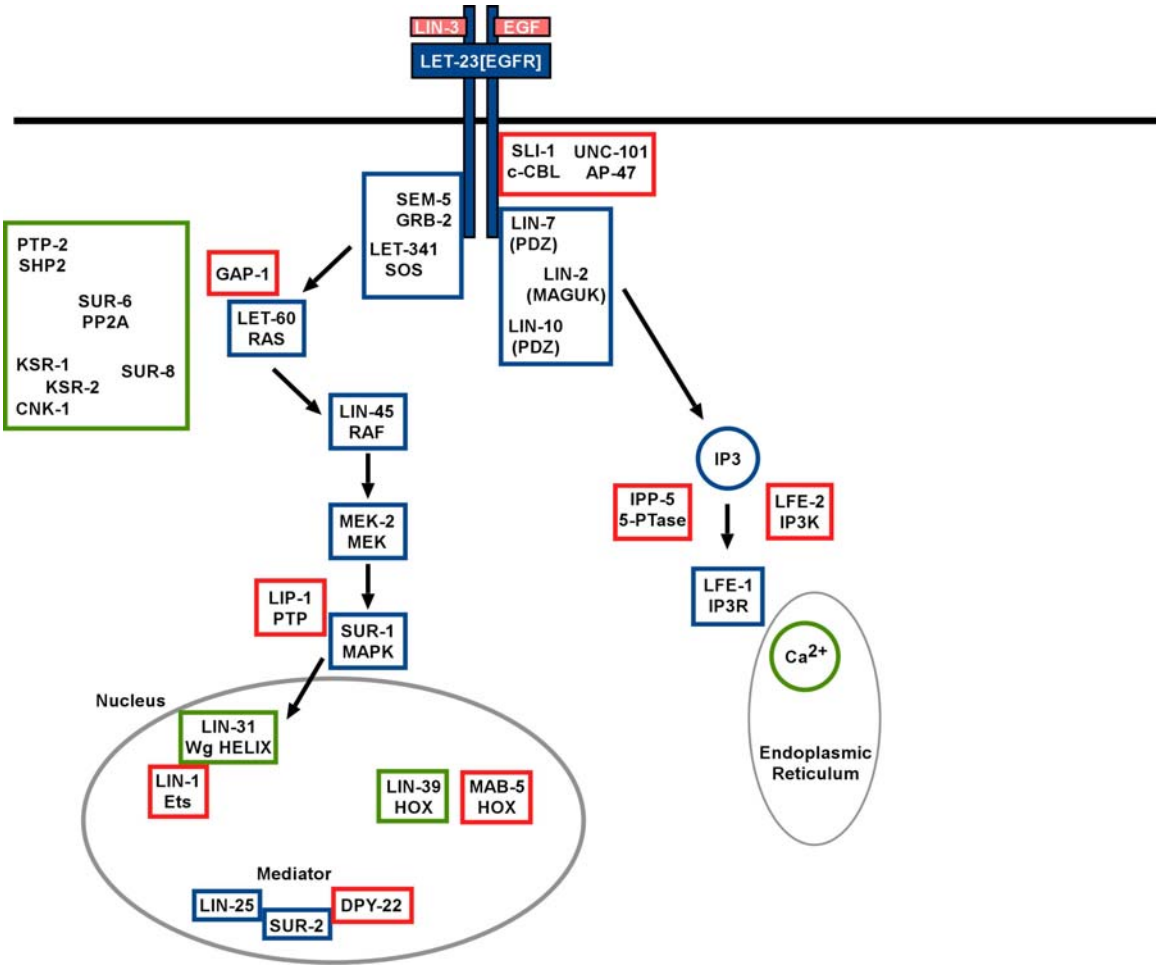

Figure 3. EGFR/RAS pathway signalling in *C. elegans*.

A summary of major components of the pathway with core players boxed in blue, positive regulators in green, and negative regulators in red. Adapted from (Moghal and Sternberg, 2003).

An EGFR/RAS pathway is used for multiple developmental events in *C. elegans*, controlling larval viability and the development of male mating structures, posterior ectoderm, ventral uterine tissue, and the vulva (Aroian and Sternberg, 1991; Chamberlin and Sternberg, 1994; Jiang and Sternberg, 1998; Newman and Sternberg, 1996). In addition, the EGF receptor is required in the somatic gonad to promote ovulation via the regulation of IP3, which is independent of RAS (Clandinin et al., 1998; Yin et al., 2004). Studies describing RAS pathway regulation of vulval development, in particular, have

provided a wealth of insight into positive and negative regulators, in addition to contributing a genetic framework that can be used for analysis of potentially new interactions.

Null or strong loss of function mutations in core EGFR/RAS pathway genes lead to early larval lethality; arrest is associated with defects in osmoregulation, such that the animals appear to fill with fluid and assume a rod-like posture. Mosaic analysis using *let-60*/RAS indicated that the lethality was due to a loss of the excretory duct cell, suggesting that this is the essential site of pathway activity (Yochem et al., 1997). However, it has been reported that *let-23* activity may be required in other tissues as well (Koga and Ohshima, 1995). Genetic analysis has suggested that a typical linear RAS pathway is utilized to promote viability, although other accessory proteins and nuclear target genes do not exhibit a lethal phenotype unless pathway activity is compromised by a second modifier mutation (Moghal and Sternberg, 2003). The isolation of non-null mutations with tissue specific phenotypes has enabled further investigation of RAS pathway function.

The spicules are a pair of male specific structures in the tail that are required for mating and may aid in the transfer of sperm. Each spicule is composed of a sensory neuron surrounded by socket and sheath cells and accessory cells that secrete sclerotic cuticle to provide support (Sulston et al., 1980). All of the cells that produce the spicules are derived from the anterior daughter of the male blast cell, B.a. Its eight daughter cells are positioned posterior to cells of the F and U lineage, which supply an inductive signal that is required for spicule development (Chamberlin and Sternberg, 1993). *lin-3* is expressed in F and U, and LET-23, LET-60, and LIN-45 are required in B.a for anterior

fates, suggesting that the EGF ligand provides the inductive signal to the B.a progeny, where RAS pathway activation promotes spicule development (Chamberlin and Sternberg, 1994).

Development of the posterior ectodermal cells is regulated by LIN-3/LET-23 in cooperation with the Wnt pathway. Early in the L1 stage, the two posterior-most ventral cord precursor cells, P11 and P12, are both competent to assume the P12 fate; if one cell is ablated, the other always becomes P12 (Sulston and White, 1980). The cells divide to produce distinct sets of neural and hypodermal progeny that can be identified based on their morphology. Mutations in *lin-44*/Wnt or *lin-17*/Fz lead to a loss of P12 and duplication of P11 fates (Herman and Horvitz, 1994; Jiang and Sternberg, 1998). Similarly, mutations in EGFR/RAS pathway genes also lead to a duplication of P11 fates, and furthermore, gain of function mutations lead to duplications of the P12 fate. Both pathways converge at the level of the Hox gene, *egl-5*. A loss of *egl-5* activity results in duplication of the P11 fate and overexpression can rescue the 2 P11 phenotype of mutation in either RAS or Wnt pathway genes (Jiang and Sternberg, 1998). This is similar to the convergence of RAS and Wnt pathways' activity at the Hox gene *lin-39* during vulval induction (Maloof and Kenyon, 1998).

Ovulation involves contraction of the gonadal sheath cells in coordination with dilation of the spermatheca, which pulls an oocyte into the spermatheca to be fertilized. The process is controlled by a LIN-3/LET-23 mediated signal from the oocyte to the distal spermatheca that is independent of RAS. Suppressors of sterile mutations in *lin-3* and *let-23* identified an IP3 kinase and IP3 receptor, which suggested that LET-23

regulates IP3 levels to promote ovulation, likely through regulation of calcium levels (Clandinin et al., 1998; McCarter et al., 1999).

Vulval development, as a model for organogenesis, incorporates intercellular signalling, cell fate specification, and the coordinated regulation of numerous transcription factors. An inductive signal from the somatic gonad stimulates a RAS cascade in the centre-most vulval precursor cell, P6.p, which leads to the activation of lateral signalling in adjacent cells via LIN-12/Notch. This directs the P6.p cell to take on a 1° fate, while P5.p and P7.p adopt 2° fates. The cells divide to produce seven types of progeny that acquire separate characteristics as each express distinct sets of transcription factors (Inoue et al., 2002; Inoue et al., 2005). The integration of multiple signalling factors, from both synergistic and antagonistic interactions, establishes a precise order of events that effect an invariant pattern of development to form the mature organ. The synchronized development of the uterine tissue allows establishment of a functional connection between the uterus and vulva (Newman and Sternberg, 1996). Together, the combination of these processes demonstrates an impressive level of complexity for such an outwardly simple animal.

Prior to the onset of induction, the VPCs must be competent to respond to instructive cues from the signalling cell, meaning that they express the necessary receptor and related components. Furthermore, their position relative to the signal-producing cell needs to be tightly regulated so that the appropriate amount of signal is received. The VPCs are derived from twelve ventral neuroblast cells during the L1 stage. The P cells divide to produce ventral cord neurons from the anterior daughters and hypodermal cells from the posterior daughters (Hedgecock et al., 1987; Sulston and Horvitz, 1977). The

Hox gene *lin-39* is expressed in P3.p-P8.p and ensures that these cells do not fuse with the major hypodermis (hyp7) in the L2 stage and instead are competent to act as VPCs. Expression of *lin-39* is controlled by a Wnt signal (primarily *cwn-1* and *egl-20*) via *bar-1*/β-catenin, together with a proposed supporting role for LIN-3/RAS signalling. This leads to *lin-39*-dependent regulation of the EFF-1 fusogen, restricting its ability to promote a fused fate (Eisenmann et al., 1998; Mohler et al., 2002; Myers and Greenwald, 2007; Shemer and Podbilewicz, 2002). Once vulval induction begins, the distal VPCs P3.p, P4.p, and P8.p, divide and fuse with hyp7, while the LIN-3 inductive signal promotes vulval fates in more proximal cells. *lin-39* is a downstream target of RAS signalling and is upregulated in P6.p following induction by the AC, where it is required to promote the 1° fate (Clandinin et al., 1997; Maloof and Kenyon, 1998). A second Hox gene, *mab-5*, is expressed in the posterior region of the animal and negatively regulates *lin-39* in P7.p and P8.p. It appears to reduce the ability of these cells to respond to the inductive signal, relative to P6.p. In addition, *mab-5* functions to position the VPCs relative to the anchor cell (Clandinin et al., 1997).

The specification of vulval cell fates occurs via a combination of inductive and lateral signalling processes that have been well characterized. Early in the L3 stage, anchor cell (AC) expression the EGF ligand, LIN-3, induces three of the six equivalent VPCs to adopt vulval cell fates via LET-23/EGF receptor activation of a RAS/MAPK cascade (Aroian and Sternberg, 1991; Beitel et al., 1990; Han and Sternberg, 1990). The P6.p cell is positioned closest to the AC and receives the highest amount of signal, leading to the generation of 1° fates. The adjacent P5.p and P7.p cells receive a lesser

amount of signal, and acquire 2° fates (Figure 4) (Hill and Sternberg, 1992; Katz et al., 1995; Kimble, 1981).

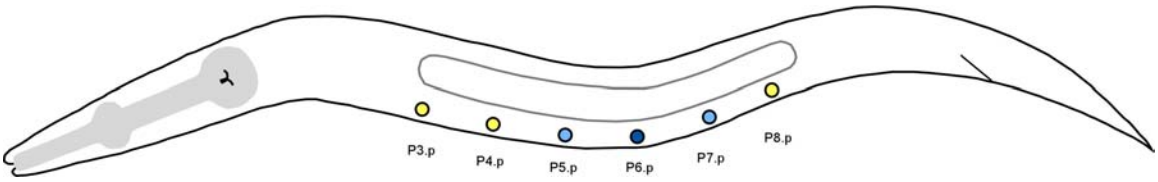

Figure 4. Six vulval precursor cells are located on the ventral mid-body of the worm.

Furthermore, activation of LET-23/EGFR in P6.p promotes the expression of Notch ligands, *lag-2*, *apx-1*, and *dsl-1*, which signal to LIN-12/Notch in the adjacent VPCs (Chen and Greenwald, 2004; Greenwald et al., 1983). Activation of Notch is necessary for the specification of 2° fates and, in turn, down regulates *let-23* expression in P5.p and P7.p. In this way, Notch signalling both prevents adjacent cells from adopting a 1° fate, and promotes the specification of the 2° fate (Figure 5). Expression of the Notch receptor is suppressed in P6.p in response to the inductive signal, leading to reciprocal negative regulation between the RAS and Notch pathways, and strengthens the 2°-1°-2° pattern of fates necessary for proper vulval development (Berset et al., 2001; Shaye and Greenwald, 2002; Sternberg and Horvitz, 1989; Yoo et al., 2004). In addition, although intermediate levels of *lin-3* have been demonstrated to promote 2° fates, the LIN-12/Notch lateral signal is necessary and sufficient to obtain a 2° fate. Thus the LIN-3 inductive signal and lateral signal may cooperate to promote 2° fates (Katz et al., 1995).

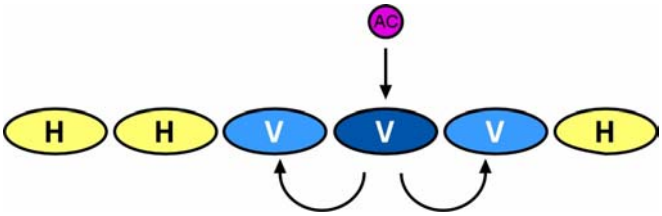

Figure 5. An inductive signal from the anchor cell (AC) generates a lateral signal that is received by adjacent VPCs such that they acquire distinct vulval fates.

Over expression of *lin-3/egf*, or a gain of function RAS mutation leads to a multivulva (Muv) phenotype where more than three VPCs acquire vulval fates. Conversely, loss of function mutations produce a vulvaless (Vul) phenotype where VPCs adopt hypodermal fates instead of vulval fates (Figure 6). Similarly, a *lin-12*(*gf*) mutation results in all VPCs acquiring 2° fates, however, a *lin-12* (0) mutant is also Muv due to a duplication of the AC in the L2 stage (Hill and Sternberg, 1992; Sternberg and Han, 1998; Sternberg and Horvitz, 1989).

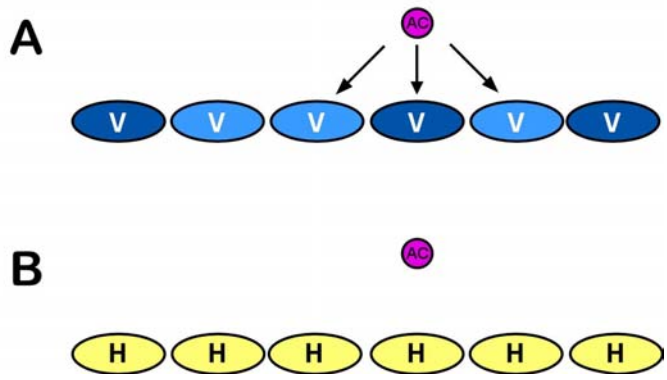

Figure 6. Gain or loss of function RAS pathway mutations lead to Muv and Vul phenotypes.

(A) Over expression of LIN-3/EGF or gain of function mutations cause extra cells to adopt vulval cell fates. **(B)** Loss of RAS pathway activity leads to a loss of vulval cell fates. Instead cells acquire a hypodermal fate.

Since six VPCs are capable of responding to these signals, but only three are required for development of a normal vulva, a number of negative regulatory mechanisms are in place to control excessive inductive signalling. As previously mentioned, a number of proteins that antagonize LET-23 activity, including GAP-1, SLI-1, and LIP-1, have been identified (Berset et al., 2001; Hajnal et al., 1997; Jongeward et al., 1995). In advance of LET-23 activation, however, a set of proteins antagonize EGFR/RAS/MAPK signalling by restricting the activity of the ligand. The synthetic multivulva (synMuv) genes are predicted to act redundantly to negatively regulate the transcription of *lin-3* (Cui et al., 2006). The synMuv genes are grouped into two main classes, A and B. Single mutations from either class exhibit wild-type characteristics, but a class A-B double mutant leads to a multivulva phenotype. Many of the synMuv proteins have orthologs with roles in chromatin remodelling and transcriptional repression, suggesting a mode of action for suppression of LIN-3 signalling (Andersen and Horvitz, 2007; Lu and Horvitz, 1998; Unhavaithaya et al., 2002; von Zelewsky et al., 2000). The synthetic Muv phenotype is proposed to result from derepression of *lin-3* in hyp7 (Figure 7). The synMuv phenotype requires the activity of EGFR/RAS signalling as it can be suppressed by mutations in RAS pathway genes. Regulation of *lin-3* expression is discussed further in chapter four.

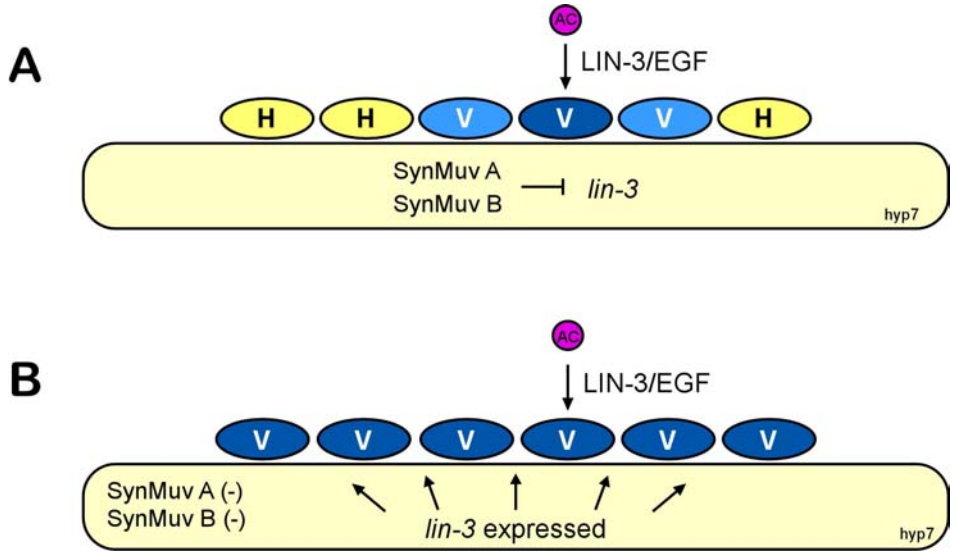

Figure 7. SynMuv activity restricts the expression of *lin-3/egf*.

(A) In wild type animals the SynMuvA and SynMuvB genes function redundantly to repress *lin-3* expression in the hypodermis (hyp7). **(B)** In a SynMuvAB double mutant, *lin-3* expression is derepressed, leading to LET-23 pathway activation in extra VPCs, and a SynMuv phenotype. Adapted from (Cui et al., 2006).

In addition to its dependence on inductive and lateral signalling, the patterning of vulval cell progeny receives input from the Wnt pathway. P6.p divides to produce eight progeny that acquire vulE and vulF fates in a symmetric pattern. P5.p and P7.p assume 2° fates, dividing to generate seven progeny each in a mirror image fashion, producing vulA, vulB1, vulB2, and vulC cell fates. The symmetry of the 2° lineages is dependent on Wnt signals via *lin-17*/Fz and *lin-18*/Ryk receptors and utilizes the *pop-1*/Tcf/LEF transcription factor. When these signals are lost, the polarity of the P7.p lineage is reversed (Deshpande et al., 2005; Inoue et al., 2004).

While vulval development is taking place, cell divisions occur in the overlying somatic gonad to produce the cells of the future uterus and prepare for the establishment of the vulva-uterine connection. During the L3 stage, the AC specifies two sets of cells

that are required for patterning the vulva and uterus; LIN-3/EGF expression induces three of six VPCs to adopt vulval cell fates, and LAG-2/DSL directs a subset of VU progeny to acquire the π cell fate via LIN-12/Notch (Hill and Sternberg, 1992; Newman et al., 1995). In this way, the uterus and vulva develop such that they are properly aligned in preparation for the formation of the vulval-uterine connection. As vulval morphogenesis proceeds, the 1° (and some 2°) progeny vulval cells invaginate so that the vulF cells lie adjacent to the AC and π cells. *lin-3* expression from the vulF cells induces four of the π cells to adopt a uv1 fate via LET-23 (Chang et al., 1999) and the uv1 cells later connect the vulF cells to the uterine seam cell (utse) (Figure 8).

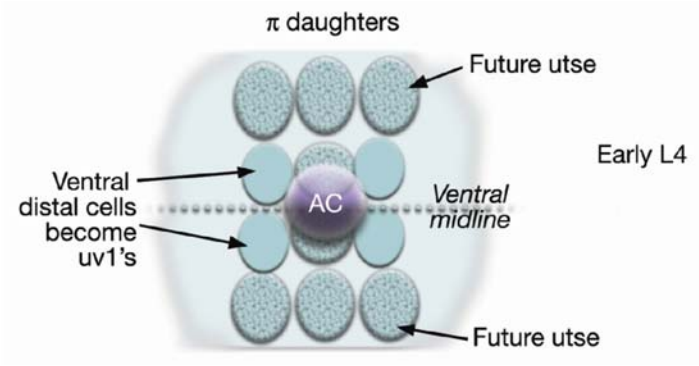

Image courtesy of WormAtlas (www.wormatlas.org)

Figure 8. Relative positions of π cells prior to the formation of the utse cell.
Ventral view of the π cells and their positions relative to the anchor cell.

The remaining π cells, together with the AC, fuse to form the utse cell. This is followed by antero-posterior migration by the π nuclei to reveal a thin laminar process separating the uterus and vulva (Newman et al., 1996). The vulF cells, uv1 cells, and the utse cell are connected by adherens junctions and together form the vulval-uterine connection; at the L4 molt, the vulva everts in preparation for egg laying.

Several transcription factors are required for the correct specification of uterine cell fates. Stimulation of the LIN-12 receptor in the π cells occurs via activation of *lag-2* expression in the AC by the zinc finger protein *lin-29* (Newman et al., 2000). Moreover, the LIM homeodomain protein *lin-11* is first expressed in 2° vulval cell lineages, and later in π cells in response to LIN-12/Notch signalling where its expression is required for the differentiation of the π cells and for fusion of the AC with the utse cell (Gupta and Sternberg, 2002; Inoue et al., 2005; Newman et al., 1999). Additionally, expression of the Pax gene *egl-38* directs the formation of the uv1 cells by positively regulating *lin-3* expression in the vulF cells. The *egl-38(n578)* mutation leads to defects in vulval morphogenesis in addition to a loss of uv1 cells (Chamberlin et al., 1997; Chang et al., 1999). Studies of these factors, among others, have been instrumental in revealing the reiterative use of the EGFR and Notch pathways to pattern the uterus and vulva.

1.4 Thesis overview

The goals of this project were to characterize *let-765*, and investigate its role in *C. elegans* development with the aim of proposing a function for the protein. In chapter two, I discuss the identification of *let-765* and refine the gene model to include additional sequence at its 5' end. By comparison with DExD/H box family orthologs, I have identified additional sequence conservation that predicts an enzymatic activity, which was subsequently confirmed using recombinant LET-765. Transcriptional and translational GFP reporter transgenes were created to describe the expression of *let-765* throughout development and I have quantified its expression at developmental stages using real-time RT-PCR. Additionally, tissue-specific expression and rescue of the lethal phenotype have predicted essential sites of activity for the gene. In chapter three, I

present an analysis of the mutant and reduction of function phenotypes for *let-765*. I have used fluorescent reporter transgenes to investigate the effect of *let-765* on the development of the excretory system, the hypodermis, and the T cell lineage. Finally, in chapter four, I investigate the role of *let-765* in promoting vulval development. I have demonstrated that *let-765* is required for EGFR/RAS pathway activity during vulval induction and for the expression of the EGFR pathway target gene, *egl-17*, in the vulval precursor cells. I provide support for *let-765* activity in promoting the P12 fate in posterior ectodermal cells. I also show that *let-765* is required for the hyperinduced phenotype in synMuvAB animals, but not for synMuvB specific phenotypes. Lastly, I have identified *let-765* as a positive regulator of *lin-3*/*egf* expression during the initiation of vulval induction.

In the course of this study, I revised the gene model for *let-765* to include two predicted gene models, F20H11.2 and F20H11.6 (Figure 9). Throughout the thesis, I have referred to these elements separately, as some of the experiments were completed prior to the identification of the 5' end of the gene. I refer to the updated coding region as *let-765*, and all of the references to specific residues correspond to the new structure. I suggest that the revised intron-exon structure be identified as F20H11.2, as this model contains the domains which provide homology to related proteins.

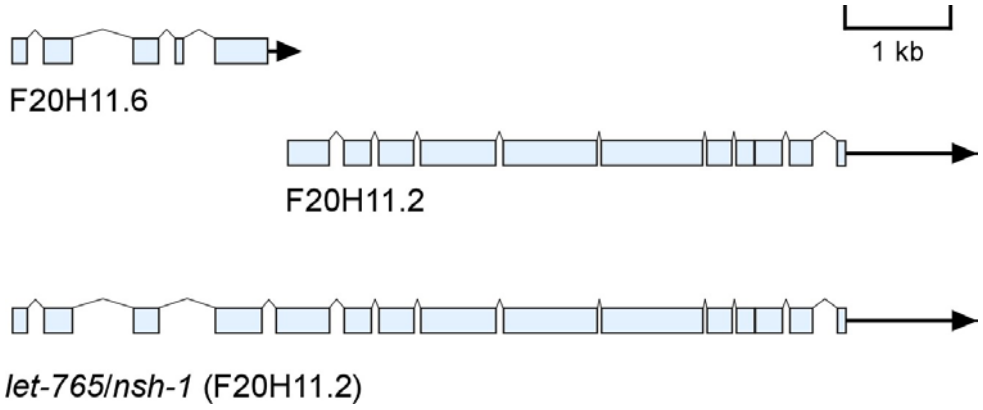

Figure 9. Predicted gene models for F20H11.6 and F20H11.2 and their relation to the updated model corresponding to *let-765/nsh-1*.

CHAPTER 2: IDENTIFICATION AND EXPRESSION OF *let-765/nsh-1*

2.1 Introduction

Essential genes are defined as those that are required for the formation of a fully fertile adult. These include zygotic lethal mutations (*let*), leading to embryonic or larval arrest; maternal-effect lethal mutations (*mel*), where a hermaphrodite homozygous for the mutation produces inviable progeny; and sterile mutations (*mes*), which result in a lack of fertilized eggs in a homozygous individual and are often due to defects in germline or somatic gonad development (Johnsen, 1997). The number of essential genes in the *C. elegans* genome is estimated to be 20–30%, although functional redundancy may well conceal the essential phenotype of some. The identification of essential genes has typically involved large scale mutagenesis screens in regions where chromosomal duplications or rearrangements can act as balancer chromosomes, enabling maintenance of the lethal mutation in a heterozygous context (Edgley et al., 2006). However more recently, PCR based methods, which screen a mutagenized population for intragenic deletions, have been used to target individual genes for knockout (Jansen et al., 1997). In addition, RNA interference (RNAi) has been used to screen for essential and non-essential phenotypes generated by knockdown of gene function and can be used to screen for synthetic lethality, caused by reducing the function of two or more genes at once (Gonczy et al., 2000; Kamath et al., 2003; Sonnichsen et al., 2005).

Two alleles of *let-765* were isolated from an EMS mutagenesis screen for essential genes on the left arm of chromosome III (Janke et al., 1997). They were mapped to a region defined by the overlap of the duplication *sDp8* and the deficiency *sDf125*, along with a second gene, *let-755* (Figure 10). Subsequent transgenic rescue experiments established that both genes reside in the region included in cosmid F20H11. In this study, I have identified *let-765* as F20H11.2/*nsh-1,* and, with the assistance of a former undergraduate student, Phoenix Chen, we identified *let-755* as F20H11.3/*mdh-1,* which encodes malate dehydrogenase.

let-765(s2575) males exhibit a lack of asymmetry at the division of a male-specific blast cell in the tail (H.Chamberlin, pers.comm). The B cell normally divides to produce a large anterior daughter cell and a smaller posterior daughter. The B.a cell produces all the cells of the copulatory spicules, while the B.p cell produces rectal epithelium and support cells (Chamberlin and Sternberg, 1993). In *let-765* animals, the B cell divides symmetrically and the daughter cells fail to divide further before arrest. The asymmetry defect suggested a potential function for *let-765* in fate specification or cell division; I opted to characterize its phenotype and expression pattern to lend insight into its role in development.

In this section, I describe the experiments that identified the affected gene in *let-765* alleles and characterize its spatial and temporal expression during *C. elegans* development. Using transgenic rescue, I determined that *let-765* is encoded by F20H11.2/*nsh-1*, a DExD/H box protein homologous to *Drosophila strawberry notch* and mammalian SBNO1; in both cases, null mutations in these genes result in embryonic lethality. Genetic lesions corresponding to the two alleles were identified and correlate

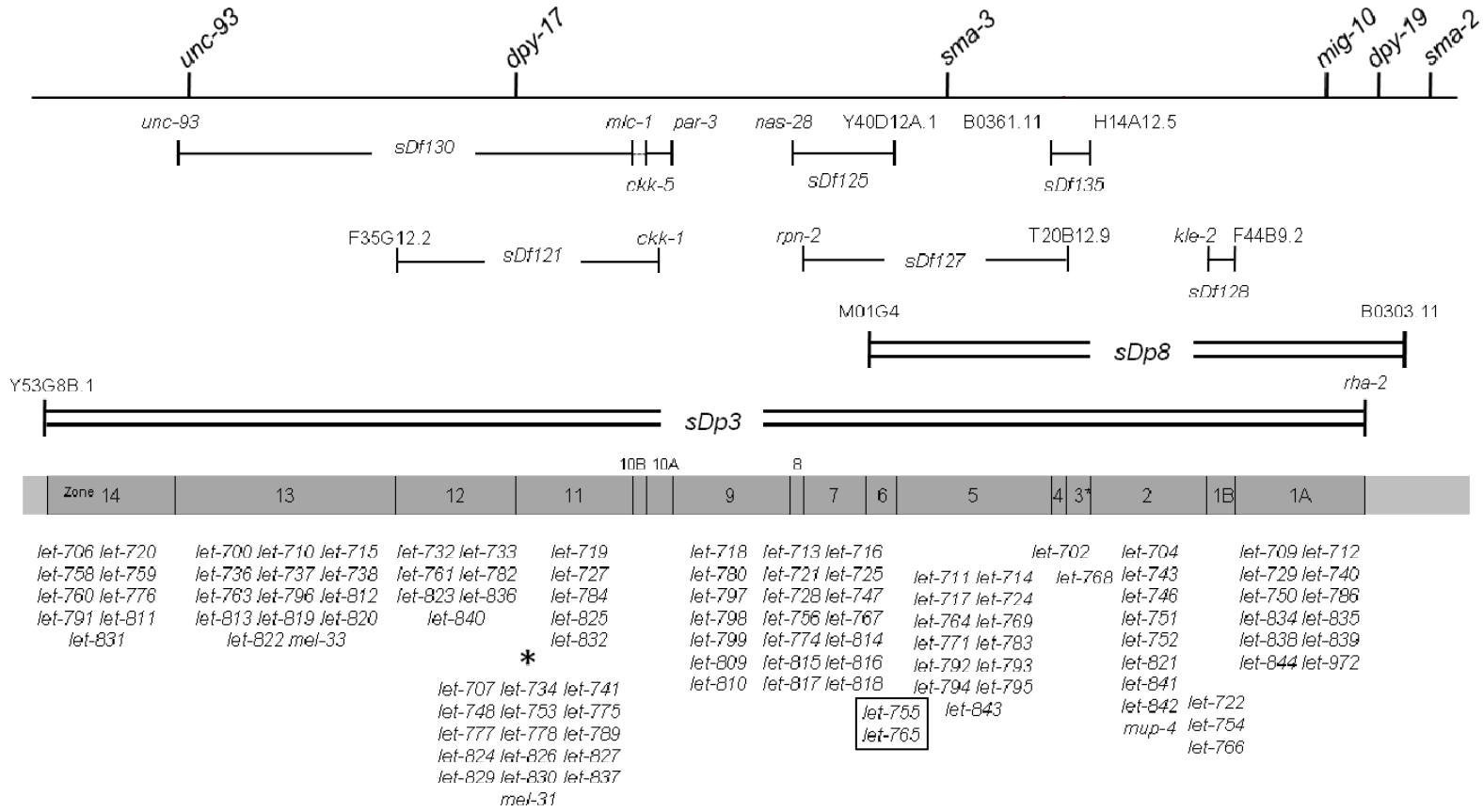

Figure 10. Genetic map of the *dpy-17* region of chromosome III.

let-765 and *let-755* are located in zone 6, which is included in *sDp8*, and deleted by *sDf125*. Deficiencies are indicated by single lines and duplications are indicated by double lines. Image courtesy of M.Jones.

well with the larval arrest phenotype and, further to this, I have refined the gene model to include additional sequence at the 5' end of F20H11.2. Comparative analysis with other related proteins allowed the discovery of motifs that are predicted to provide ATPase activity – this was confirmed by ATPase assay using recombinant LET-765 protein. I have determined spatial and temporal expression patterns, which have allowed insight into potential sites of essential activity as well as correlation with reduction of function phenotypes, presented in the following chapter.

2.2 Materials and methods

2.2.1 Strains and maintenance

C. elegans were cultured using standard methods (Brenner, 1974) and experiments were performed at 20°C unless otherwise noted. Bristol N2 was used as wild type. A complete list of strains used can be found in Appendix A.

2.2.2 Generation of transgenic strains for rescue

2.2.2.1 Cosmid and fosmid rescue constructs

Cosmid DNA was prepared using standard plasmid DNA preparation techniques. To generate F20H11 subclones, cosmid DNA was incubated with either KpnI or XhoI for one hour at 37°C, followed by 15 minutes at 65°C to inactivate the restriction enzyme. T4 DNA ligase and 10× ligase buffer were added (to a final concentration of 1×) and the reaction incubated at 15°C overnight. The ligation product, consisting of a religated cosmid 'shrink', was transformed into DH5α cells and positive colonies were expanded, miniprepped and digested to confirm the presence of the correct insert.

The KpnI-XhoI subclone was made by digesting the F20H11_XhoI cosmid clone with KpnI and Xho, column purifying to remove restriction enzymes, and ligating the mixed products to KpnI-XhoI digested pBluescript. Clones with the 12 kb insert were identified and one chosen for injection.

2.2.2.2 Germline transformation

DNA was injected into the syncytial gonad of wild type or *dpy-5*(*e907*) worms as described in (Mello et al., 1991). DNA from cosmid subclones was injected at a concentration of 10 ng/µL together with 100 ng/µL of pCeh361 (*dpy-5* rescuing plasmid) (Thacker et al., 2006) and 50 ng/µL *pgp-12:rfp* (Zhao et al., 2005). Fosmid DNA was injected at 3 ng/µL together with 100 ng/µL pCeh361 and either 50 ng/µL *pgp-12::rfp* or 50 ng/µL *myo-2::gfp*. Wild type F1 worms were individually plated and F2 worms that express the co-injected marker were selected to establish transgenic lines. The presence of cosmid or fosmid DNA was confirmed by PCR amplified using total DNA from worm lysates as a template and primers specific to the vector sequence.

2.2.3 Integration of extrachromosomal arrays

Young adult transgenic hermaphrodites were treated with low-dose X-ray irradiation (1,500 R). 12 P_0 were transferred singly to plates after one hour, the animals were allowed to lay eggs for 18–24 hours before removing them. Seven days later, mid to late larval wild-type F_2 animals were picked and set up (one/plate) at 23°C. F_2 plates were screened for the absence of Dpy-5 animals,indicating stable inheritance of the array. Integrated strains were outcrossed at least three times.

2.2.4 Complementation testing of *let-765* alleles

2.2.4.1 Testing for complementation between alleles of *let-765*

N2 males were crossed to *sDp3; dpy-17, let-765(s**X**), unc-32* hermaphrodites. The resulting heterozygous males were crossed to *sDp3; dpy-17, let-765(s**Y**), unc-32* hermaphrodites (where **X** and **Y** are different alleles) and individual F1 Dpy-Uncs (*dpy-17,s**X**,unc-32/dpy-17,s**Y**,unc-32*) were picked and scored for arrest (Figure 11).

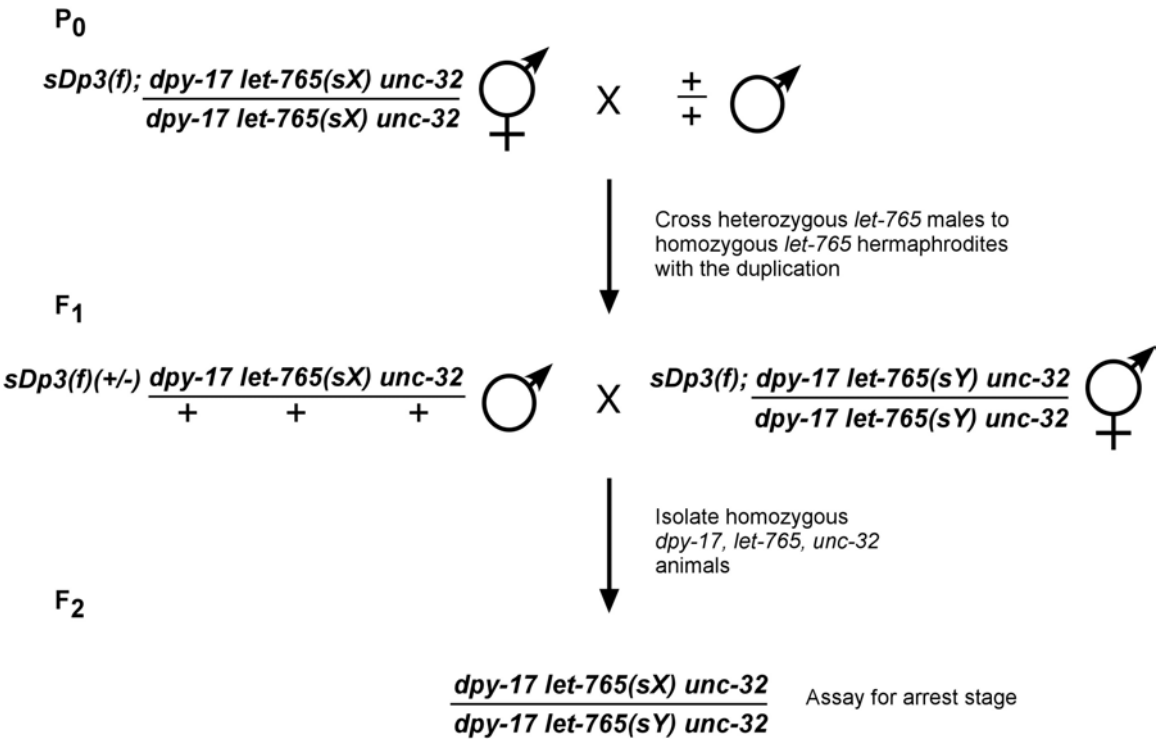

Figure 11. Cross scheme for complementation testing between *let-765* 's' alleles.

2.2.4.2 Re-balance '*s*' alleles over hT2

I.) N2 males were crossed to *sDp3; dpy-17, let-765, unc-32* hermaphrodites. The resulting heterozygous males were crossed to *dpy-17, unc-32* hermaphrodites and individual non-Dpy Unc hermaphrodites were selected from the resulting progeny (either *dpy-17 + unc-32/+ let-765 unc-32* **or** *sDp3; dpy-17 + unc-32/dpy-17 let-765 unc-32*). From these, individual Uncs were picked from lines that segregated Let non-Dpy Uncs (*let-765, unc-32/dpy-17, unc-32*) (Figure 12).

II.) *let-765, unc-32/dpy-17, unc-32* hermaphrodites were crossed to GFP expressing *hT2(qIs48)* males [+/*hT2*(I); +/*hT2*(III)]. Individual GFP positive hermaphrodites were isolated and lines that gave non-GFP Let Unc progeny were retained (Figure 13). One line was selected to establish BC7808 (*s2575*) or BC7726 (*s2630*).

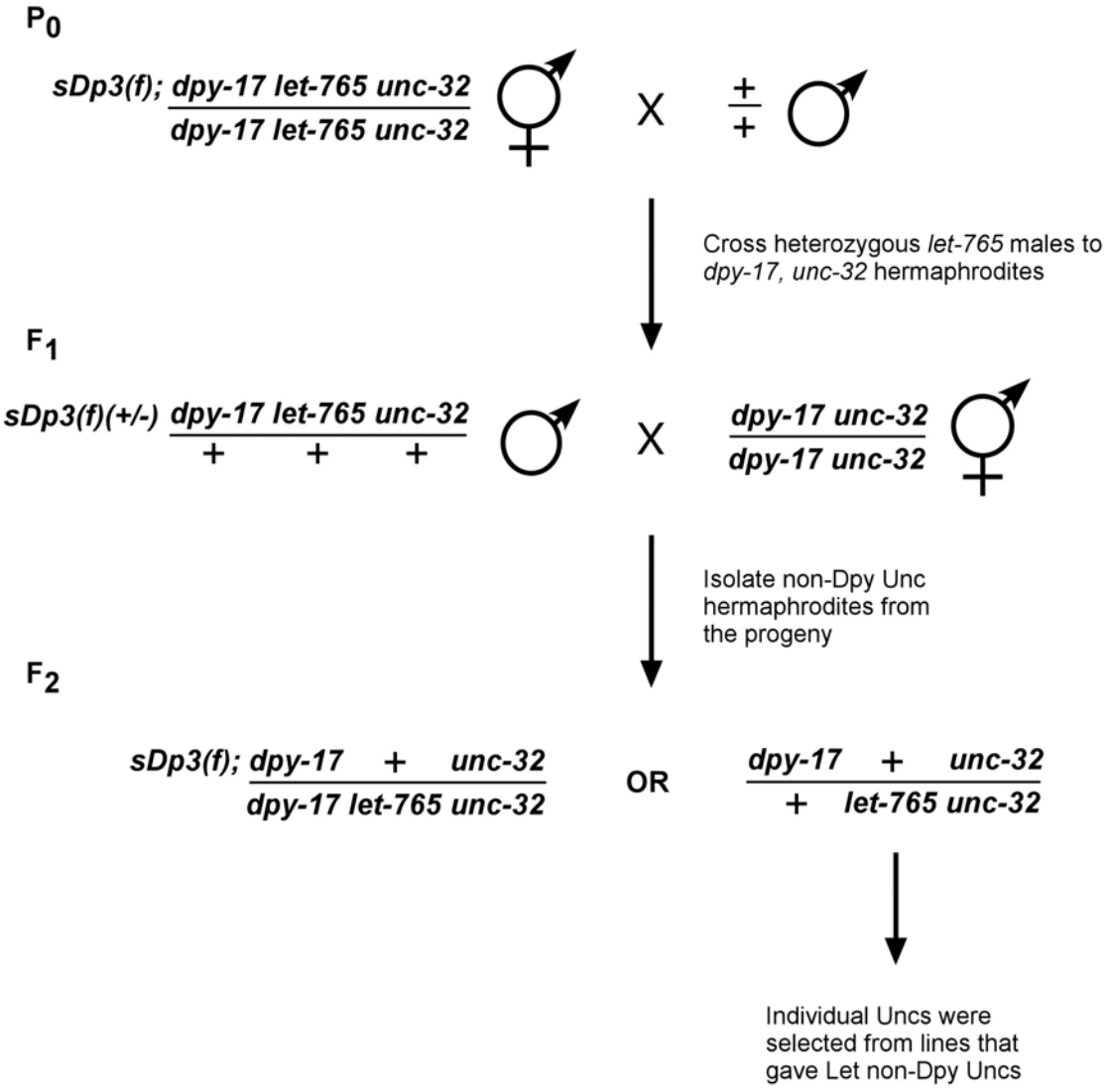

Figure 12. Cross scheme to remove *dpy-17* from the *let-765* chromosome.

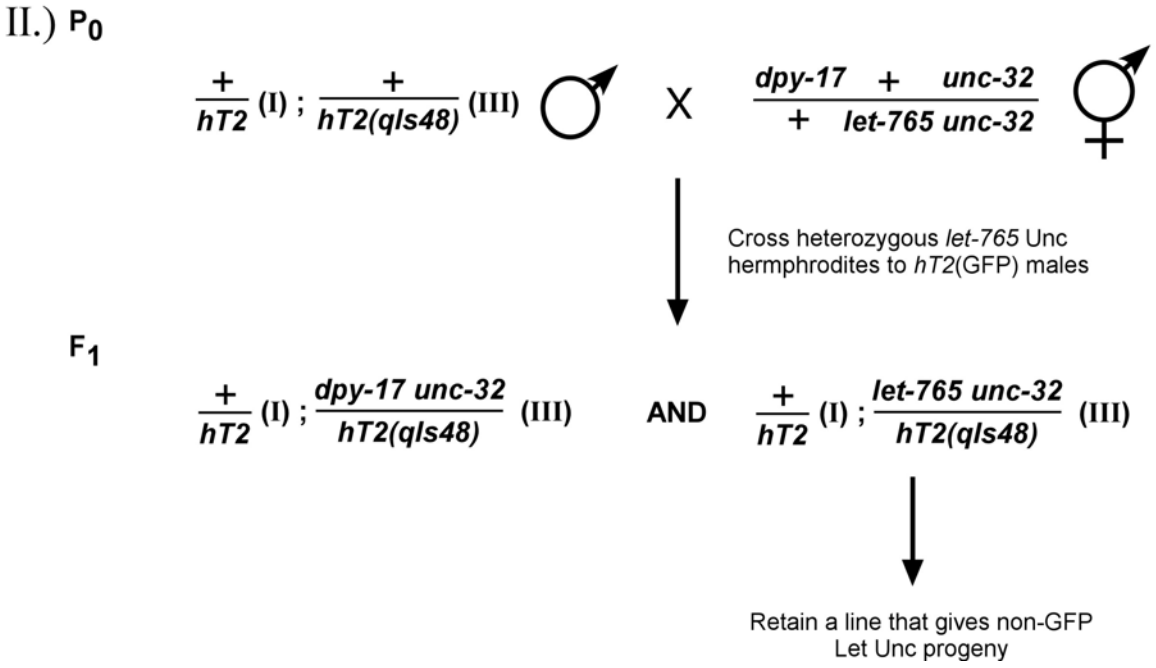

Figure 13. Cross scheme to re-balance *let-765* over *hT2*.

2.2.4.3 Testing for complementation with rescuing constructs

Rescue experiments using cosmid transgenic strains marked with pCes1943(*rol-6*) were completed as in Figure 14. N2 males were crossed to *sDp3, dpy-17, let-765, unc-32* hermaphrodites. The resulting heterozygous males were crossed to roller transgenic hermaphrodites. Dpy-Unc hermaphrodites from heterozygous roller parents were assayed for viability.

Rescues using arrays of cosmid subclones, fosmid, or plasmid clones were assayed as follows (see Figure 15). Transgenic hermaphrodites were crossed to N2 males. Progeny males that expressed the fluorescent marker were crossed to *hT2*-balanced *let-765* hermaphrodites. Non-*hT2* hermaphrodites that expressed the co-injected marker were isolated and progeny from lines that gave Let Uncs were assayed for viability.

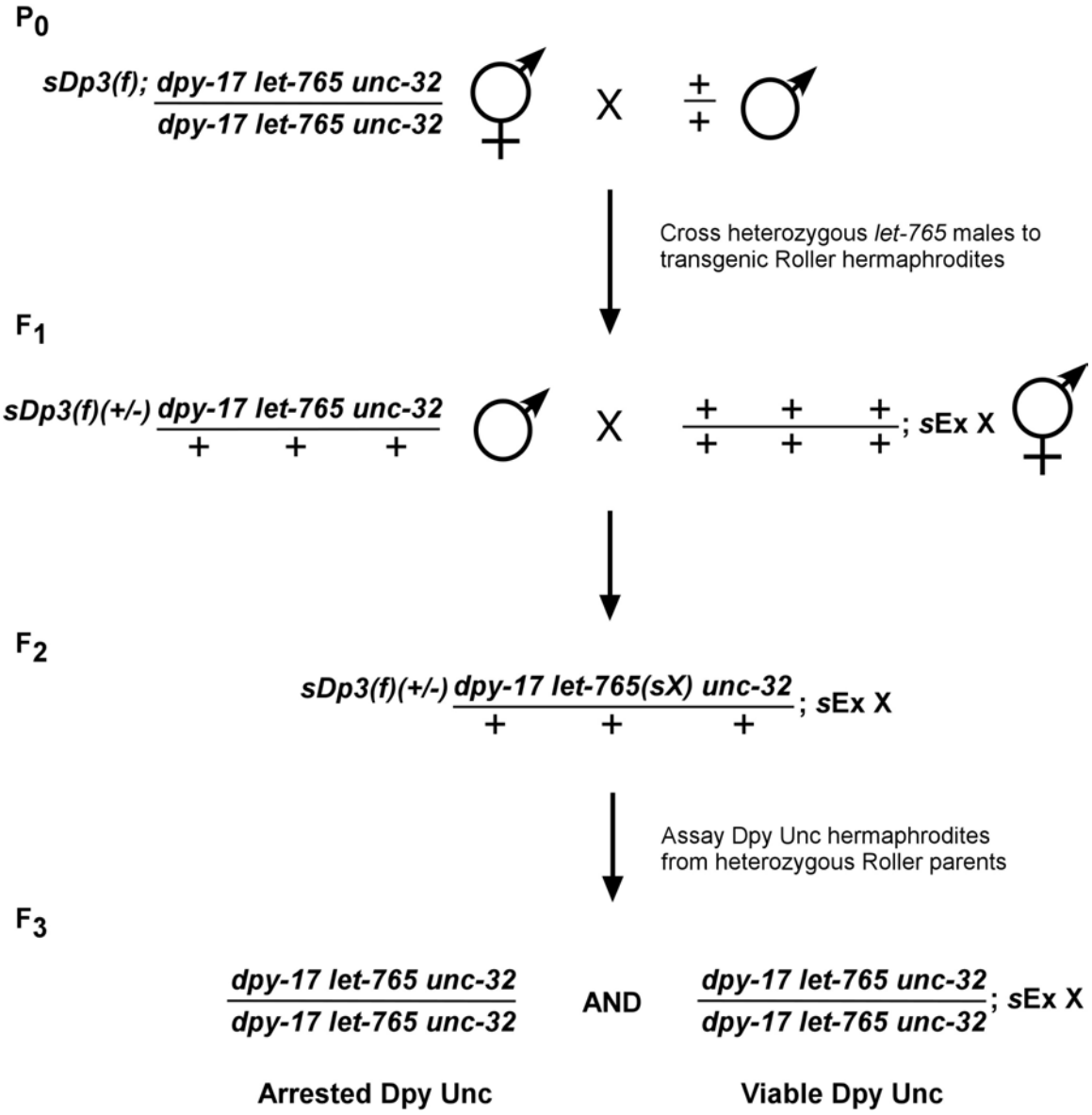

Figure 14. Cross scheme for rescue experiments using roller transgenic strains.

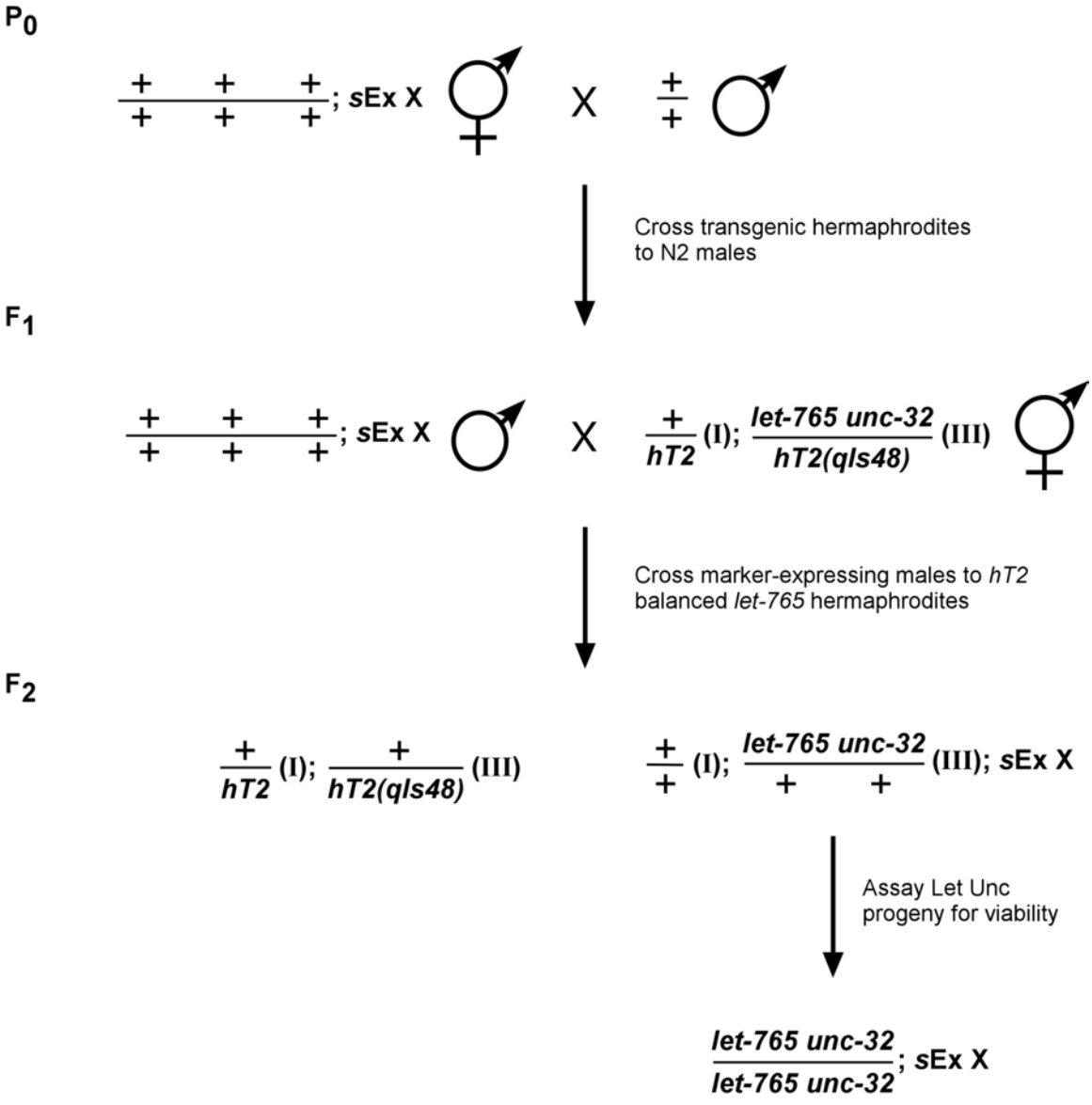

Figure 15. Cross scheme for rescue using transgenic with a fluorescent marker.

2.2.5 Determination of sequence changes in *let-765* alleles

Ten to fifteen homozygous Dpy-Unc progeny from strains BC4215(*s2575*) or BC4270(*s2630*) were picked into 5 µL worm lysis buffer [10mM Tris pH8.3, 50 mM KCl 2.5 mM MgCl2, 0.45% Tween20, 0.05% gelatin, 100ug/mL proteinase K] and flash frozen at -80°C. Worms were digested by incubating at 60°C for one hour followed by 95°C for 15 minutes. 1 µL of lysate was used as template for PCR amplification of the F20H11.2 genomic region. Three overlapping templates were amplified using multiple 20 µL PCR reactions for each; the products were pooled, gel extracted and sent for sequencing. Primers were designed every 500 bp, alternating on each strand, and are listed in Appendix B.

2.2.6 RT-PCR and sequencing *let-765* cDNAs

2.2.6.1 Preparation of yk clones for sequencing

cDNA clones yk536c4 and yk1729e03 were courtesy of Yuji Kohara (National Institute of Genetics, Japan). Clone yk536c4 was received as a phage stock and the pBluescript phagmid was excised essentially as described in the *lambda* ZAPII protocol (Stratagene). Briefly, the phage stock was diluted in 500 µL SM buffer/chloroform and incubated at RT for 1 hour. 200 µL of phage suspension and 1 µl of f1 helper phage was added to 250 µL fresh XL1-Blue cells and the cells incubated at 37°C for 15 minutes. 5 mL LB was added and the cells incubated for a further 3 hours at 37°C. Lysis was achieved by heating the tube to 70°C for 20 minutes. Supernatant containing the excised phagemid particles was added to XL-1 Blue cells, incubated at 37°C for 15 minutes and plated on LB ampicillan overnight.

Plasmids for yk536c4 and yk1729e03 were prepared from overnight cultures by plasmid miniprep and sent for sequencing.

2.2.6.2 Total RNA isolation and purification

Total RNA was prepared from both developmentally staged N2 worms as well as a mixed population, as follows: worms were synchronized by treating wild-type young adults with hypochlorite to collect eggs, hatching eggs in M9 buffer overnight, and plating aliquots on 10 cm plates seeded with OP50 bacteria. Animals were collected at the desired stage based on size and degree of gonad development. Worms were collected in M9, washed 3-5 times to remove bacteria and 2 volumes of Trizol added before freezing in liquid nitrogen. Samples were thawed at 37°C and vortexed, an additional 2 volumes of Trizol added, and two further freeze thaw cycles performed, vortexing each time. After incubating at room temperature (RT) for about 15 minutes, 200 µL of chloroform was added per 1 mL of Trizol used and samples vortexed for at least 15 seconds. After a further 15 minutes at RT, samples were centrifuged at 12,000 rpm/15'/4°C. The aqueous layer was removed and a second chloroform extraction completed. One volume of isopropanol was added to the aqueous layer and left for 15 minutes at RT, followed by centrifugation at 12 000 rpm/20'/4°C to precipitate RNA. The supernatant was removed and the pellet rinsed with 500 µL 70% EtOH, then spun at 8000 rpm/5'/4°C. Pellets were dried and resuspended in 50 µL DEPC H_2O. RNA samples were DNase treated by adding 1U DNase per 1 µg RNA and incubating at RT for 15 minutes. Reactions were stopped by adding 1 µL 25 mM EDTA and heating at 65°C for 10 minutes. Samples were purified using a QIAGEN RNeasy Mini kit and eluted in DEPC-treated water.

2.2.6.3 cDNA preparation and sequencing

1 µg of total RNA was used in each cDNA reaction. First strand synthesis was performed using Superscript II reverse transcriptase (Invitrogen) and oligo$(dT)_{17}$ primer as per the manufacturer's instructions. 1 µL of cDNA reaction was used in a 50 µL PCR reaction with gene-specific primers and SL primers. RT-PCR products were gel purified and sent for sequencing.

2.2.7 Analysis of the LET-765 protein sequence

The full LET-765 protein sequence was analyzed using SMART and Pfam. Homologous proteins were identified using BLASTp. Alignments were created using ClustalW (http://www.ebi.ac.uk/Tools/clustalw2/index.html). Some sequence motifs were identified by direct comparison between LET-765 and consensus sequences for DExD/H box family orthologs (Cordin et al., 2006; Cordin et al., 2004).

2.2.8 Generation of transcriptional reporter constructs

Transcriptional promoter:GFP constructs were made using a PCR fusion method as described in (Hobert, 2002). Genomic sequences containing promoter regions were amplified using gene specific primers. A reporter cassette was generated by amplification from a GFP vector sequence (pPD95.67) (Addgene) and the two products fused using nested primers. The GFP amplicon includes a nuclear localization signal (nls) sequence and an *unc-54* 3' untranslated region. Linear PCR products (~50 ng/µL) were co-injected with pCeh361(100 ng/µL). Multiple independent lines were isolated that exhibited the same pattern of GFP expression.

2.2.9 Recombineered fosmid:GFP

A cassette containing the GFP coding sequence was inserted into the fosmid WRM0625dF01 by homologous recombination using the method outlined in (Dolphin and Hope, 2006). The fosmid was chosen based on its ability to rescue alleles of *let-765*. Briefly, fosmid DNA was introduced into competent *swi106 E. coli* by electroporation, followed by two rounds of *lambda* Red recombinase-induced insertion of PCR generated DNA cassettes. The RT (*rps*L-*tet*A(C)) and GFP cassettes were PCR amplified such that they contain 50 bp of sequence on either end that flanks the desired insertion site (homology arms), thus allowing for homologous recombination to occur. Cassette primers were PAGE purified to ensure generation of full length homology arms and PCR products were gel-purified prior to electroporation. First a counter-selection (RT) cassette that contains positive and negative selection markers was introduced, and recombinant colonies isolated. In the second recombination step, the GFP cassette replaced the RT cassette. A summary of the selection protocol is shown in Figure 16. At each step, positive colonies were tested for insertion of the DNA cassette by PCR using primers that flank the insertion site (Figure 16 C).

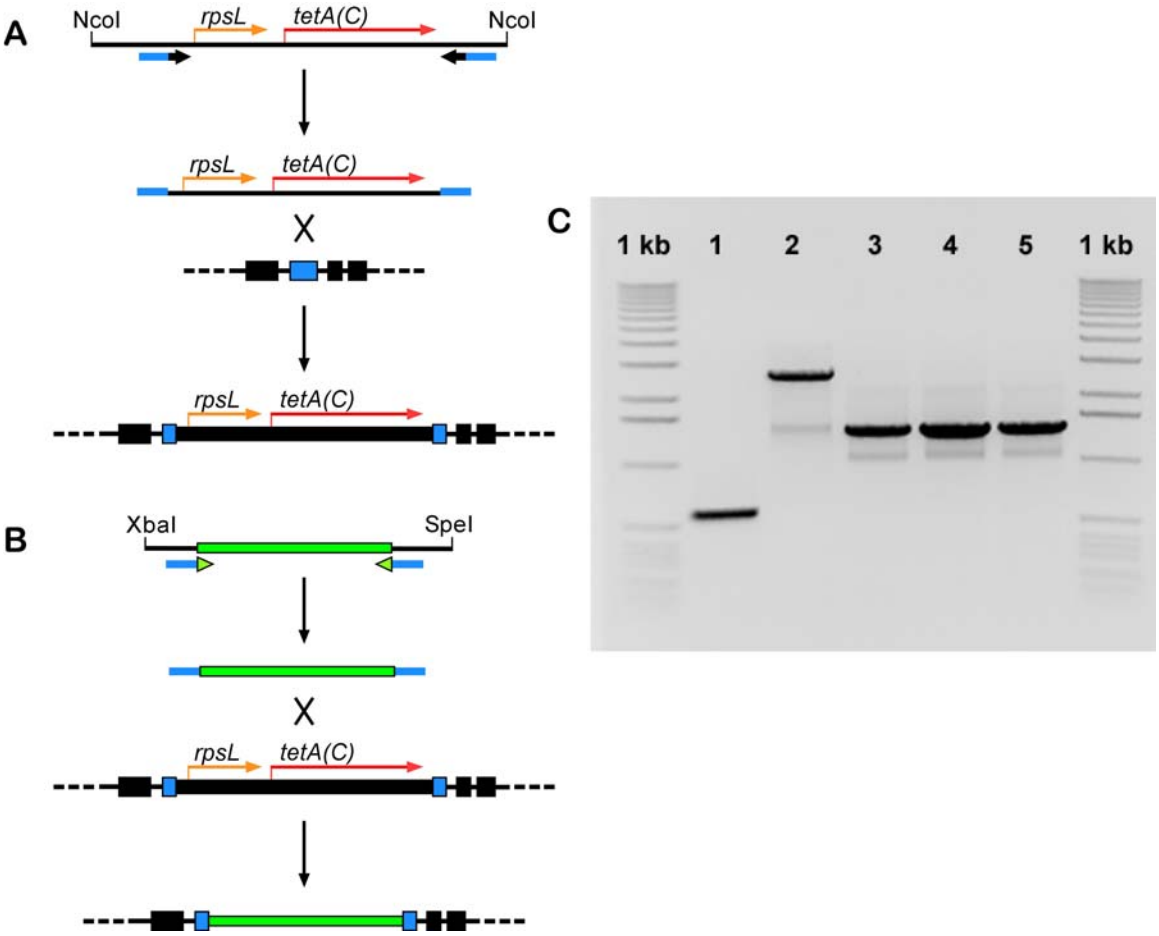

Figure 16. Method for generating recombineered fosmid::GFP.

(A) In step one, a counter selection cassette is introduced and positive selection by the tetA(C) marker allows for identification of successful recombinants. **(B)** In step two, the RT cassette is replaced with the GFP coding sequence and counter selection is achieved using the rpsL^{+} gene. An rpsL^{-} host exhibits a Str^{R} phenotype, however, when rpsL^{+} is introduced, it confers a dominant Str^{S} phenotype. Consequently, non-recombinants will be StrS, and are selected against, while GFP containing clones are Str^{R} revertants. **(C)** The presence of the recombineered insert is confirmed by PCR with primers flanking the insertion site. Lane1: empty fosmid, Lane 2: fosmid wth RT cassette inserted, Lanes 3-5: fosmid with GFP insert.

2.2.10 Generation of subclones used for rescue

The construct containing F20H11.2 together with the upstream intergenic 'promoter' region (*sEx1644*) was made by PCR amplifying the genomic region relative to F20H11.2 [-376 to 5774] and cloning into pBluescript via PstI digest.

A *dpy-7*p::gfp transcriptional reporter (*sEx1653*) was generated by amplifying a 216 bp genomic fragment of the *dpy-7* promoter and cloning into pPD95.75 using HindIII/PstI. Hypodermal GFP expression was confirmed in transgenic worms. The XmaI-SpeI gfp::*unc-54* 3'UTR was replaced with a genomic fragment containing F20H11.2 [-10 to 5950] that was PCR amplified and digested with XmaI-SpeI, to obtain *dpy-7*p::F20H11.2 (*sEx1739*).

Heat shock promoter-driven constructs were built by amplifying the genomic fragment F20H11.2 [-10 to 5445] and cloning into the NheI-KpnI sites in pPD49.78 (*hsp 16-2*, hypodermis and neural expression) and pPD49.83 (*hsp16-41*, gut expression) toobtain *hsp 49.78*::F20H11.2 (*sEx1354*, *sEx1355*) and *hsp 49.83*::F20H11.2 (*sEx1356*, *sEx1357*).

All constructs were sequenced to confirm that junctions and insert sequences were correct. Constructs were injected at 10-20 ng/µL together with 100 ng/µL pCeh361 and either 50 ng/µL *pgp-12::rfp* or 50 ng/µL *myo-2::gfp*.

2.2.11 Real-time RT-PCR using developmentally staged and *glp-4* RNA

Total RNA was isolated and purified as in 2.2.6.2. 1 µg of RNA from each developmental staged sample was used in first strand cDNA synthesis with Superscript II reverse transcriptase (Invitrogen) and an oligo$(dT)_{17}$ primer.

To obtain *glp-4* total RNA, a synchronized population of *glp-4*(*bn2*) animals was obtained by hypochlorite treatment and hatching embryos in M9 buffer overnight. The larvae were raised at the restrictive temperature (25°C) and collected as young adults. Total RNA was isolated and purified as in 2.2.6.2. cDNA samples were prepared as above.

Staged cDNA samples were used as template for each real time RT-PCR reaction. Reactions were run in triplicate on a Biorad MyIQ Real-time thermocycler and consisted of the following: 50 ng of RT products, 10 µL of 2× SYBR Green Supermix (Biorad), and 1µM of each primer. Cycling parameters were as follows: 3' 95°C, 34 cycles of 10" 95°C/20" 58°C/45" 72°C, and a final 2' at 72°C. Relative fold change was calculated using the ΔΔCt method and data normalized using *rpl-19*, which encodes a large ribosomal subunit protein. A melt curve analysis was performed for each set of reactions to check for amplified-products homogeneity. Primer efficiency was calculated after testing on serial dilutions of mixed stage cDNA and genomic DNA. Two independent sets of primers for *let-765* were used and gave nearly identical results. *rpl-19* was found to be expressed at relatively constant levels and was used as an internal reference. Total levels of transcript are shown in Figure 17.

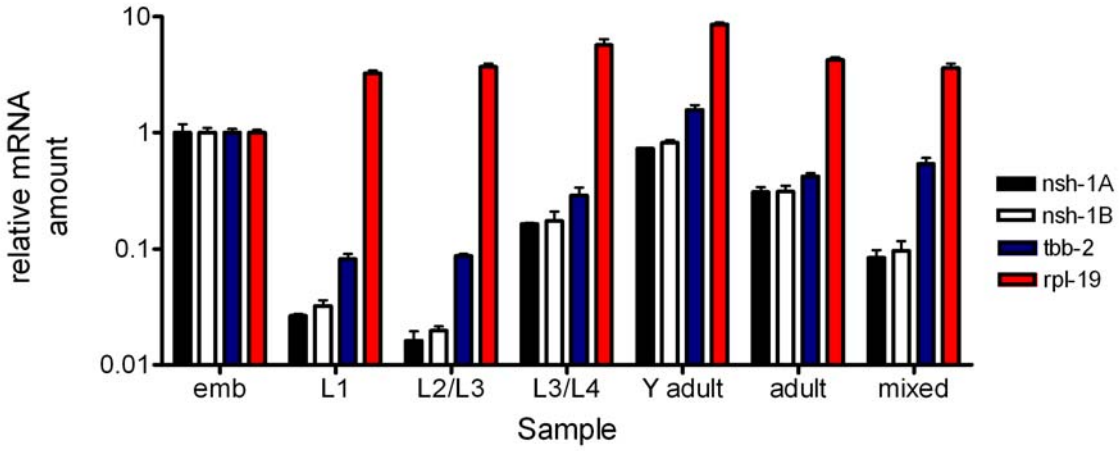

Figure 17. Relative mRNA levels in non-normalized samples.

Stage specific real-time RT-PCR of the indicated transcripts. The data has not been normalized for loading control, however the consistency of *rpl-19* expression across samples is notable and therefore it was chosen as a reference. Conversely, β-tubulin (*tbb-1*) expression levels were found to be much less stable. Two sets of primers for *let-765/nsh-1* behave similarly and *nsh-1a* was used in subsequent experiments. Plotted bars indicate mRNA amount relative to the embryo sample, and represent the average of three replicates.

2.2.12 Recombinant protein expression

The sequence corresponding to amino acids 626 to 1542 of the updated protein was amplified from *let-765* cDNA using primers that contained SmaI and XhoI restriction sites. The PCR product was digested and cloned into pGEX-6P1. DH5α cells were transformed with the ligation reaction and colonies screened for a positive clone. Clones were sequenced to confirm successful insertion of the cDNA in frame. One clone was chosen and transformed into BL21(DE3) cells for protein expression and purification. . Cells were first incubated at 37°C until the mid-logarithmic stage (OD_{600} ~ 0.6) and transferred to an 18°C incubator before induction with 1 mM IPTG in the presence of 1% ethanol (to induce bacterial chaperones). The induction was allowed to

proceed overnight before the cells were cracked using a French Press. The protein was purified over glutathione sepharose beads, dialyzed in a PBS buffer containing 50% glycerol and stored in aliquots at 80°C

2.2.13 Assay for ATPase activity

ATPase activity of the recombinant protein was measured by incubating 50 μM [γ-^{32}P]-ATP with ~100 ng/mL protein in PBS buffer, supplemented with 5 mM MgCl2 at 37°C for 15 minutes. The reactions were quenched in 20% formic acid. The products (inorganic phosphate) were resolved from unreacted ATP by PEI cellulose thin-layer chromatography with 0.5 M KH_2PO_4 pH 3.5 as a mobile phase. The TLC was dried and scanned using a Typhoon (Molecular Dynamics) phosphorimager. Reactions where RNA was present, ~5 μM 74-nt *in vitro* transcribed RNA was added to the reaction.

2.2.14 Microscopy

Analysis of GFP transgenic and *hT2* balanced mutants was performed using a Zeiss Stemi SVC11dissecting microscope equipped with epiflourescence. Images were collected using a Zeiss Axioscop equipped with epiflourescence and a QImaging camera or a WaveFX spinning disc confocal microscope (Zeiss Axio Observer microscope and Hammamatsu EMCCD camera) using Improvision software. Images of *sIs15339* were collected using a Leica DMRXA microscope with a Hammamatsu OrcaAD with Openlab software. Animals were mounted on a pad of 2% agarose in a drop of 2mM levamisole in M9.

2.3 Results Part I: *let-765* is encoded by F20H11.2/*nsh-1*

2.3.1 *let-765* is rescued by subclones containing F20H11.6 and F20H11.2

The cosmid F20H11 successfully rescued the *s2575* allele, resulting in ten candidate genes that could encode *let-765*. I completed subsequent transformation rescue attempts using the overlapping cosmid F27B3 and found that it failed to complement the lethal phenotype. With the expectation that *let-765*(RNAi) would reflect the essential nature of the gene, only three coding elements remained to be likely candidates for *let-765*; F20H11.3, F20H11.6 and F20H11.2, as RNAi against these genes by injection results in embryonic lethality. Further rescues with subclones generated by digest and religation of the cosmid reduced the number of potential gene models. A XhoI digested clone containing four genes, F20H11.3, F20H11.4, F20H11.6 and F20H11.2, rescued the lethal phenotype. In contrast, a KpnI digested clone that contains F20H11.3 and F20H11.4 failed to rescue – all homozygous progeny arrested at the L2 stage. This identifed *let-765* as either F20H11.6 or F20H11.2 which was also confirmed by transformation rescue with a KpnI-XhoI subclone of F20H11 (Figure 18).

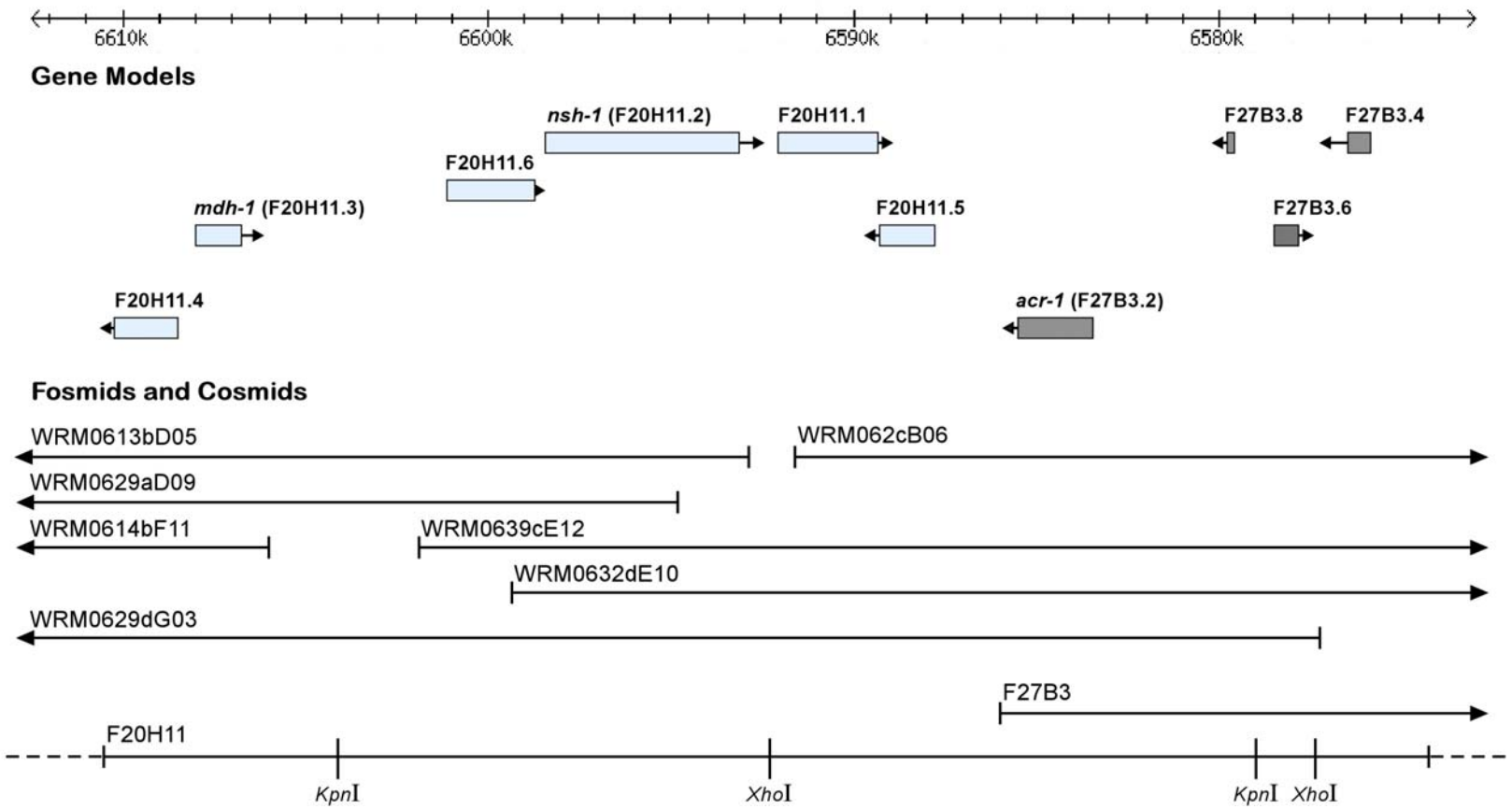

Figure 18. Genomic region of the F20H11 cosmid.

Scale representation of fosmid clones that span the region, as well as the overlapping cosmids used for rescue. Restriction sites used for generating cosmid shrinks are noted on F20H11. Dashed lines indicate vector sequence. Adapted from Wormbase (WS203).

I subsequently used several fosmid clones to refine further the region that complements *let-765* (http://elegans.bcgsc.ca/perl/fosmid/CloneSearch). Two overlapping fosmids containing both genes provided rescue, while WRM0632dE10, that is missing most of F20H11.6 and its promoter, did not (Figure 19). F20H11.6 and F20H11.2, together with F20H11.1, were predicted to reside in an operon, indicating that they are likely co-transcribed and the upstream promoter region may be required for expression of F20H11.2 (and F20H11.1). The results implied that either F20H11.6 was the corresponding coding region for *let-765*, or F20H11.2 encoded the gene, but required an upstream promoter and /or cis acting regulatory sequences to produce a fully functional F20H11.2 gene product. I later discovered, using SL2 RT-PCR, that the F20H11.6 gene model was in fact part of F20H11.2, clearly resolving the identity of *let-765*.

2.3.2 *let-765* alleles contain point mutations in F20H11.2/*nsh-1*

To identify the molecular lesions associated with each *let-765* allele, I isolated genomic DNA from homozygous mutant animals, PCR amplified and sequenced the F20H11.2 region. The template DNA was amplified in three overlapping segments of about 2000 bp, covering the F20H11.2 coding region, 5' UTR and 3' UTR. A sufficient number of sequencing primers were used to obtain a minimum of five-fold coverage throughout the gene. I identified a G>A transition in *s2630* that converts a conserved tryptophan to a stop codon at residue 940 of the predicted protein. The *s2575* allele has a C to T transition located upstream of the previously annotated ATG that I subsequently identified as part of the F20H11.2 coding sequence. As a result, both alleles are predicted to cause premature chain termination of the protein, which correlates well with the

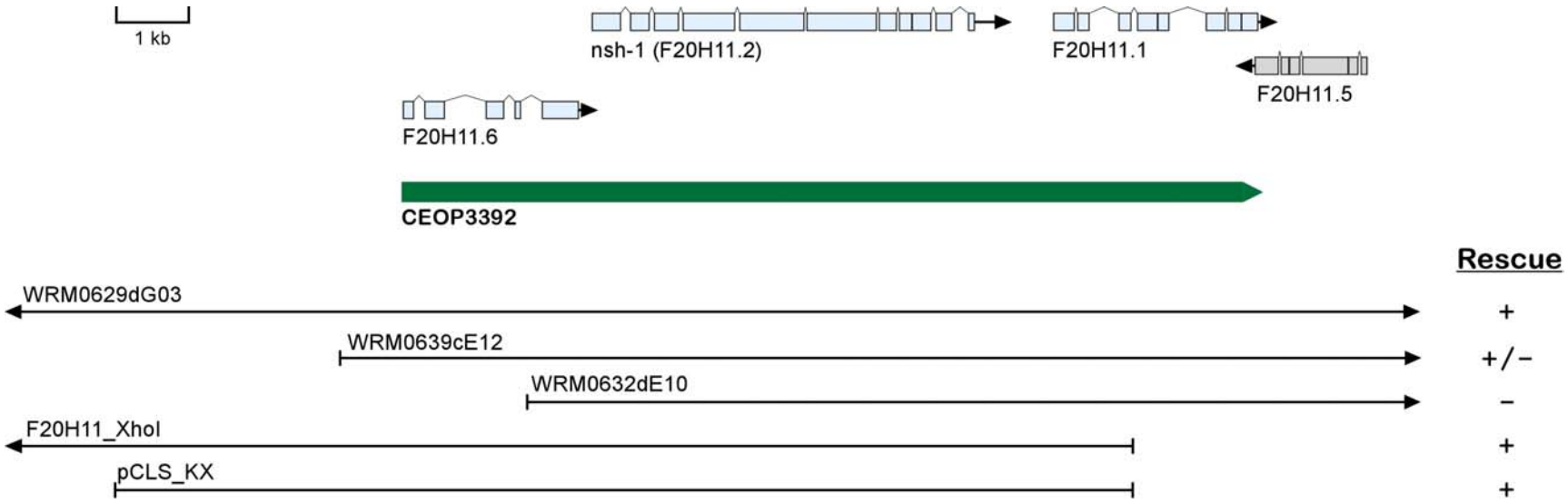

Figure 19. Rescue of the lethal phenotype defines the upstream regulatory region for *let-765*.

Schematic of fosmids and cosmid subclones used to rescue the lethal phenotype. The predicted operon (CEOP3392) is shown along with the corresponding gene models. Results from rescue experiments are listed at right: +: full rescue, +/-: partial rescue, -: no rescue. Adapted from Wormbase (WS203)

observed early larval arrest phenotype. Together with the rescue data, this confirmed that F20H11.2 encodes *let-765*.

In addition to our existing alleles, the *C. elegans* Gene Knockout Consortium generated a deletion allele (*ok2058*) in F20H11.2/*nsh-1* that removes 1541 bp and inserts a C at the 5' end of the deletion site – the deletion and frameshift result in a truncation at residue 839 of the predicted protein. Animals homozygous for *ok2058* display the same early larval lethality as *s2575* and *s2630* and all three alleles fail to complement one another, verifying that they are allelic, and providing further confirmation that I have identified *let-765* as F20H11.2/*nsh-1*.

```
                ....|....| ....|....| ....|...*| ....|....| ....|....| ....|....| ....|....| ....|....|
                    5         15         25         35         45         55         65         75
F20H11.2        ATCGAATGGA CCAACCCATC TCCTCCGACG AACCACAACA ACTGGTCAAC CAACTCGCGG AGCTCCAGTA GGAATGGCTG
N-36            ---------- ---------- -----CGATG AACCACAACA ACTGGTCAAC CAACTCGCGG AGCTCCAGTA GGAATGGCTG
N-37            ATCGAATGGA CCAACCCATC TCCTCCGATG AACCACAACA ACTGGTCAAC CAACTCGCGG AGCTCCAGTA GGAATGGCTG
N-38            ATCGAATGGA CCAACCCATC TCCTCCGATG AACCACAACA ACTGGTCAAC CAACTCGCGG AGCTCCAGTA GGAATGGCTG
N-A1            ATCGAATGGA CCAACCCATC TCCTCCGATG AACCACAACA ACTGGTCAAC CAACTCGCGG AGCTCCAGTA GGAATGGCTG
N-2             ATCGAATGGA CCAACCCATC TCCTCCGATG AACCACAACA ACTGGTCAAC CAACTCGCGG AGCTCCAGTA GGAATGGCTG
N-3             ---------- ---------- ---------- ---------- ---------- ---------- ---------- ----------
N-4             ---------- ---------- ---------- ---------- ---------- ---------- ---------- ----------

                ....|....| ....|....| ....|....| ....|....| ....|....| ....|....| ....|....| ....|....|
                    85         95        105        115        125        135        145        155
F20H11.2        CTCGTCACGC AGTTCGTGGT GGAACTGTTT ATGGTGGTGG TAATGGATAT CGAGTAAATC TTGTTGGCCG TGGAACTGGT
N-36            CTCGTCACGC AGTTCGTGGT GGAACTGTTT ATGGTGGTGG TAATGGATAT CGAGTAAATC TTGTTGGCCG TGGAACTGGT
N-37            CTCGTCACGC AGTTCGTGGT GGAACTGTTT ATGGTGGTGG TAATGGATAT CGAGTAAATC TTGTTGGCCG TGGAACTGGT
N-38            CTCGTCACGC AGTTCGTGGT GGAACTGTTT ATGGTGGTGG TAATGGATAT CGAGTAAATC TTGTTGGCCG TGGAACTGGT
N-A1            CTCGTCACGC AGTTCGTGGT GGAACTGTTT ATGGTGGTGG TAATGGATAT CGAGTAAATC TTGTTGGCCG TGGAACTGGT
N-2             CTCGTCACGC AGTTCGTGGT GGAACTGTTT ATGGTGGTGG TAATGGATAT CGAGTAAATC TTGTTGGCCG TGGAACTGGT
N-3             ---------- ---------- ---------- ---------- ---------- ---------- ---------- ----------
N-4             ---------- ---------- ---------- ---------- ---------- ---------- ---------- ----------
```

Figure 20. Sequencing results for *let-765*(*s2575*).

The top sequence is wild type (F20H11.2) followed by 7 overlapping reads from *let-765(s2575)* homozygotes. The C>T mutation is marked with an asterisk.

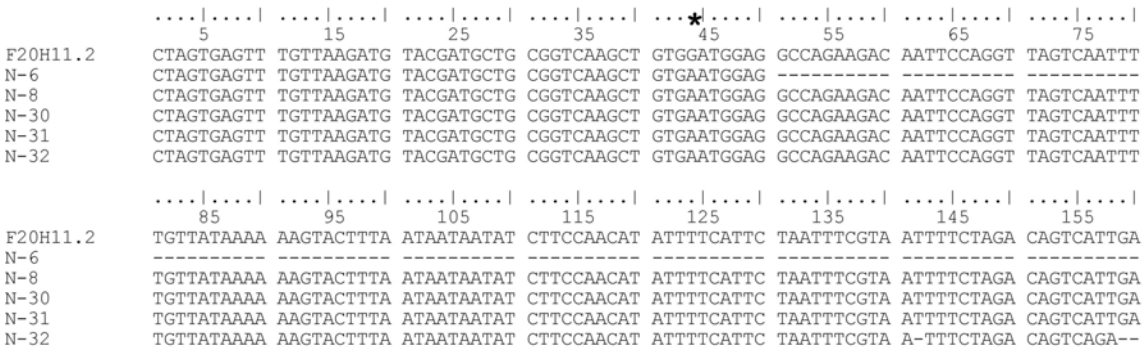

Figure 21. Sequencing results for *let-765*(*s2630*).

The wild-type sequence is followed by 5 overalapping sequence reads from *let-765*(*s2630*) homozygotes. The G>A mutation is marked with an asterisk.

2.3.3 Refinement of the *let-765* gene model using RT-PCR

Once the residues affected by *let-765* mutations were identified, I proceeded to confirm the gene model for F20H11.2. I obtained two cDNA clones, yk536c4 and yk1729e03, from the laboratory of Yuji Kohara (National Genetics Institute, Japan). Plasmid DNA was prepared for each clone and sequenced using the original *let-765* sequencing primers. The two cDNAs provided overlapping sequences that confirmed all exons and splice junctions from the predicted gene model (WS203) except for an extra intron and 11th exon at the 3' end of yk536c4. I noted that the yk1729e03 cDNA contains an unspliced intron between exons 8 and 9 and is missing the 11th exon – possibly as a result of a failure to splice the last intron as well. Furthermore, neither of the cDNA clones contained a spliced leader at their 5' end, as would be predicted if the gene were in an operon, so I attempted to amplify the full length transcript using RT-PCR.

Several overlapping RT-PCR products were amplified and sequenced, allowing confirmation of the 11 exons identified in the previous cDNA sequences, however,

evidence of the 10 exon transcript predicted by yk1729e03 was lacking. To assess whether a subset of my reaction products matched the alternate cDNA sequence, a mixed stage RT-PCR sample was amplified across the last four exons. A unique HindP1 site in the sequence of intron 10 allowed for the potential identification of a product that matched yk1729e03; the intronic sequence would not be spliced out and instead would remain as part of the 3'UTR (Figure 22). However, the reaction products did not contain a band corresponding to the unspliced version of the cDNA, so I have not been able to confirm the alternate 3' end.

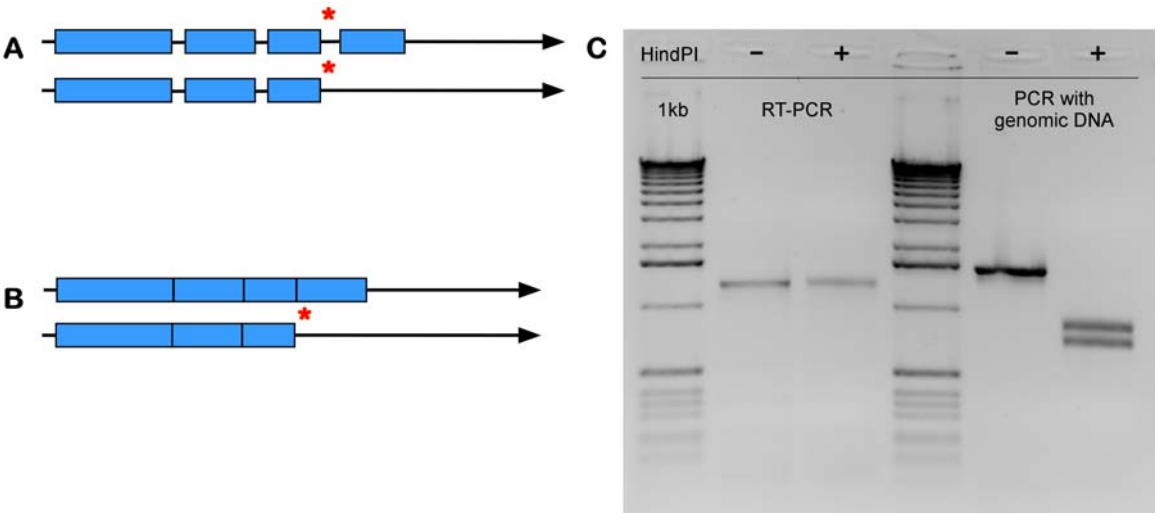

Figure 22. Investigation of an alternate 3' end.

(A) Genomic structure of the 3'end of *let-765*. The top product corresponds to cDNA results from this study; the bottom product represents the predicted gene model. A unique HindPI site is present in the intron between the 3rd and 4th exons (asterisk). **(B)** Schematic of the possible RT-PCR products that would be obtained from the two alternatively spliced genes as outlined in in A. The 3 exon product would still contain the HindPI site, and, as a result, would be expected to be recognized by the restriction endonucelase. **(C)** An agarose gel showing the digestion products of RT-PCR and genomic PCR products. The RT-PCR products are not digested by HindPI, suggesting that *let-765* spliced transcript is composed of 4 exons.

In addition, RT-PCR using an SL2 primer identified a further four exons at the 5' end that had been annotated as the upstream gene F20H11.6. Several attempts to identify a possible alternate start site at the 5' end of the F20H11.2 sequence using 5' RACE failed to generate any other transcripts. From this, it is likely that the *let-765* sequence encompasses all 15 exons. As a result of the upstream sequence being added to the existing F20H11.2 gene model, the mutation identified in *s2575* would be classified as an R>Stop, and better correlates the strong loss of function phenotype (Figure 23). Translation of the updated open reading frame results in a protein of 1866 amino acids in length.

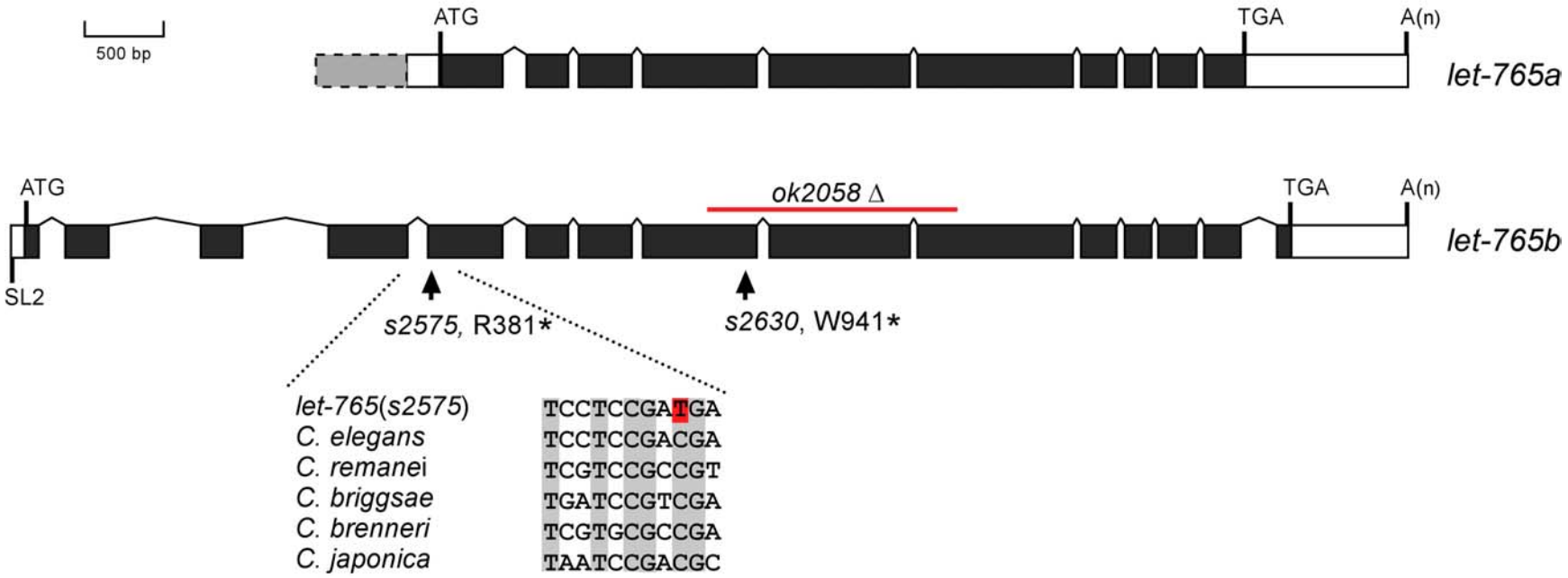

Figure 23. Schematic of *let-765* gene structure.

The Wormbase prediction(WS203) is labelled *let-765a* and the structure based on SL2 RT-PCR is marked *let-765b*. Exons are shown as black boxes, 3' and 5' untranslated regions are shown as white boxes. In *let-765a*, the predicted upstream gene is dashed and shaded grey. Translational start and stop sites and polyadenylation sites are indicated and the *s2575* and *s2630* mutations and *ok2058* deletion are shown. The *s2575* mutation affects a residue that is conserved among *Caenorhabditis* species. Image is to scale.

2.3.4 *let-765* encodes a protein from the DExD/H box helicase family

F20H11.2, also known as *notch signalling pathway homolog-1* (*nsh-1*), encodes a DExD/H box helicase (Cordin et al., 2004; Tanner and Linder, 2001) – a family of proteins defined by a set of characteristic motifs including the DExD/H box. LET-765 contains an Asp-Glu-Cys-His (DECH) in place of the signature DEAD box 'Walker B' motif and sequence searching using Pfam (Finn et al., 2008) and SMART (Schultz et al., 2000) databases identified a C-terminal helicase domain. Closer inspection of the protein sequence revealed that LET-765 shares with other helicase proteins nearly all of the conserved residues that are required for their enzymatic activity (Figure 24).

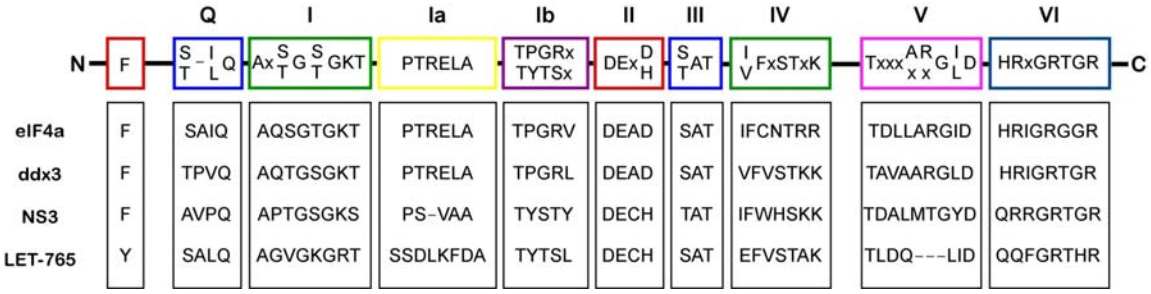

Figure 24. Consensus motifs of DExD/H box orthologs and LET-765.
Motifs I through VI are found in all DExD/H box proteins with some correlation between subgroups (note motif II and motif VI in DEAD versus DECH). The Q motif may function specifically in DEAD box proteins. Motifs (Q), I, II, and VI participate in nucleotide binding and hydrolysis, while Ia, IV, and V bind RNA. Adapted from (Cordin et al., 2006; Kwong et al., 2005).

let-765 is the *C. elegans* homolog of *strawberry notch* (sno) in *Drosophila melanogaster*, (41% identity) and of mammalian *strawberry notch homolog 1* (SBNO1) (44% identity); both are members of a novel family of DExD/H box proteins. It is well conserved with the *Drosophila* and human orthologs in the functional domains (Figure 25), with greater divergence at the terminal portions of the protein, as is typically found

when comparing DExD/H box orthologs (Cordin et al., 2006) (Full alignment Appendix C). BLAST searches revealed that mammalian genomes contain two *sno* homologs, while *Drosophila* and *C. elegans* have a single member. In addition, proteins from the *strawberry notch*-like gene family are found in plant and animal species, but yeast or bacterial homologs have not been identified, suggesting that they may be specific to multicellular organisms.

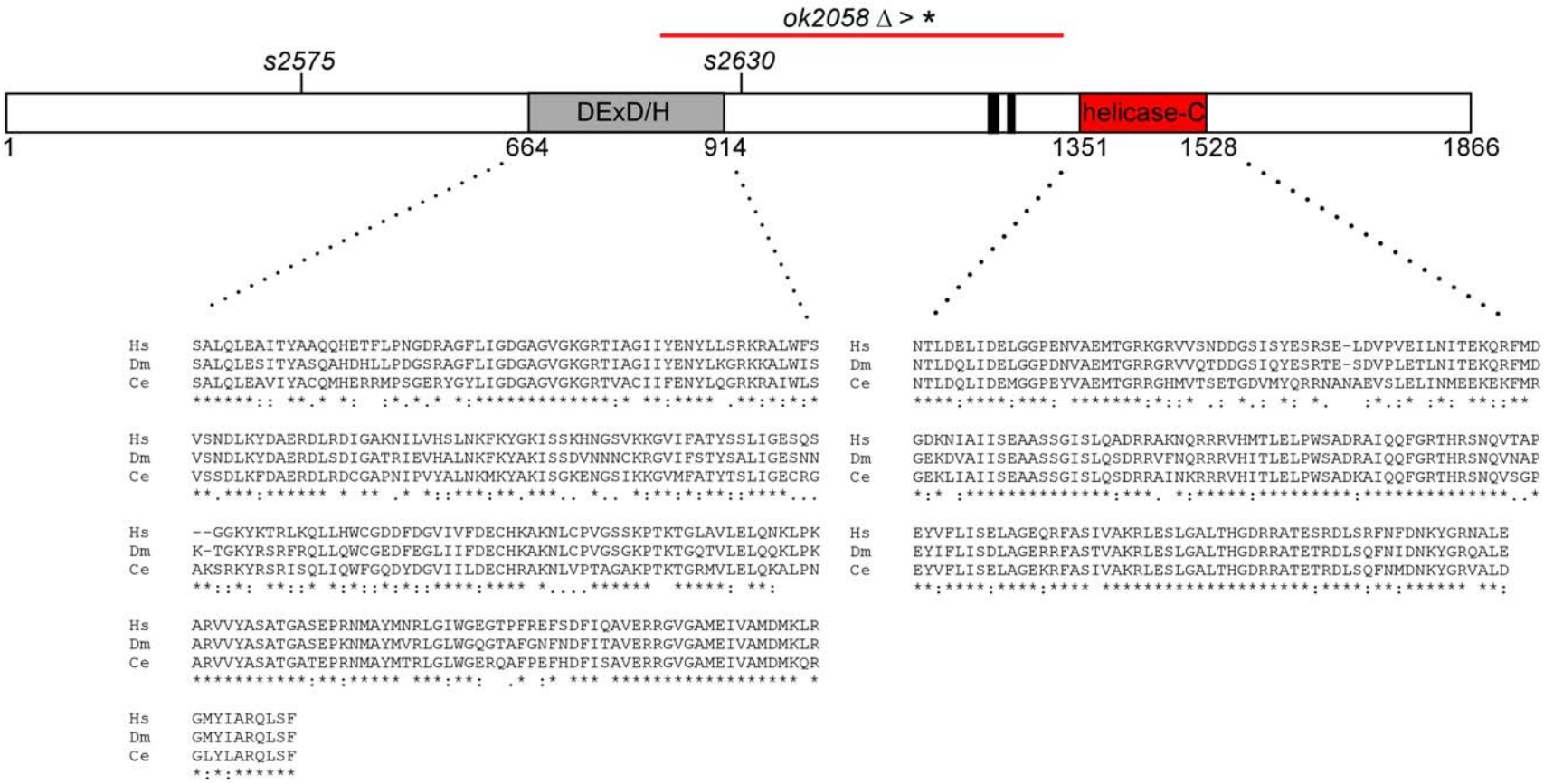

Figure 25. Schematic of the LET-765 domain structure.

The location of the DExD/H domain and helicase C-terminal domain are shown and the mutation sites marked. The nuclear localization sequences are indicated by black bars. Alignments demonstrate that the domains are well conserved between species: Hs (H.sapiens SBNO1), Dm (Drosophila sno), and Ce (LET-765).

2.4 Results Part II: Characterization of *let-765* expression

2.4.1 *let-765p:gfp* is expressed throughout larval development in multiple cell types

The updated gene model for *let-765*/*nsh-1* indicates that the promoter should lie upstream of the predicted gene F20H11.6. In order to observe the expression pattern of *let-765*, I generated a transcriptional reporter construct using 3 kb of sequence upstream of the F20H11.6 translational start site fused to a green fluorescent protein (GFP) sequence that contains a nuclear localization signal (nls). Expression of *let-765p::nls::gfp* (*sEx1800*) was observed in hypodermal cells, including the seam cells, in the excretory system, and in neurons in the head and tail. GFP was also strongly expressed in the somatic gonad from early in the L3 stage through the L4 stage (Figure 26).

Prior to the identification of the true 5' end of *let-765*, I designed a transcriptional reporter containing 376bp of sequence at the 5'end of F20H11.2 including the predicted upstream intergenic region and end of the neighbouring gene, F20H11.6. The *F20H11.2p*:*nls*:*gfp* transgene (*sIs1578*) was expressed throughout larval development in hypodermal-derived cells and neurons in the head and tail. A second, overlapping promoter fusion construct, *sIs15339*, generated by the *C. elegans* gene expression (CEII) project produced an identical expression pattern (Figure 27). The intensity and consistency of the hypodermal expression in animals carrying *sIs15339*, together with the overlap in expression pattern with the formal promoter, implied that the expression generated by the *sIs15339* construct may be genuine, however, when I used this 'promoter' sequence to drive expression of an F20H11.2 genomic clone, it failed to rescue the lethality of *let-765* alleles. This, together with the lack of 5' RACE evidence

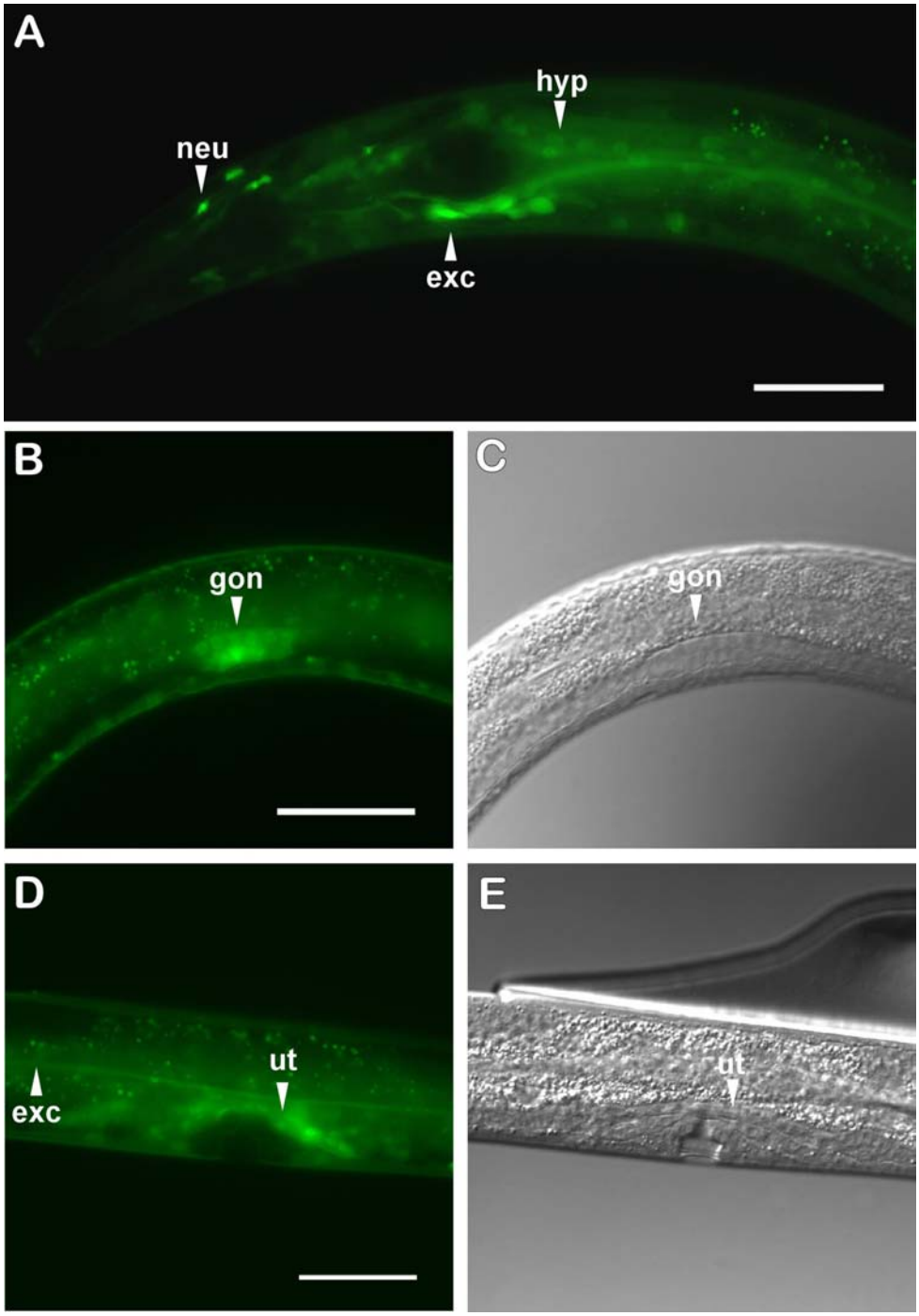

Figure 26. Transcriptional expression pattern of *let-765*.

Animals expressing a *let-765p::gfp* transgene (*sEx1800*), which contains 3 kb of gene regulatory sequence. GFP was visible in the hypodermis (hyp) and head neurons (neu) beginning in early larval stages **(A)** and throughout development. Expression was particularly strong in the excretory system (exc) in early larvae. Somatic gonad (gon) cells express GFP from the L2 stage **(B-C)** through to the L4 stage in the developing uterus (ut) **(D-E)**, until it fades in adult animals. Scale bar 25 µm.

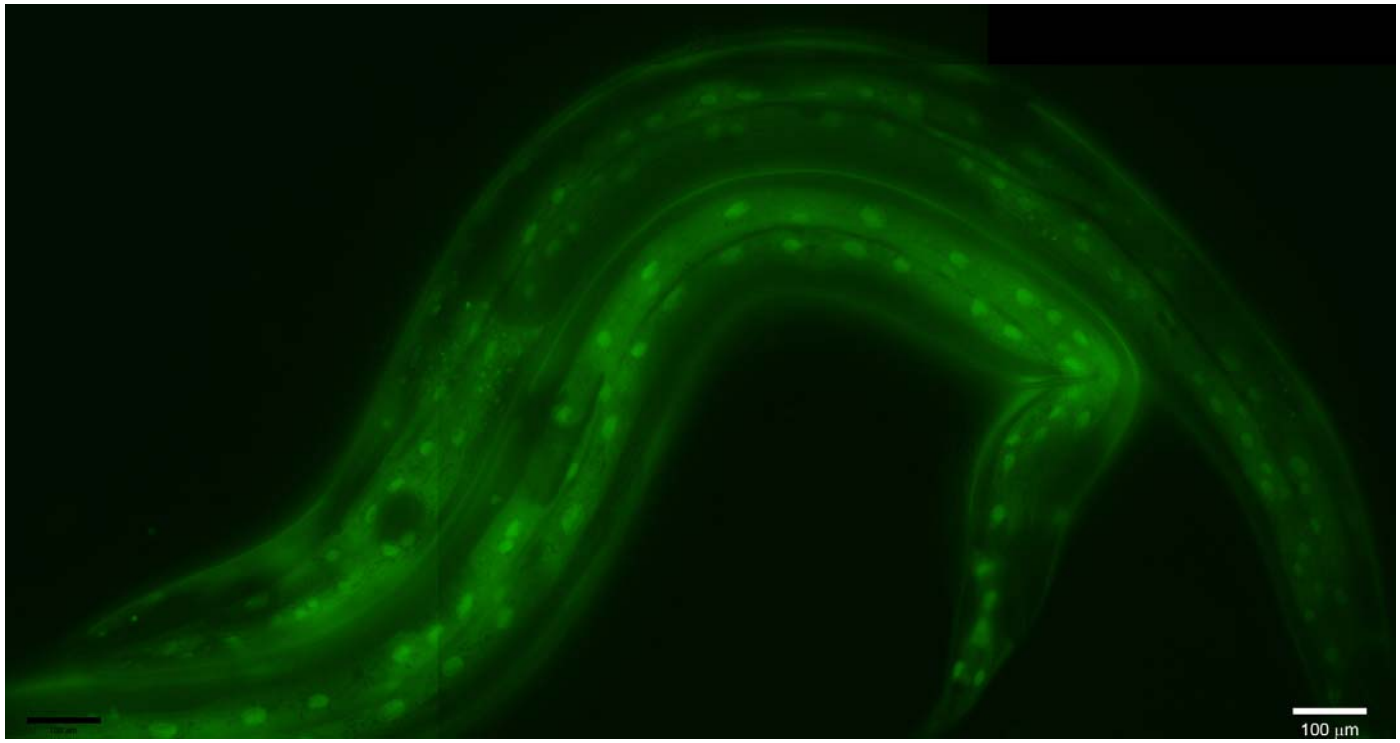

Figure 27. *sIs15339* is expressed in hypodermal cells

A GFP fusion construct made using the predicted intergenic region between F20H11.2 and F20H11.6 displayed hypodermal expression throughout post-embryonic development. Scale bar 100 µm.

for an alternate start site, suggests the *sIs15339* GFP expression is an artefactual result specific to the sequence used in these constructs. A summary of GFP reporter constructs is described in Figure 28.

2.4.2 A translational LET-765:GFP fusion construct is broadly expressed and nuclear-localized

To verify the complete pattern of gene expression, I used homologous recombination to insert a cassette containing the GFP coding sequence into the rescuing fosmid clone WRM0629dG03 at amino acid position 497. The resulting translational fusion construct, LET-765:GFP (*sIs1637*), is expressed in nearly all cells of the embryo from about the 100 cell stage. In larvae and adults, GFP is detectable in neurons, hypodermal cells and the seam cells, the excretory system, and intestinal cells (Figure 29). I noted expression in the vulval precursor cells and their descendents during mid-larval stages, and strong somatic gonad expression in early L3, similar to that seen in *sEx1800* animals. GFP expression was visible in the nucleus but restricted from the nucleolus in all expressing cells, consistent with a role in RNA metabolism or the regulation of gene expression.

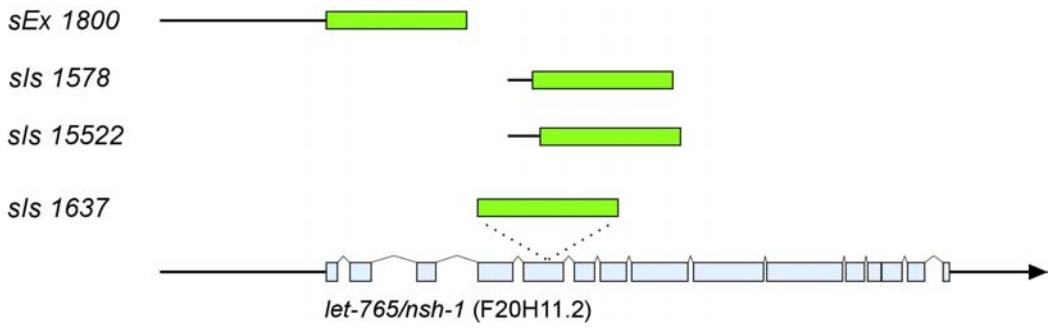

Figure 28. Summary of *let-765:gfp* reporter transgenes.

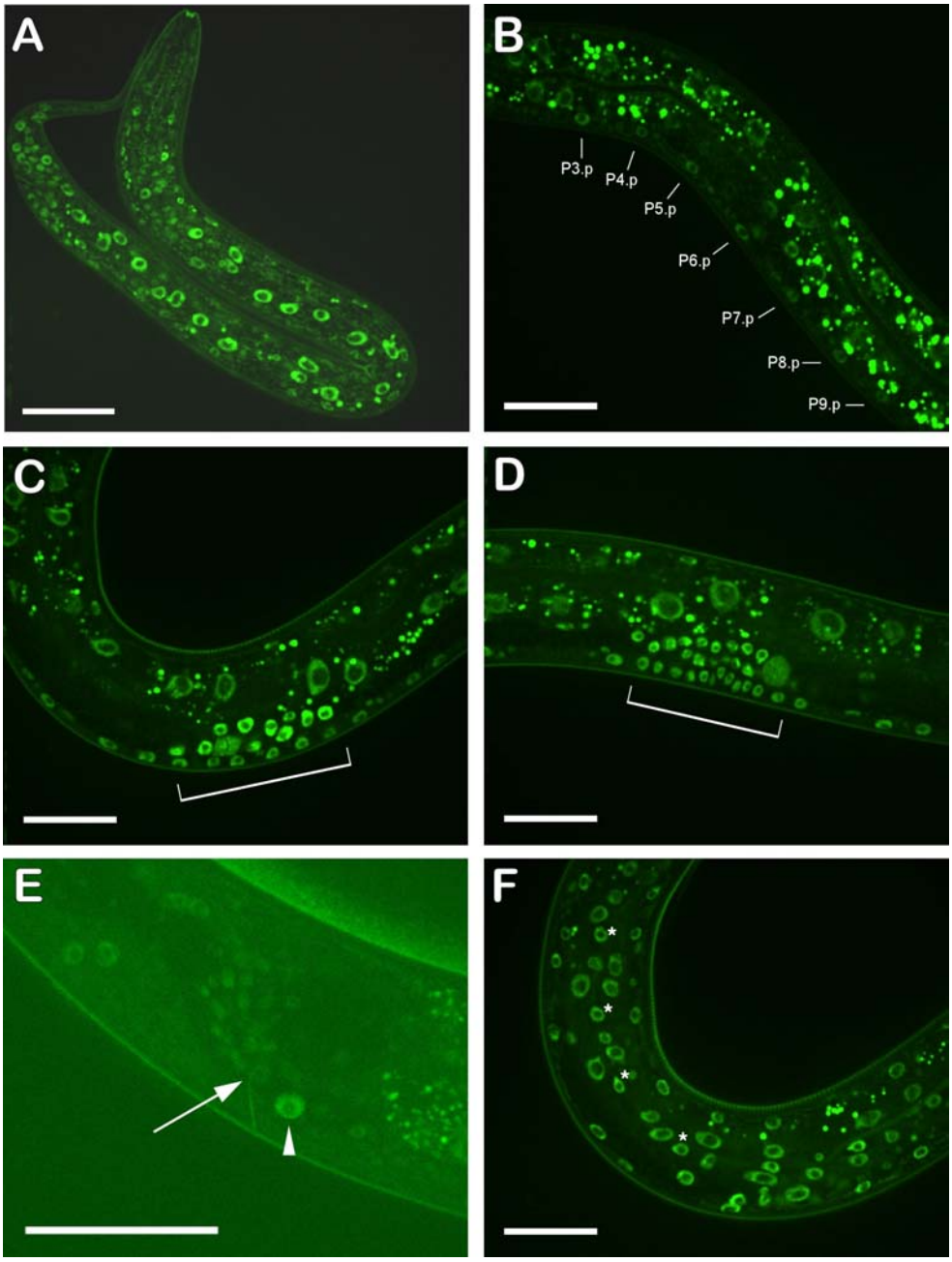

Figure 29. A LET-765::GFP translational fusion protein is broadly expressed.

Expression of the *sIs1637* transgene is strong in hypodermis and neurons from the L1 stage **(A)** through to adult **(F)**. GFP is visible in Pn.p cells at the L2 stage **(B)**. During the L3 stage expression is visible in the developing vuval cells and, more strongly, in the somatic gonad **(C-D)**. The excretory cell body (arrowhead) and excretory duct cell (arrow) express GFP throughout larval development **(E)**. The developing vulva and somatic gonad cells are bracketed in **(C-D)**. Seam cells in **(F)** are marked with asterisks. Gut granule autofluorescence is visible as strong foci in the midbody of animals in **B-D**. Scale bar 25 μm.

2.4.3 The germline and major hypodermis are essential sites for *let-765* activity

The fosmid:GFP transgene successfully rescued all three of the *let-765* alleles to a sterile adult, reflecting silencing of transgene activity in the germline; as the expression of multicopy transgenic DNA arrays is strongly suppressed in germ cell nuclei (Kelly et al., 1997). The notable lack of embryos or oocytes in the gonad implies that LET-765 may be required for normal development of the germline in addition to larval viability. Reducing *let-765* expression using RNAi also produced a sterile phenotype (see section 3.3.2), providing further support for a role in germline development and /or maintenance.

Since hypodermal expression was prominent in both the transcriptional and translational reporter transgenes, I suspected that *let-765* activity might be of particular importance in these cells. To test this hypothesis, I used a hypodermal specific promoter, *dpy-7*(-338 to -122), to drive expression of an F20H11.2 genomic clone (Bulow et al., 2004; Gilleard et al., 1997). The transgene was able to rescue the larval arrest phenotype of animals homozygous for either *s2575* or *ok2058*, indicating that the hypodermis is an essential site of *let-765* activity. Rescued animals that reached adulthood were sterile and exhibited a protruding vulva phenotype, consistent with a role for LET-765 in cells other than the hypodermis to promote vulval or uterine morphogenesis. Together, these results demonstrate that *let-765* expression in the hypodermis and germline supports larval viability and fertility respectively.

In order to provide temporally controlled rescue, I generated heat shock inducible constructs consisting of the F20H11.2 genomic clone driven by the *hsp 16-2* and *hsp 16-41* promoters. Several transgenic lines were obtained and, in all cases, animals were sick and slightly dumpy in appearance. Upon heat shock, these phenotypes worsened and the

strains became inviable, preventing an opportunity to test for rescue. The detrimental effects of overexpression suggest that *let-765* activity is tightly regulated. The low level of expression seen in our qRT-PCR data (section 3.3.4) and that relatively few ESTs that have been isolated for the gene (WS203) add further support to this proposal.

2.4.4 *let-765* mRNA is detectable at all stages of development and is enriched in the germline

To investigate the temporal expression of *let-765*, RNA was isolated from developmentally staged wild type worms and used in real time RT-PCR reactions. *let-765* is expressed throughout the life cycle, suggesting that it is required for multiple developmental processes. The level of *let-765* mRNA was significantly higher in young adults and embryos, supporting a role for *let-765* in germline development and embryogenesis, and the lowest levels of transcript were observed in total RNA from L1/L2 stage animals. The relative abundance of *let-765* transcript at each developmental stage is shown in Figure 30.

To confirm that the level of *let-765* transcript is enriched in the germline, I assayed *let-765* expression in *glp-4(bn2)* adults compared to wild type. When raised at the restrictive temperature, *glp-4* hermaphrodites fail to produce a germline. qRT-PCR analysis revealed that there is >10 fold more *let-765* transcript in samples from wild-type young adults when compared to samples from *glp-4* young adults (Figure 31). This result not only supports the suggestion that *let-765* is maternally contributed to the embryo, but also that germline development requires LET-765 function. This is consistent with results from the staged qRT-PCR experiments and with reported RNA in situ

hybridization data (NextDB – http://nematode.lab.nig.ac.jp/db2/index.php) which revealed strong germline expression.

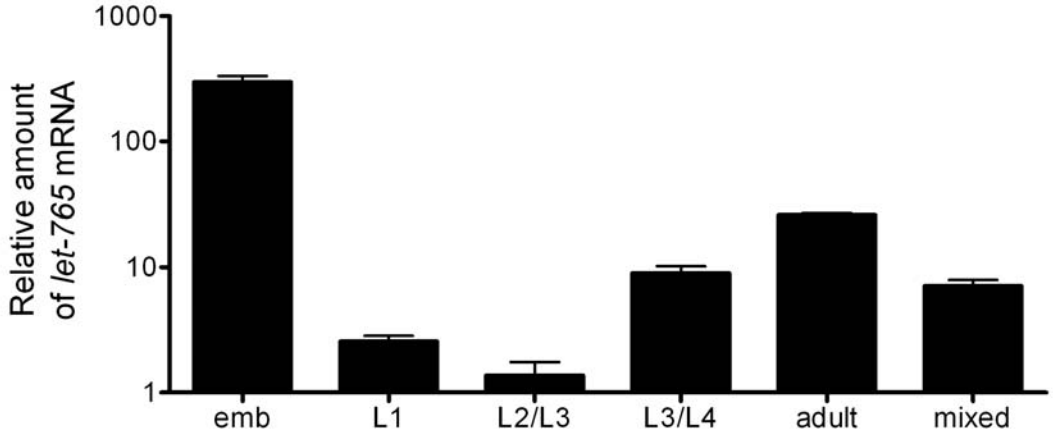

Figure 30. The level of *let-765* mRNA varies across developmental stages.

The level of *let-765* transcripts was analyzed by real-time RT-PCR using total RNA from staged populations of wild-type worms. Transcript levels are significantly enriched in embryos, consistent with the expectation that it is expressed in the germline and plays a role in embryonic development. Increased abundance in late larval and adult stages correlates with development of the germline. *rpl-19* was used as an internal reference. Mean values and standard deviations for relative *let-765/rpl-19* ratios from three replicates are shown

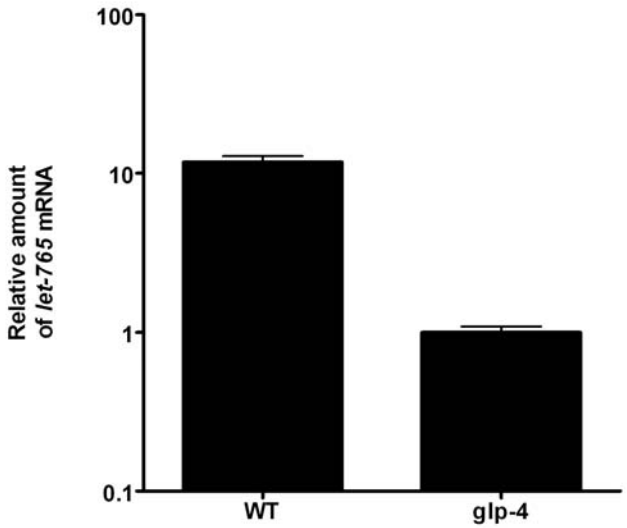

Figure 31. Relative abundance of *let-765* mRNA is decreased in hermaphrodites without a germline.

Total RNA from young adult wild type and *glp-4* animals was used for real-time RT-PCR reactions. The level of *let-765* transcript is more than 10-fold enriched in animals that develop a germline, compared to animals that do not. This supports a role for LET-765 in germline development and is consistent with staged real-time RT-PCR experiments. *rpl-19* was used as an internal reference. Mean values and standard deviations of relative *let-765/rpl-19* ratios from three replicates are shown.

2.4.5 ATPase assay using recombinant LET-765

DExD/H box proteins possess motifs that are involved in binding and hydrolyzing ATP in order to generate energy for nucleic acid unwinding and /or disrupting protein-nucleic acid interactions. Since LET-765 shares these conserved elements with DExD/H box proteins, I prepared bacterially expressed LET-765 protein in order to investigate its enzymatic activity. I designed a fusion protein containing the predicted functional domains of LET-765, from amino acid position 626 to 1542, fused to glutathione-S-transferase (GST). The purified protein was used to assay for ATPase activity. Interestingly, the fusion protein was found to hydrolyze ATP but not GTP, albeit in an RNA independent manner (Figure 32). As a control, purified GST was found not to support this activity.

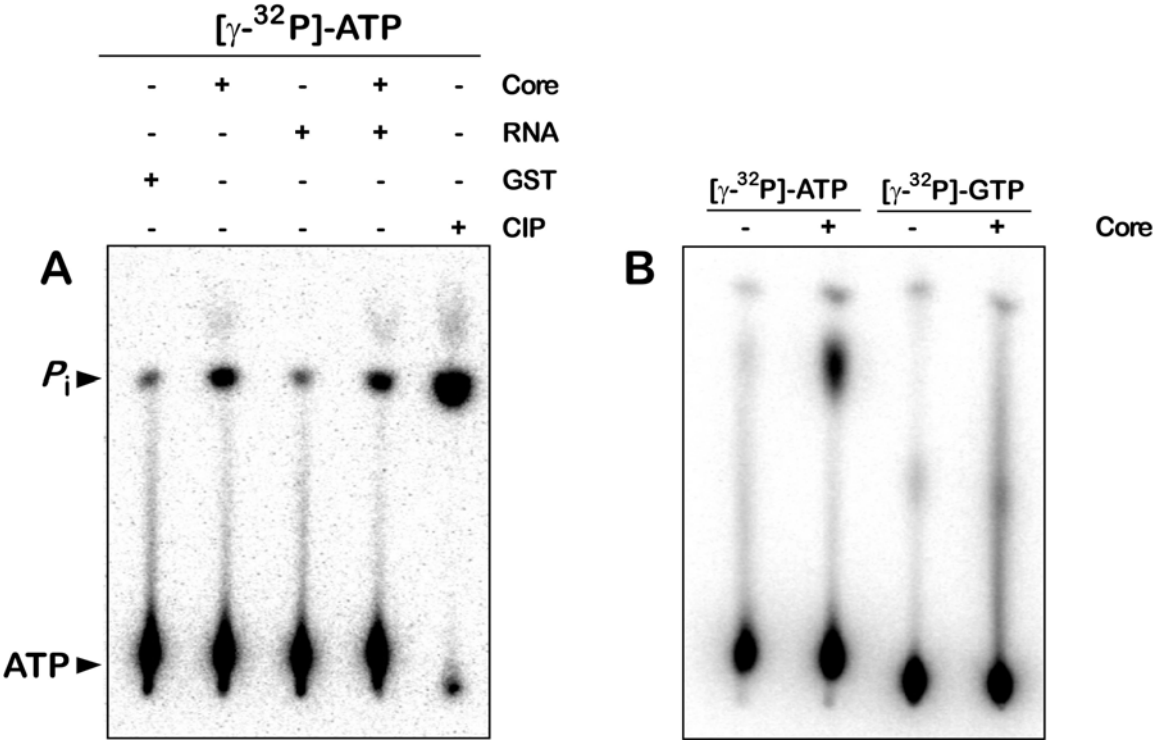

Figure 32. The enzymatic core residues of LET-765 exhibit ATPase activity.

(A) Recombinant LET-765 protein consisting of the core enzymatic residues was incubated in the presence of radio-labelled ATP, with and without RNA (CORE = amino acids 626 to 1542). The hydrolysis of ATP was increased in CORE samples relative to GST control, although the addition of RNA did not have a noticeable effect. CIP activity provided a positive control. **(B)** The CORE protein specifically hydrolyses ATP and not GTP.

CHAPTER 3: AN ANALYSIS OF *let-765* MUTATIONS AND REDUCTION OF FUNCTION PHENOTYPES

3.1 Introduction

The *C. elegans* model organism possesses several characteristics that make it particularly well suited for studying the development of cells and tissues. Aside from the low cost and ease of maintenance in the laboratory, it is well established as a genetic model system, such that ample genetic tools are available including duplications, balancers, and deletions as companions to an array of mutant strains. In addition, the existence of hermaphrodite and male sexes provides an opportunity to establish clonal lines, as well as a means for outcrossing. It has a relatively simple body plan that is generated by an essentially invariant cell lineage, enabling the identification of cell division or lineage defects. Furthermore, it is completely transparent, allowing visualization of internal structures in a live animal. This, in turn, has led to the use of fluorescent reporters as the method of choice for studying gene expression, protein localization, identifying cis-regulatory elements, and as markers to track specific cells or tissues (Chalfie et al., 1994; Mah et al., 2007).

In addition to traditional forward genetic methods, the discovery that the presence of dsRNA can lead to specific degradation of the corresponding mRNA prompted the development of RNAi (Fire et al., 1998). This technique permits a reverse genetic approach that targets the gene of interest and produces a transient knockdown of the gene's activity without altering the chromosomal DNA. There are three methods to

introduce dsRNA into the worm: injection of *in vitro* transcribed dsRNA, which provides the most effective knockdown of gene function, by soaking in a solution of dsRNA, or by feeding the worms bacteria that express dsRNA (Fire et al., 1998; Tabara et al., 1998; Timmons and Fire, 1998). RNAi by feeding is the most efficient and can be scaled up for highthroughput screening, but produces the highest variability of phenotypes. Finally, dsRNA can be delivered in a tissue specific manner using a plasmid construct that, when transcribed, generates a dsRNA hairpin expressed in a promoter-specific context (Timmons et al., 2003).

Although RNAi usually produces a phenotype in wild type animals, some tissues, most notably neurons and possibly the hypodermis, are resistant to standard methods. Experiments using the RNAi hypersensitive strains *rrf-3*, *eri-1*, and *eri-1; lin-15B*, can generate stronger, and sometimes additional, phenotypes than those seen in wild type (Kennedy et al., 2004; Simmer et al., 2002; Wang et al., 2005). In this study, I have used *rrf-3(pk1426)* to examine RNAi phenotypes using a feeding strategy targeting *let-765*. I found that the penetrance of larval lethality and sterility was considerably higher than when using wild type.

In this section, I describe the phenotypic characterization of animals with a loss or reduction of *let-765* function. I find that mutations in *let-765* confer an early larval lethal phenotype that is associated with excretory system defects and a loss of excretory duct morphology. RNAi against the gene produces pleiotropic phenotypes that include vulval defects and a variety of male tail phenotypes. I use fluorescent reporters to assess affected tissues in order to aid in determining the source of the defects. Many of the

phenotypes resemble those caused by mutations in RAS pathway genes, suggesting a convergence of activity between LET-765 and RAS signalling.

3.2 Materials and methods

3.2.1 RNAi

3.2.1.1 Preparation of dsRNA for injection

dsRNA for injection was prepared using the method and primer sequences as described in (Gonczy et al., 2000). PCR products targeting F20H11.2 that contained T3 and T7 sites at the 5' and 3' ends were produced by PCR amplification using genomic DNA. Single stranded RNA was transcribed using the Ambion MEGAscript T3/T7 kit as per manufacturer's instructions. Products of the T3 and T7 reactions were purified, combined and annealed by heating to 68°C for 10 min and 37°C for 30 min to obtain dsRNA. Single and double stranded RNAs were analyzed by electrophoresis before injecting wild-type worms.

3.2.1.2 RNAi by feeding

RNAi by feeding was performed as described in (Kamath et al., 2003) with the following modifications: worms were grown on NGM lite plates containing 50 µg/mL carbenicillian, 12.5 µg/mL tetracycline and 4 mM IPTG. L4 animals were plated on HT115 bacteria expressing F20H11.2 dsRNA or empty vector control (pPD129.36) and incubated at 23°C for 24-30 hours. P_0 hermaphrodites were removed and progeny were allowed to develop. Experiments were repeated a minimum of two times to confirm phenotypic results.

3.2.1.3 Tissue specific RNAi

The hypodermal expression hairpin construct was built starting with the *dpy-7p::gfp* plasmid (from section 2.2.10). A 728 bp fragment of the *let-765* genomic sequence was PCR amplified using primers containing appropriate restriction sites and the product cloned into SalI-BamHI digested *dpy-7p::gfp*. The ligation product was transformed, miniprepped and the insertion confirmed by restriction digest and sequencing, producing *dpy-7p*::SB. The same region was then amplified with a second set of primers and the product cloned into NcoI-XhoI digested *dpy-7p*::SB. The resulting clone, *dpy-7*p::hp, contains pair of inverted *let-765* sequences (sense and antisense) separated by a short region of GFP sequence. Primers are listed in Appendix B.

3.2.2 Scoring larval arrest in RNAi treated animals

Arrested rod-like lethal progeny of RNAi treated hermaphrodites were scored by allowing mothers to lay eggs for 24–30 hours. L1 arrested animals were counted and removed. Plates were scored every 24 hours for 4 days.

3.2.3 Crossing fluorescent markers into *let-765* alleles

Hermaphrodites carrying an integrated transgene were crossed to N2 males. Heterozygous males were then crossed to *hT2*-balanced *let-765* hermaphrodites. Progeny were sib-mated – *hT2* males crossed to non-*hT2* hermaphrodites (*let-765* heterozygotes). Individual *hT2* hermphrodites that expressed the transgene were selected and lines that gave no surviving non-*hT2* progeny were kept. A line that exhibited homozygosity for the marker was selected for further investigation.

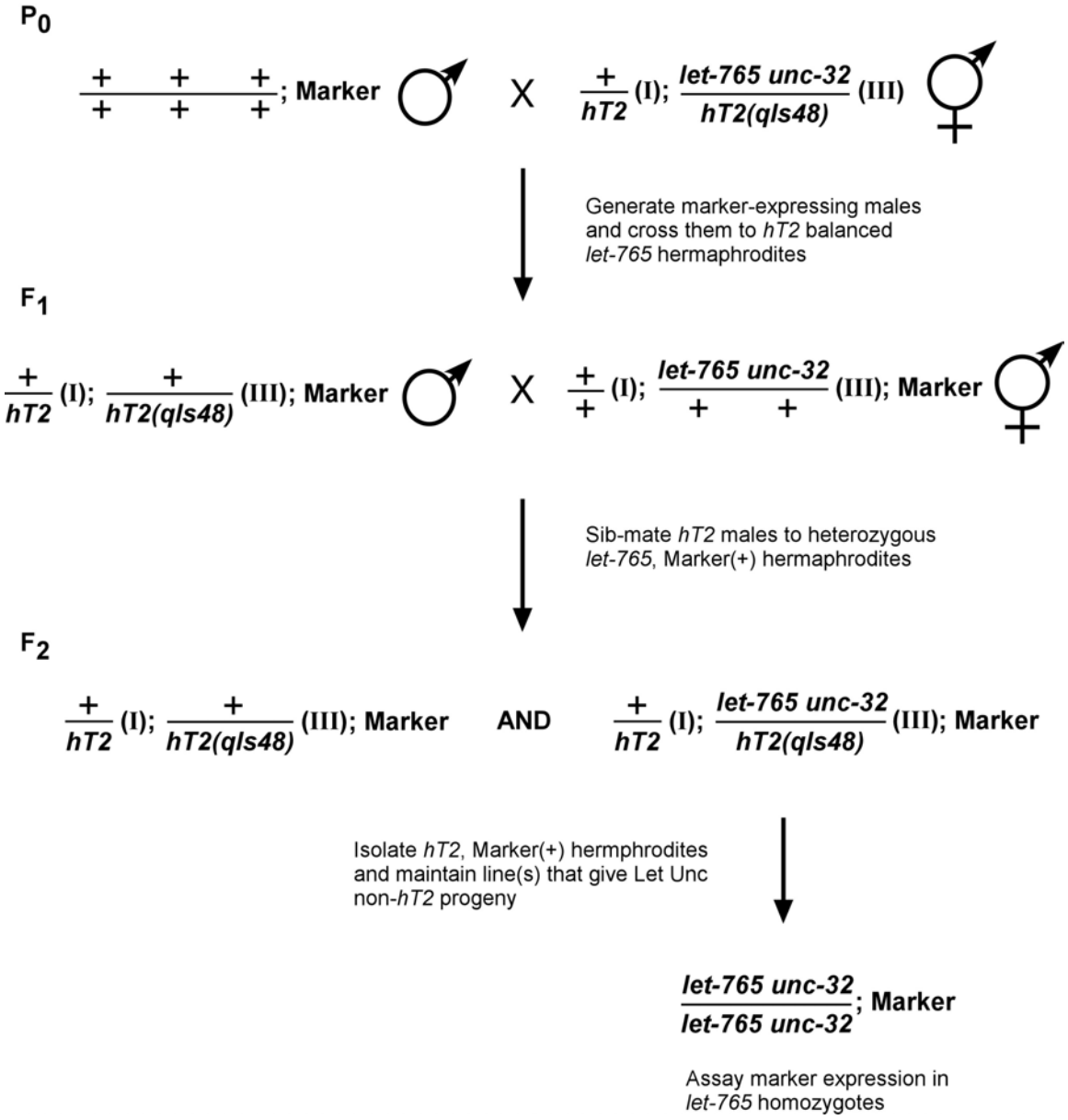

Figure 33. Cross scheme for introducing a fluorescent reporter transgene into *hT2*-balanced *let-765* strains.

3.2.4 Dye filling

Worms were washed off plates containing *hT2* balanced heterozygotes and homozygous *let-765* animals. After washing 3 times with M9, worms were incubated overnight in 10 μg/mL 1,1-dioctadecyl-3,3,3,3-tetramethylindocarbocyanin (DiI) in M9 before washing 2-3 times in M9 and plating on NGM plates for scoring. Worms used for images were rocked in M9 for 20 minutes to flush excess dye from the gut and mounted in a drop of 2 mM levamisole on 2% agarose.

3.2.5 Microscopy

Microscopy was performed as in section 2.2.13.

3.3 Results

3.3.1 *let-765* animals arrest at an early larval stage

To gain insight into *let-765* function, I began by examining the phenotype of *let-765* mutant animals. Hermaphrodites homozygous for either *s2630* or *ok2058* arrest near the L1/L2 molt, while *s2575* animals survive slightly longer, arresting during the L2 stage. Homozygous mutant animals subsist for several days after arrest, but nearly all develop a rod-like morphology similar in appearance to animals with a reduction in RAS pathway activity (Sternberg and Han, 1998; Sundaram, 2006), although the *s2575* and *s2630* alleles exhibit less severe morphological defects, perhaps due to a synergistic effect from the linked *unc-32(e189)* mutation (Figure 34). The *let-765* larval arrest phenotype is fully penetrant and recessive, and placing *s2630* or *ok2058* over the deficiency *sDf125* did not affect the timing of arrest, indicating that these two alleles severely reduce, if not eliminate *let-765* function. From this, I concluded that the *let-765*

null phenotype is larval arrest near the L1/L2 molt when zygotic activity is lost and animals obtain a wild-type maternal contribution.

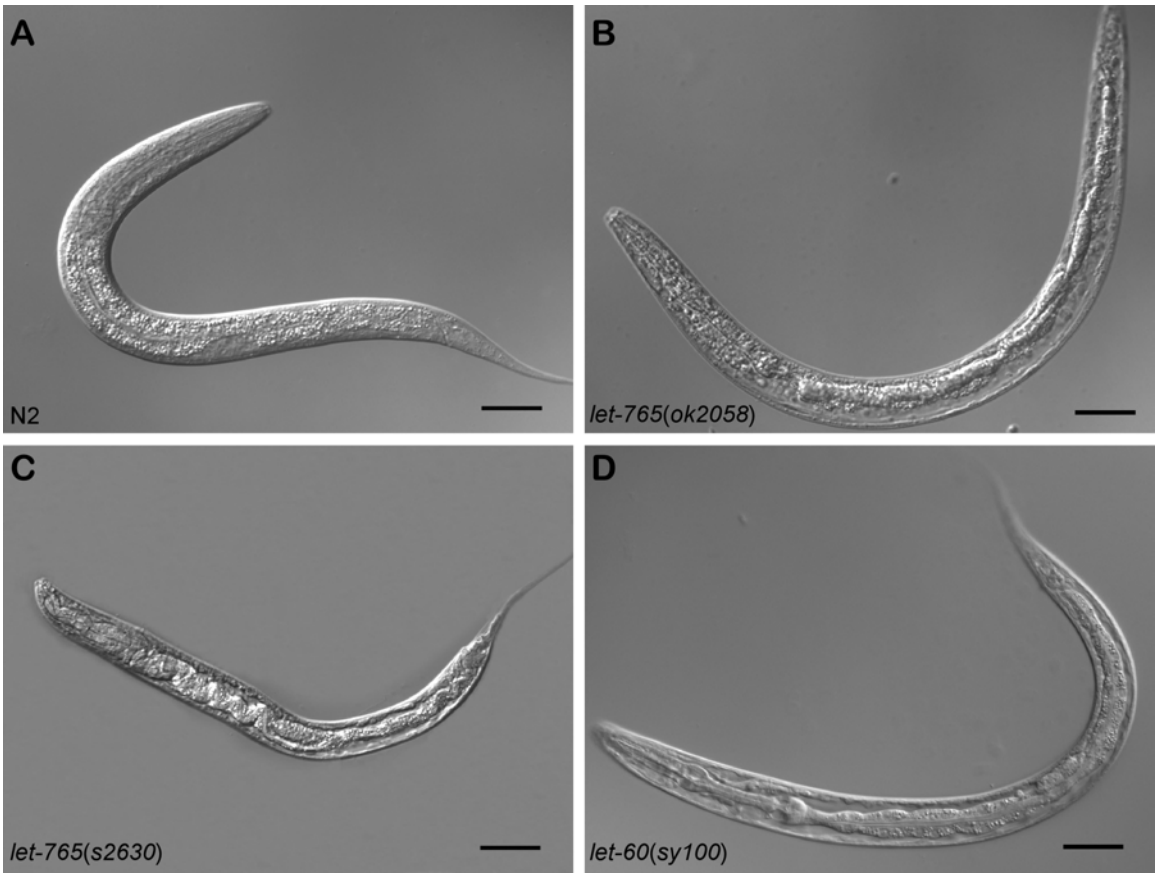

Figure 34. *let-765* animals exhibit early larval arrest with a RAS-like phenotype. When compared to early L2 stage wild-type animals **(A)**, *let-765* larvae exhibit L2 arrest with osmoregulation defects **(B,C)** that resemble those seen in *let-60*/RAS null mutants **(D)**. Scale bar: 25 μm.

3.3.2 Reducing the level of *let-765* expression leads to pleiotropic phenotypes

Since the larval lethality of *let-765* mutants precluded observation of later developmental stages, I used RNAi by feeding to assess a reduction-of-function (*rf*) phenotype (Kamath et al., 2003; Timmons et al., 2003). As RNAi by injection had

resulted in some embryonic lethal progeny and a lack of any post-embryonic phenotypes, I chose to use a feeding strategy rather than injection in further assays.

Experiments using the RNAi-hypersensitive strain *rrf-3*(*pk1426*) (Simmer et al., 2003) resulted in a significant proportion of rod-like lethal progeny (46%; n=183). Animals that survived exhibited slow growth, gonad migration defects, and a protruding vulva (Pvl) phenotype (Figure 35C). In addition, nearly all animals that developed to adulthood were sterile, with only rare cases (< 5%) of embryos present in the uterus.

A Pvl phenotype can be caused by any one of a number of defects in cell specification or morphogenesis, but I began with the suggestion that *let-765* might be required for vulval development. To investigate the possibility that *let-765*(RNAi) may lead to reduced vulval induction, I examined the vulval cell lineage in early L4 stage animals. I found that 30% of the animals displayed less than wild-type induction (n=27), with an average of 1.1 vulval cells induced in these animals compared to 3.0 in wild type. This suggests that, in wild type animals, *let-765* functions to promote vulval induction.

In addition, the Pvl phenotype was nearly fully penetrant however, the disrupted migration of the gonad arms often led to crowding of the uterine cells, which could account for a failure in vulval-uterine morphogenesis. Signalling between the anchor cell and developing uterus is required to specify the π cells, which will form part of the vulval-uterine connection (Newman et al., 1995). A marker for the π cells, the transcription factor *lin-11*, was usually expressed in *let-765*(RNAi) treated animals, although there were rare cases where the signal was lost (Figure 36) (Newman et al., 1999). A loss of pi cell specification could lead to morphogenetic defects and a Pvl phenotype.

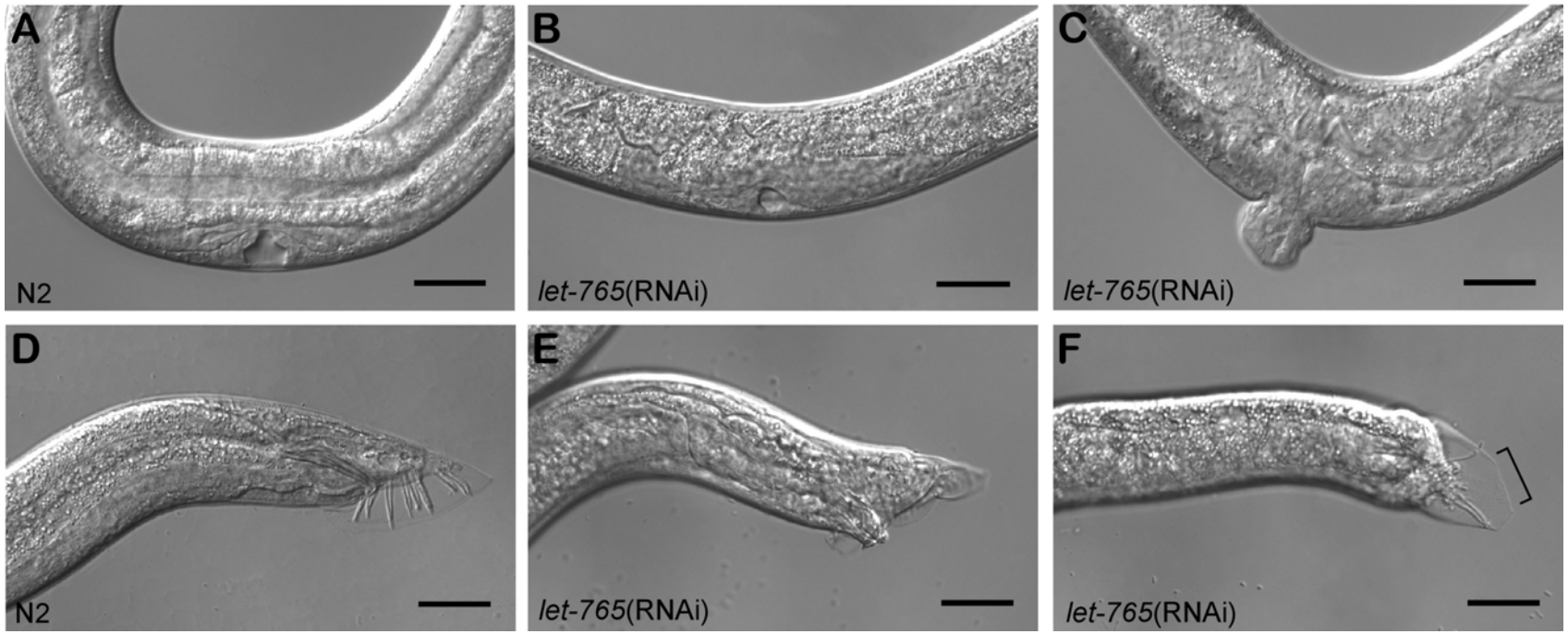

Figure 35. *let-765*(RNAi) produces defects in vulval development and male tail development.

(A-B) Nomarski images of vulval development in L4 stage hermaphrodites. **(A)** Wild-type vulval cells with a typical division pattern. **(B)** *let-765*(RNAi) treated larva with a hypo-induced phenotype. **(C)** Adult *let-765*(RNAi) treated animal with a protruding vulva phenotype. **(D-F)** Adult male tails. **(D)** Wild-type adult male. **(E-F)** Males with a reduction of *let-765* function exhibit multiple tail defects including shortened spicules **(E)** and missing rays **(F)**. Animal in **(F)** is facing ventrally with the location of missing rays bracketed. Scale bar: 25 μm.

let-765(RNAi) treated males had variable tail defects including underdeveloped club-like tails, spicule defects, and missing rays (Figure 35, D-F). This, together with reduced vulval induction and the early larval arrest phenotype, strongly resemble those seen in animals with compromised RAS pathway activity and suggest that *let-765* may function in cooperation with the RAS pathway to promote development and viability.

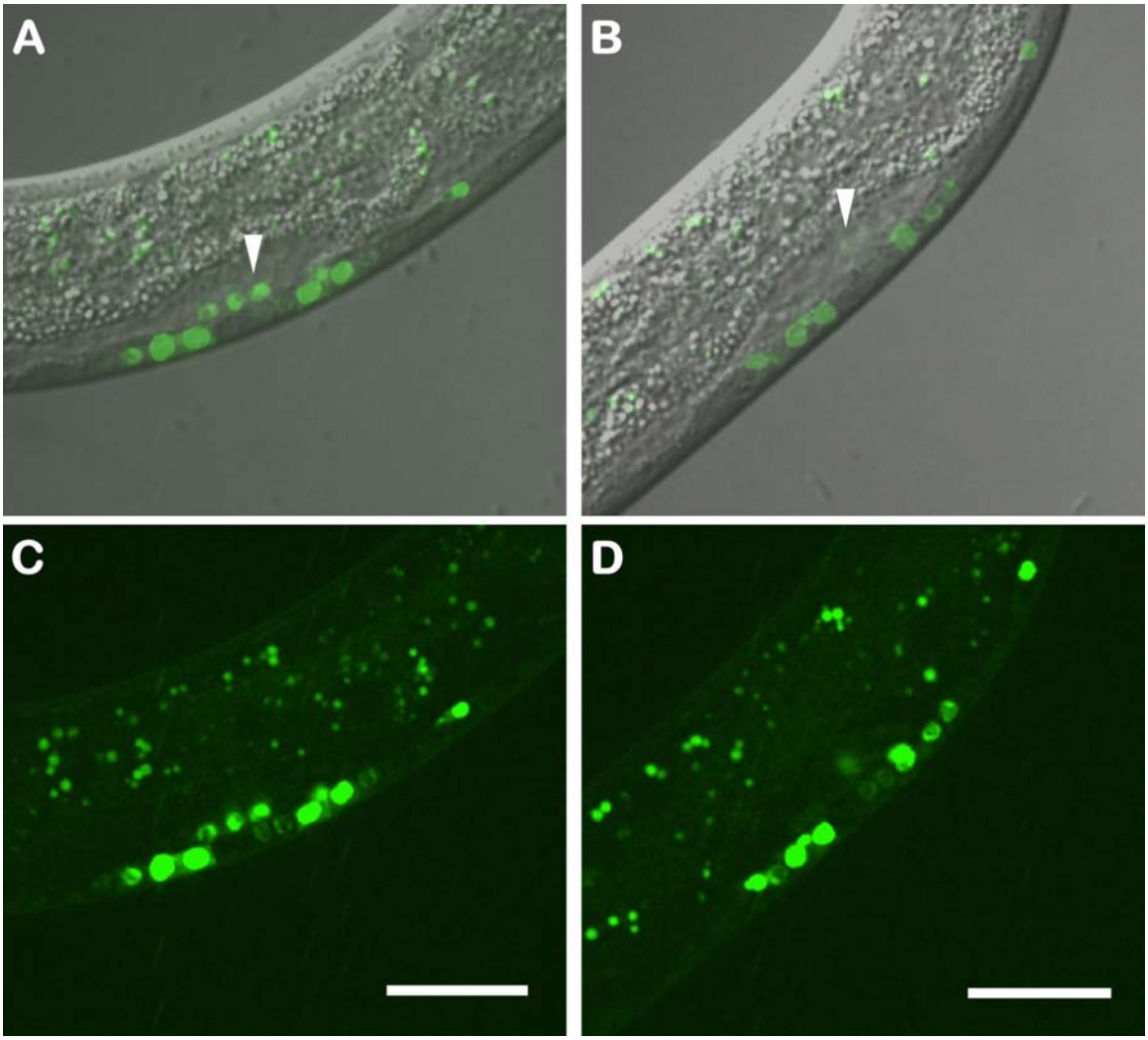

Figure 36. Expression of a π cell marker in *let-765*(RNAi) animals.

Animals expressing a *lin-11::gfp* transgene (*syIs103*) were raised on *let-765*(RNAi) plates. Many animals exhibited wild-type GFP expression at the L3 stage **(A,C)**. There were rare instances where animals had lost expression in the π cells, but not in the vulval cells that had acquired a 2° fate. **(B,D)** Arrowhead marks the developing π cells. Top panels are merged GFP and Nomarski images. Scale bar: 25 μm.

3.3.3 Larval arrest in *let-765* animals is associated with excretory system defects

Animals with a loss or reduction of *let-765* function exhibit morphology that suggests defects in osmoregulation, specifically a rod-like posture and fluid filled body cavity. This phenotype is seen in loss of function mutants of core RAS pathway components where it is thought to result from a failure to specify the excretory duct cell (Sundaram, 2006; Yochem et al., 1997). The excretory duct functions to connect the excretory cell body, which provides the main osmoregulatory function in the nematode, to the pore cell and the external environment. To investigate whether the phenotype exhibited by *let-765* mutant animals is caused by duct cell loss, I assayed expression of a cell-specific marker, *lin-48*::*gfp* (*saIs14*) (Johnson et al., 2001). 10% of dying *ok2058* homozygotes (n=35) were lacking duct cell expression, suggesting that the cell was missing. This phenotype has also been observed in *let-60* null mutants (Tiensuu et al., 2005). The remainder of *ok2058* L1 larvae examined did express GFP upon arrest although, in these animals, the duct cell and the excretory cell display abnormal morphology. The excretory duct cell body is present, but the duct is missing or tracks away from the body wall (Figure 37). It is possible that *let-765* is required for duct cell specification, but in some *let-765* mutants, the maternal contribution is sufficient to partially rescue defects in the duct cell; alternatively, *let-765* activity may contribute to the functional properties of the duct cell or excretory system.

To further examine the development of the excretory system, I used a transcriptional reporter, *pgp-12*::*rfp,* to visualize the excretory cell body and canals (Zhao et al., 2005). The cell body is located on the ventral side of the animal, just anterior to the second pharyngeal bulb. Four canals extend outward from the cell body,

Figure 37. *let-765* animals display defects in excretory duct cell morphology.
The excretory duct cell body can be visualized using the cell-specific marker *lin-48::gfp* (*saIs14*), which expresses in the duct cell and amphid neurons. In wild type, the duct itself (du) can be seen curving away from the cell body towards the body wall of the animal **(A,C)**. The position of the duct cell body is marked with an arrowhead. Some *let-765(ok2058)* animals exhibit a loss of the duct cell **(B, D)**. Many *let-765(ok2058)* animals appear to have generated a duct cell, but the duct process does not extend to the body wall. Instead it tracks away from the wall or down the body **(E-G)**. Expression in the amphid neurons is not affected by mutations in *let-765*. Scale bars are 25 um. **(A, B**, **E**, **F)** are Nomarski images merged with the GFP images in **(C**, **D**, **G**, **H)**.

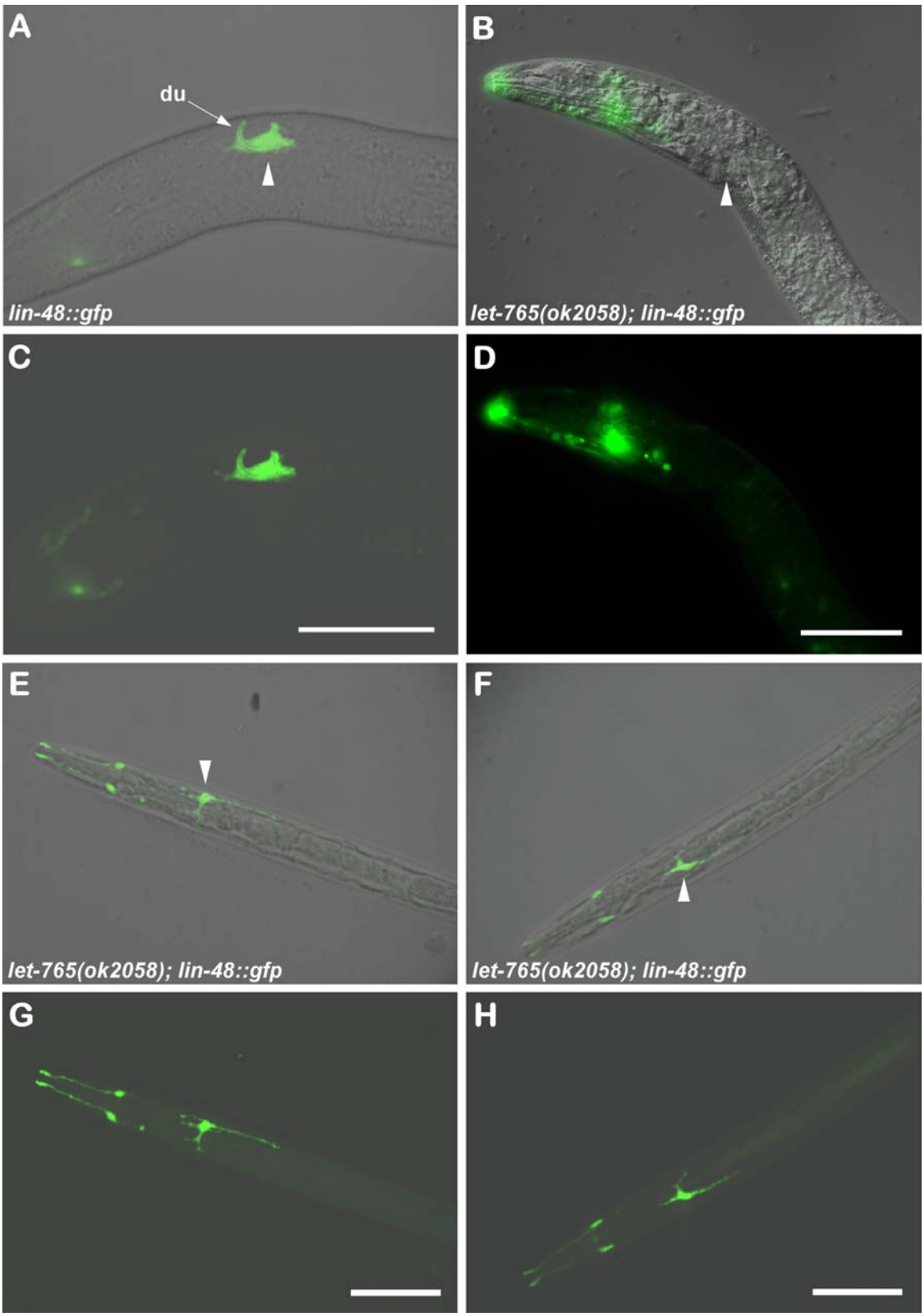
A
du
lin-48::gfp
B
let-765(ok2058); lin-48::gfp
C
D
E
let-765(ok2058); lin-48::gfp
F
let-765(ok2058); lin-48::gfp
G
H

two to the anterior and two to the posterior, such that they form an H shape that runs the length of the animal. When the excretory system was examined in *let-765* mutants, the canals were extended but had a jagged appearance and the lumen of the canals was fuller than in wild type. Furthermore, in 38% of animals observed (n=15), branching occurred at the posterior termini of the canals. In all animals, the excretory cell body was misshapen when compared to wild type, where it has a rounded appearance (Figure 38). These phenotypes hint at a regulatory role for *let-765* in the development of this system beyond its potential effect on the RAS pathway.

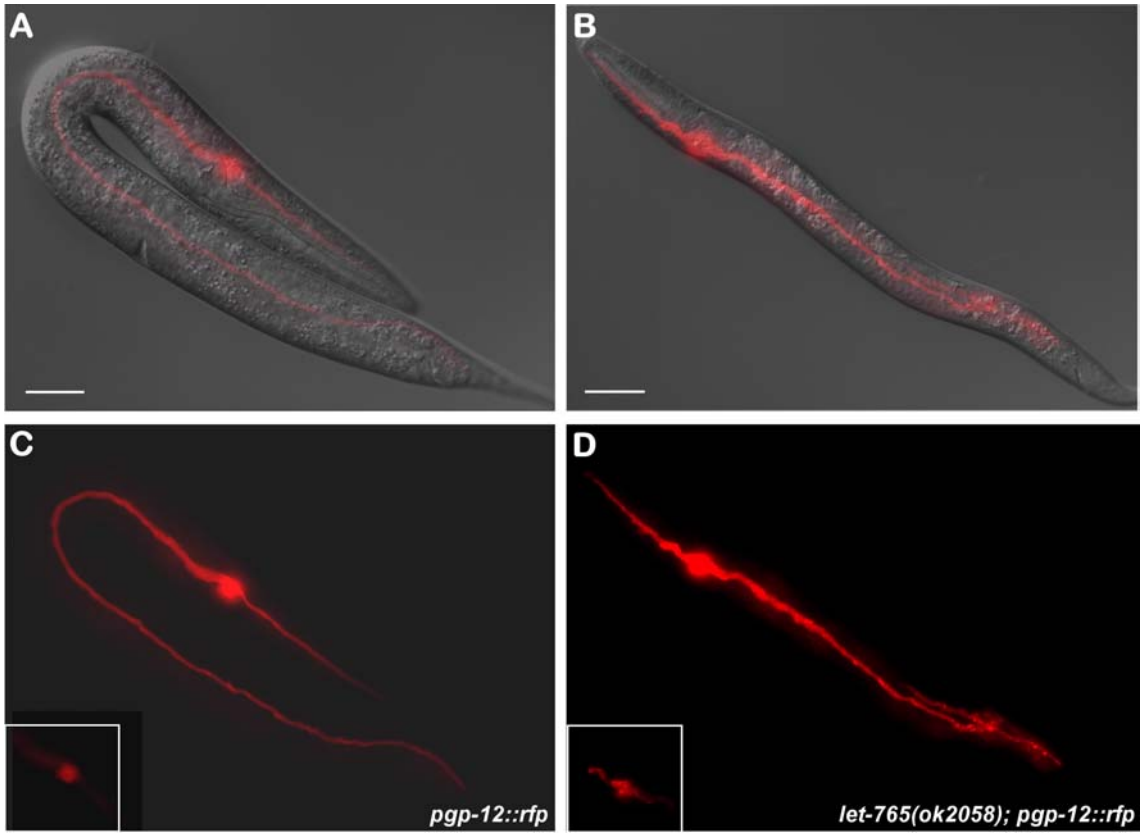

Figure 38. Excretory canal defects in *let-765*(*ok2058*) animals.

Visualization of the excretory cell and canals using *pgp-12::rfp* revealed defects in canal morphology and extension. In wild-type animals **(A**,**C)**, the posterior canals appear very smooth and extend from the cell body to the tail. In *let-765(ok2058)* animals, the canals appear jagged with a fuller lumen. Several examples were observed where the canals had branches near the posterior end **(B**, **D)**. Futhermore, the cell body is very round, with a noticeable nucleolus in wild type **(C**-inset**)**, while in *let-765* animals, the cell body is misshapen **(D**-inset**)**.Inset in **C** and **D** are of reduced exposure. Scale bar: 25 μm.

3.3.4 Reducing *let-765* expression leads to gonad migration defects without a loss of distal tip cells

let-765(RNAi) led to gonad migration defects, where the gonad extended in an anterior-posterior direction but failed to turn dorsally, or extended briefly but then knotted upon itself. Furthermore, RNAi treated animals were sterile which, together with the sterile germline in rescued animals, suggested that LET-765 functions in germline development. Two main processes, namely the specification and migration of the distal tip cells (DTC) together with the proliferation and maturation of the germ cells, are required for the growth and differentiation of the germline (Kimble and Crittenden, 2005). The DTCs are born at the end of the L1 stage when they begin to express *lag-2*, a LIN-12/Notch ligand. The DTCs possess a gonadal leader function, so that the characteristic extension and reflex of developing gonad arms occurs normally (Kimble, 1981). Furthermore, the DTCs function as niche cells where *lag-2* is required to signal the Notch receptor GLP-1 to promote mitotic proliferation of the germline stem cells through the distal region of the gonad (Austin and Kimble, 1987; Austin et al., 1989).

I first examined *lag-2* expression in *let-765* mutants to assess whether the gonad migration defects were a result of a failure to specify the DTCs (Siegfried and Kimble, 2002). *let-765* homozygotes expressed *lag-2::gfp* (*qIs56*) in the presumptive DTCs at the end of the L1 stage and gonad development appeared normal through early L2 until they reached arrest. Similarly, in *lag-2::gfp* expressing animals raised on *let-765* RNAi bacteria, the DTCs also appeared to be specified and gonad migration proceeded along the ventral side. However, in some animals one or both of the gonad arms failed to turn dorsally and extended into the tail region or up into the pharynx (Figure 39). There were

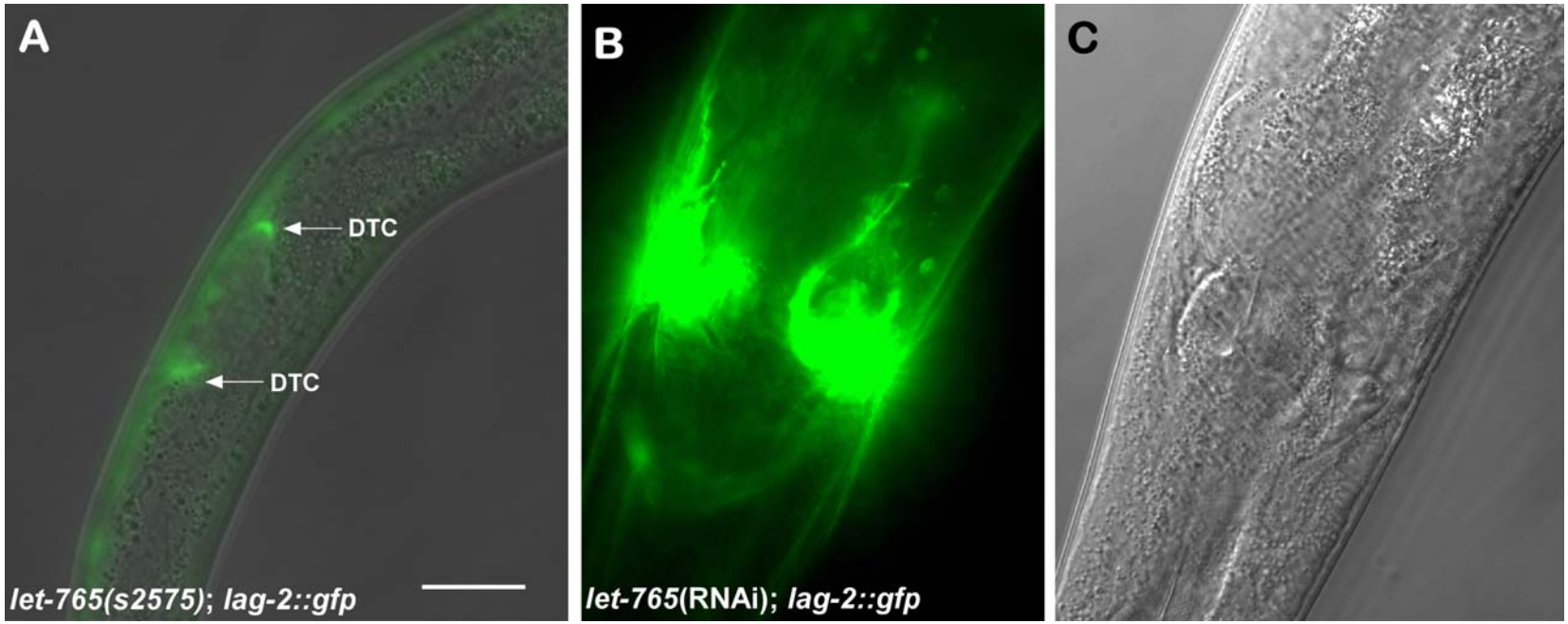

Figure 39. *lag-2* expression in *let-765* animals.

The distal tip cells (DTCs) are specified in *let-765(s2575)* animals, evidenced by *lag-2::gfp* expression at the L2 stage **(A)**. The bottom cell is out of the focal plane. When *lag-2::gfp* (*qIs56*) animals are raised on *let-765*(RNAi) plates, the DTCs fail to migrate properly. **(B-C)** cropped image of an adult where the DTCs have both extended to the base of the pharynx. Scale bar in **(A)** 25 um.

also many examples of gonads that developed a knotted appearance after extending along the ventral side. The migration defects could result from a failure in DTC function, however the degree of gonad extension was not affected and mitotic proliferation of the germline does occur. The loss of migration may be a result of a misregulation of guidance cues from the underlying hypodermis and muscle.

3.3.5 *let-765* arrested larvae exhibit a phasmid dye fill defect

An asymmetry defect at the B cell division was previously identified in *let-765*(*s2575*) males. In *C. elegans*, many asymmetric divisions are regulated by *lin-44*/Wnt and *lin-17*/Fz including the division of the B cell and the T cell (Herman et al., 1995; Sternberg and Horvitz, 1988). I examined the T cell lineage in *let-765* animals to determine whether it would reveal a lack of asymmetry similar to that seen at the B cell division.

The T cells are a pair of bilaterally symmetric cells in the tail that divide during the L1 stage to produce hypodermal cells (from T.a) and neural cells (from T.p). The T.pap and T.paa cells are the phasmid socket cells PHso1 and PHso2, which connect the phasmid neurons, PHA and PHB, to the external environment (Sulston and White, 1980). When the animals are soaked in a lipophilic dye, such as DiO or DiI, the amphid and phasmid neurons take up dye through their associated socket cells, allowing visualization of the neuronal cells (Herman and Horvitz, 1994). If the T cell lineage is disrupted, the phasmid sockets can be lost or displaced and PHA/PHB will not stain. I used a dye filling assay to test *let-765* mutants for defects in phasmid staining and found that 89% (n=54) of *ok2058* homozygotes and 92% (n=48) of *s2575* homozygotes exhibited a

phasmid dye fill defect. Conversely, the amphid neurons fully stained in all animals tested. None of the wild type animals, and few of the heterozygotes (<5%), exhibited a lack of phasmid staining (Figure 40). This suggested that the phasmid socket cells may have been lost or that the cells were present, but had failed to function.

To ascertain the source of the dye fill phenotype, I attempted to characterize the T cell lineage in *let-765* animals by examining the nuclear morphology. In wild-type animals, at the four cell stage the anterior daughter cells have acquired a hypodermal fate and their nuclei are large and flattened with a smooth appearance. The posterior cells display neural characteristics with a small nucleus and granular nucleoplasm (Sulston and Horvitz, 1977). Examination of the T cell lineage in *s2575* and *ok2058* mutants revealed that, in some animals, the T.a and T.p cells did not divide and in others the deterioration of cellular morphology resulted in indistinguishable cell types, making the results inconclusive.

Another indicator of T cell lineage fates is the expression of the Tcf/LEF gene, *pop-1*, which is regulated by *lin-44*/Wnt and *lin-17*/Fz (Herman, 2001). It is expressed in an asymmetric fashion, with high levels in T.a and lower levels in T.p. A *pop-1::gfp* transgene (*qIs74*) was introduced into *let-765* animals and GFP expression was compared to that in a wild-type background. Expression was clearly visible in L1 animals, before the T cell had divided. After the first division, GFP expression was observed in a wild-type pattern (T.a>T.p) or, less often, at equal levels in both T.a and T.p, however, equal levels of expression were also occasionally seen in wild-type animals (Figure 41). There were few animals where the T lineage had developed to the four-cell stage, however,

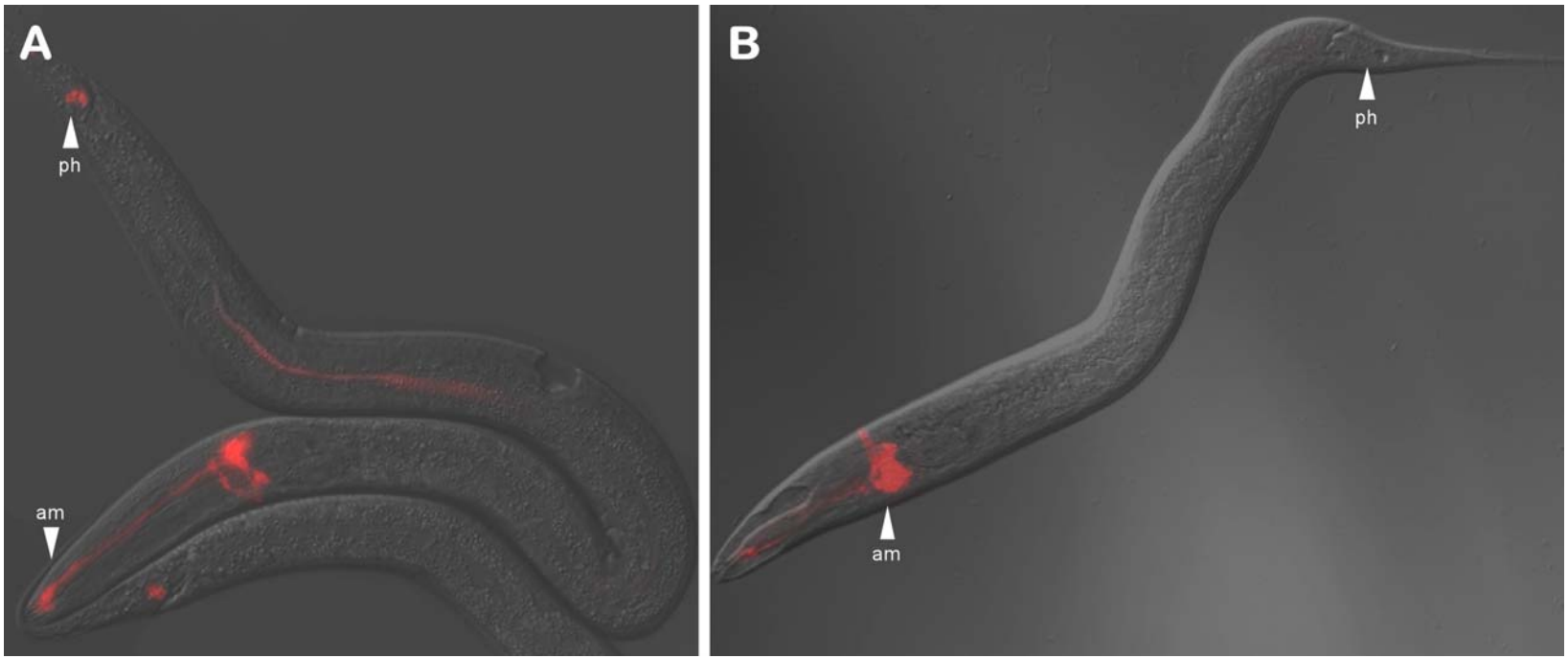

Figure 40. *let-765* animals exhibit a phasmid dye fill defect.

Wildtype animals soaked in a lipophilic dye display staining in the amphid (am) and phasmid (ph) neurons **(A)**, L4 stage animal shown. In a *let-765*(*s2575*) larva, the phasmid neurons have not stained **(B)**.

these animals displayed a wild-type expression pattern. Overall, I was unable to determine conclusively whether the T cell lineage was disrupted by mutations in *let-765*.

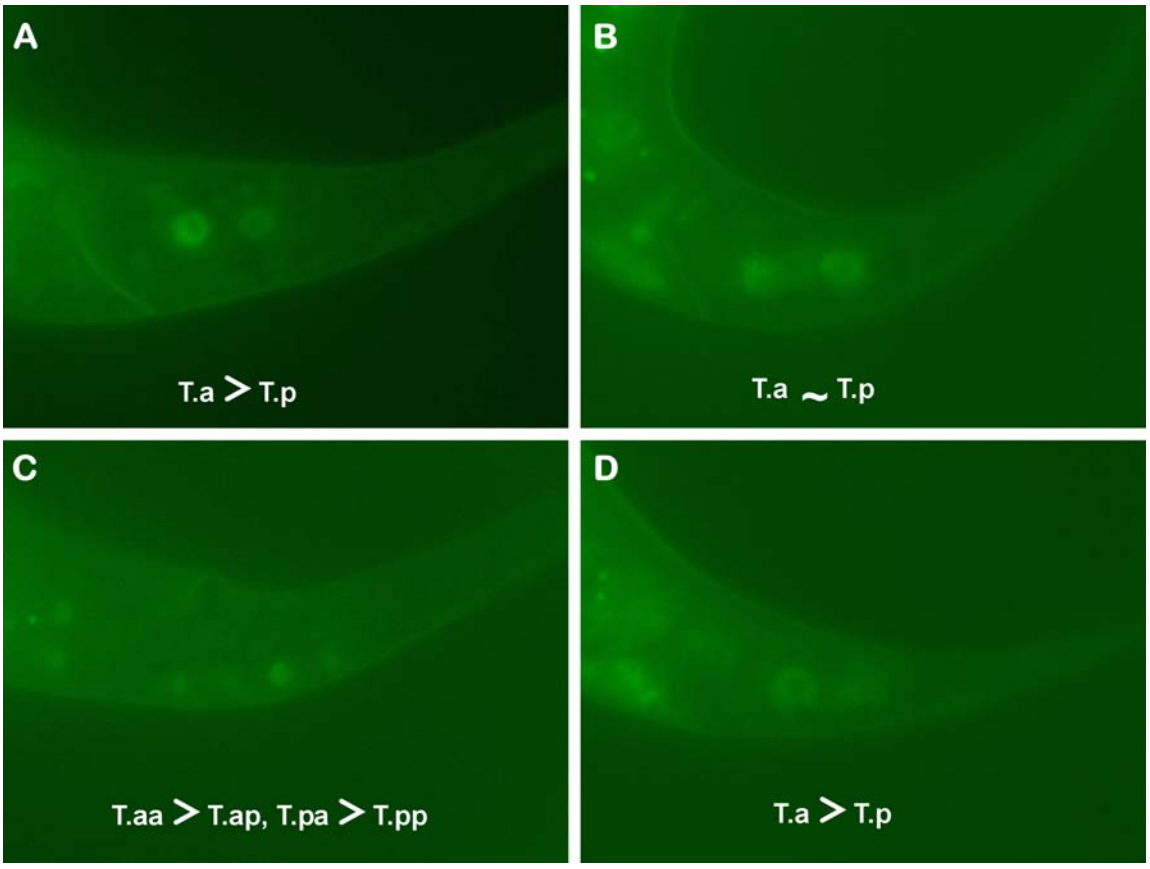

Figure 41. *pop-1::gfp* expression in *let-765* animals.

Panels **(A)** and **(C)** are wild type. Panels **(B)** and **(D)** are *let-765(s2575)*. *pop-1::gfp (qIs56)* is expressed asymmetrically in the T cell lineage with higher levels in anterior cells and lower levels in posterior cells: **(A)** after one division, and **(C)** after two divisions. *let-765(s2575)* animals appear to have equal levels in both T.a and T.p **(B)**, otherwise the expression appeared to be wild type **(D)**.

The dye fill defect could result from missing or defective phasmid neurons, so an *srb-6::gfp* (*gmIs13*) reporter was used to establish the presence of PHA and PHB in *let-765* mutants. In all animals scored, GFP was observed in both phasmids, in the correct location. Furthermore, when a *lin-44::gfp* transgene (*mnIs7*) was crossed into strains

carrying *let-765* mutations, expression was detected in the phasmid socket cells as well as in hypodermal cells of the tail (Herman et al., 1995). The same expression pattern was seen in wild-type animals, although the socket cell expression was slightly weaker (Figure 42). In summary, the data collected suggests that the phasmid dye filling phenotype is not caused by a disruption in the T cell lineage or a loss of phasmid neurons or socket cells. The lack of staining in *let-765* animals may be a result of a defect in phasmid socket cell structure, such that dye uptake is impeded.

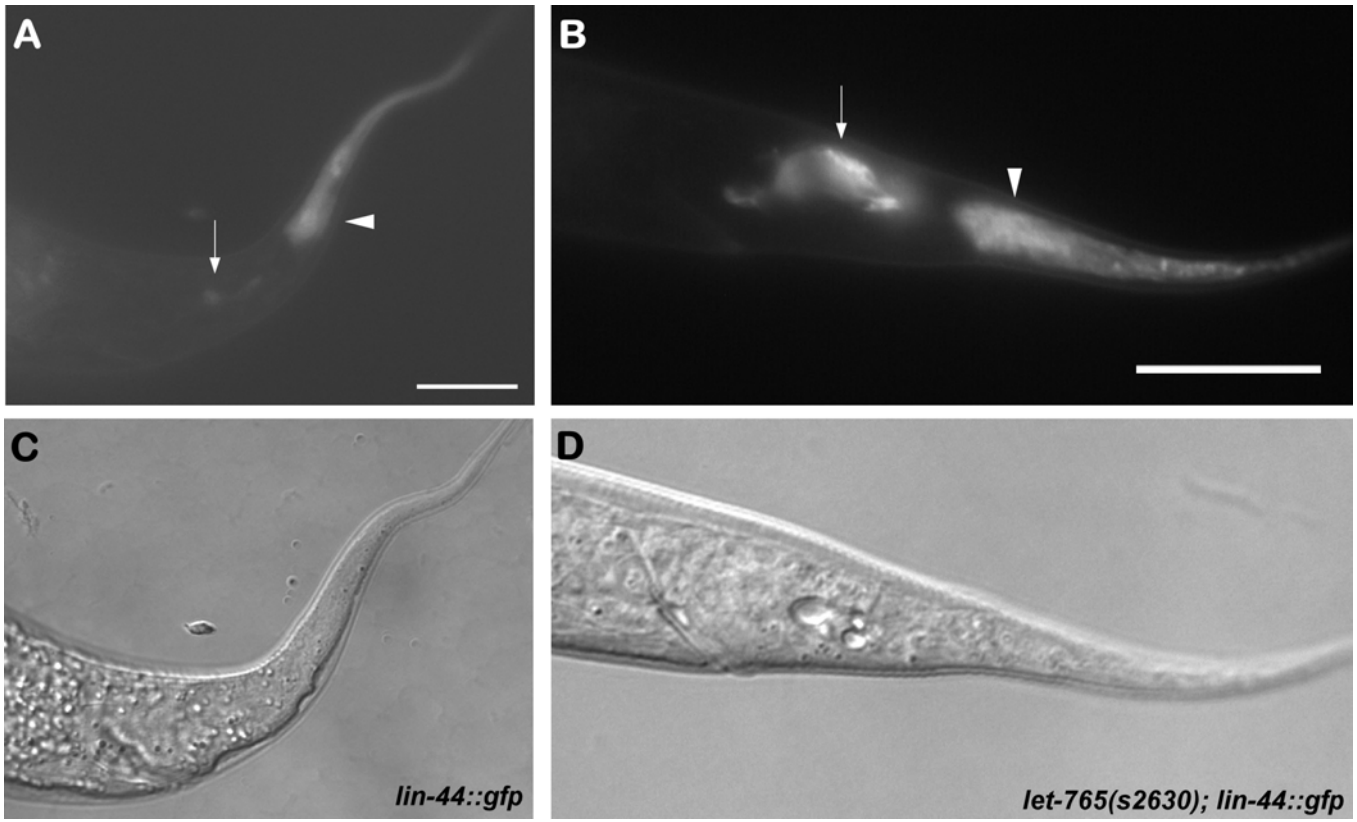

Figure 42. Expression of a *lin-44*/Wnt reporter in *let-765*.

The *mnIs7* transgene is expressed in tail hypodermis (arrowhead) and in the phasmid socket cells (arrow). In wild type animals, expression is often weaker in the phasmid sockets **(A,C)**. *let-765(s2630)* larvae display hypodermal expression similar to wild type, however, expression in phasmid socket cells was stronger than wild type **(B,D)**. The phasmid sockets are correctly positioned in *let-765(s2630)*. Scale bar: 25 µm.

3.3.6 Development of the hypodermis is unaffected in *let-765* mutants

Given that hypodermal expression of *let-765* is required for viability, I examined the structure of the major hypodermis and seam cells to confirm that they were properly developed. The seam cells are specialized hypodermal cells that are located laterally along each side of the body. There are 10 cells on a side at hatching and they divide in stem cell-like fashion at each stage to produce a seam cell and a daughter cell that differentiates into other cell types. In most cases the daughter cell fuses with the hypodermal syncytium but the posterior-most seam cell, the T cell, also divides to produce the phasmid socket cells, as previously mentioned, and in males the V5, V6, and T cells give rise to the sensory rays in the tail (Sulston et al., 1980). In adults, the seam cells form a syncitial band containing 16 nuclei that runs the length of the body. The seam cells function to regulate cuticle formation and molting, in addition to providing structural support to the worm (Thein et al., 2003).

As *let-765*(RNAi) produces missing rays in males, which could result from a loss of seam cells, the maintenance of seam cell fate was examined using SCM::gfp (*wIs51*) in *let-765* mutant animals. The correct numbers of seam cells were present in *let-765* homozygotes at hatching (Figure 43) and all cells appeared to divide upon reaching the L2 stage. SCM::gfp animals raised on *let-765*(RNAi) plates did not reveal any losses in seam cell number or division. Therefore, the mail tail defects and deficiencies in T cell daughter function do not appear to be a result of improper seam cell specification.

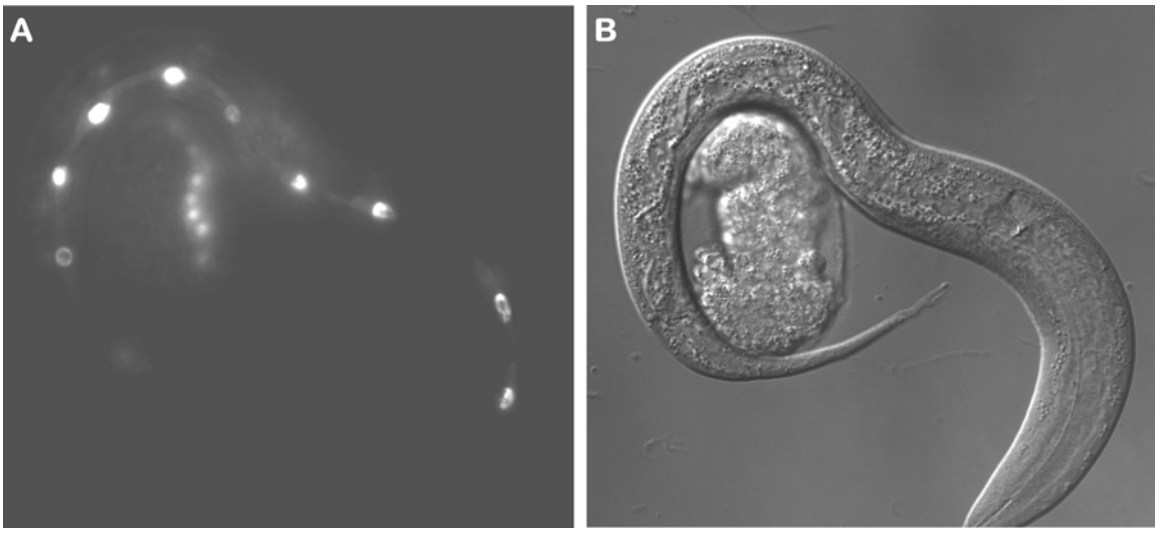

Figure 43. The correct number of seam cells are present in *let-765*(*s2630*) animals. Fluorescence can be seen in each of the seam cells at the L1 stage **(A)**. The T cell is out of focus in this image. **(B)** Corresponding Nomarski image.

To investigate the structure of the major hypodermis, an AJM-1::GFP translational fusion reporter (*syIs78*) was introduced into *let-765*(*ok2058*) mutants. The protein is present at adherens junctions and can be used to visualize seam cell development and the migrations of the hypodermal daughter cells. A wild type pattern of GFP expression was observed in *let-765* mutants with complete connections visible between seam cells. Furthermore, the P3.p-P8.p cells were visible late in the L1 stage, confirming that they remain unfused and competent to adopt a vulval cell fate, referred to as vulval precursor cells (VPCs) (Figure 44). In sum, the structure of the major hypodermis and seam cells in early larval staged *let-765* mutants does not exhibit any gross morphological defects.

Given that the major hypodermis is an essential site of *let-765* expression, I sought to determine if reducing its activity specifically in these cells could generate more

subtle phenotypes, which could lend insight into the gene's function. An expression construct consisting of the *dpy-7* promoter sequence and an inverted repeat of *let-765* sequence was built such that a dsRNA hairpin would be transcribed in hyp7, triggering an RNAi response against *let-765* transcripts (Myers and Greenwald, 2005). Unfortunately, when injected at concentrations of 5 – 15 ng/μL, a stable transgenic line could not be obtained, emphasizing the sensitive requirement for hypodermal expression of *let-765*.

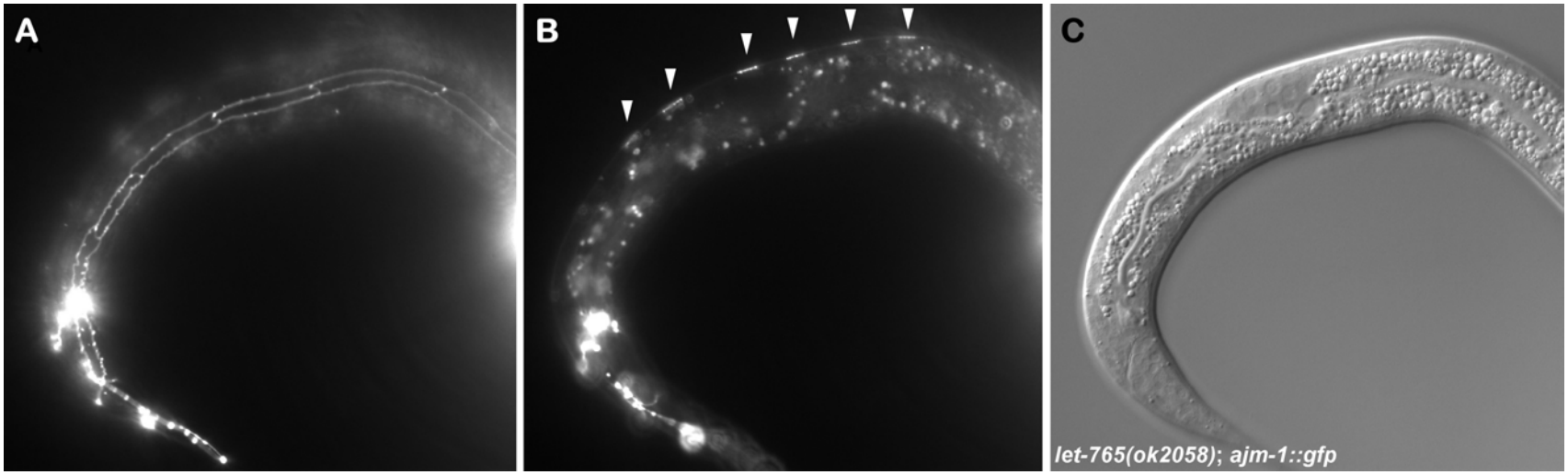

Figure 44. The seam cells and vulval precursor cells are specified in *let-765* animals.

The *ajm-1::gfp* transgene is visible at adherens junctions of the hypodermis. **(A)** The seam cells connect to one another along the length of the animal, forming a ladder-like structure. The junctions in *let-765(ok2058)* appear to have wild-type morphology. **(B-C)** By the end of the L1 stage, the P3.p-P8.p cells, positioned along the ventral side of the body, have not fused with the hypodermis as the junctions are clearly visible (arrowheads). This indicates that the cells are competent vulval precursor cells. The other posterior daughters of the P lineage have fused with hyp7. **(C)** Nomarski image of focal plane in **(B)**.

CHAPTER 4: LET-765 PROMOTES RAS PATHWAY ACTIVITY DURING VULVAL DEVELOPMENT

4.1 Introduction

The specification of distinct cell fates is often achieved through the activation of specific intercellular signalling pathways by growth factors whose expression must be spatially and temporally controlled to ensure accurate responses. Typically, a target cell expresses an excess of receptors such that the availability of its ligand is rate limiting for pathway activation. Overall, for a signal to elicit the desired response, the intensity and duration of ligand expression must be sufficient to meet its threshold concentration, and yet the signal response must be restricted to prevent excessive signalling (Freeman and Gurdon, 2002). Excessive activation of a signalling pathway can have broad deleterious effects, thus prompting a requirement for antagonistic regulation.

In *C. elegans*, an epidermal growth factor receptor (EGFR) mediated RAS pathway is used in development and differentiation of multiple types of tissues (Sundaram, 2006). In addition to an early essential requirement, EGFR/RAS signalling is also required for spicule development in the male tail (Chamberlin and Sternberg, 1994), vulval induction (Aroian and Sternberg, 1991), differentiation of the vulval-uterine connection (Chang et al., 1999) and P12 cell specification in the posterior ectoderm (Jiang and Sternberg, 1998). The development of the *C. elegans* vulva has been extensively studied as a model for understanding how multiple signalling pathways and their cues can be integrated to

specify a variety of cell fates (Horvitz and Sternberg, 1991; Sternberg, 2005; Yoo et al., 2004).

Vulval development begins when an EGF-like growth factor, LIN-3, is secreted by the gonadal anchor cell (AC) (Hill and Sternberg, 1992) to induce three of six equivalent vulval precursor cells (VPCs) to form the mature vulva (Sulston and White, 1980). All of the VPCs (P3.p through P8.p) express the EGF receptor homolog LET-23 (Aroian and Sternberg, 1991) and are capable of receiving the growth factor signal to activate a RAS/MAPK signalling pathway that specifies vulval cell fates via LET-60/RAS (Beitel et al., 1990; Han and Sternberg, 1990). Under typical physiological conditions P6.p, the cell closest to the AC, acquires the 1° fate and the two neighbouring cells, P5.p and P7.p, adopt 2° cell fates. Experiments with LIN-3/EGF indicate that the growth factor signal acts in a graded manner (Katz et al., 1995). As a result of this gradient, P6.p receives the greatest amount of the signal, acquiring the 1°cell fate, whereas intermediate amounts of signal specifies 2° cell fates in P5.p and P7.p. Distal VPCs do not receive enough growth factor signal to induce a vulval fate. Instead, they divide once and fuse with the hypodermal syncytium (hyp7). Additionally, in response to the LIN-3/EGF inductive signal, P6.p produces a lateral signal that activates LIN-12/NOTCH in P5.p and P7.p (Sternberg and Horvitz, 1989). Activation of the Notch pathway is necessary for the generation of 2° cell fates (Greenwald et al., 1983; Simske and Kim, 1995). Thus the LIN-3/EGF gradient may function synergistically with LIN-12/NOTCH to specify 2° fates (Kenyon, 1995).

Mutations that reduce the function of the EGFR/RAS/MAPK pathway components result in the induction of less than three vulva precursor cells and a vulvaless (Vul)

phenotype. Activating mutations or over expression of *lin-3*/*egf* cause distal cells to be induced and produce a multivulval (Muv) phenotype. Not surprisingly, there exists an antagonistic mechanism, which ensures that only three cells can adopt vulval fates and produce a functional vulva. This is accomplished in part by the synthetic multivulva (synMuv) genes which antagonize EGFR/RAS/MAPK signalling (reviewed in (Fay and Yochem, 2007). The synMuv genes are classified into two principal groups – synMuv A and synMuv B – based on the observation that single or double mutants from one class develop a wild-type vulva, but an A-B double mutant produces a strong Muv phenotype; the synthetic interaction implies that these genes act in two redundant processes to inhibit vulval induction (Ferguson and Horvitz, 1989). The molecular functions of synMuv A genes have not been established, but they have been predicted to play a role in transcriptional regulation (Davison et al., 2005; Huang et al., 1994). By homology comparisons to Drosophila and mammalian proteins, the large synMuv B class includes proteins predicted to act as transcription factors and chromatin modifiers, including homologs of the mammalian Rb/E2F complex (LIN-35/Rb and EFL-1/DPL-1 E2F) (Ceol and Horvitz, 2001; Lu and Horvitz, 1998; Thomas et al., 2003), the nucleosome remodelling and deacetylase (NuRD) complex (Solari and Ahringer, 2000; Unhavaithaya et al., 2002; von Zelewsky et al., 2000), histone methyltransferases (Andersen and Horvitz, 2007), and a DP/Rb/MuvB (DRM) complex (Harrison et al., 2006). The homology to Rb/E2F and NuRD complexes suggests that the synMuv proteins function in transcriptional repression. Specifically, as a result of *lin-3*/*egf* being identified as a transcriptional target of many synMuv genes (Andersen and Horvitz, 2007; Andersen et al., 2008; Cui et al., 2006), it has been proposed that synMuv genes function to repress

lin-3 expression thus inhibiting ectopic vulval induction. A number of genes have been identified that function in various aspects of chromatin remodelling and transcriptional regulation and are suppressors of the synMuv phenotype (Andersen et al., 2006; Cui et al., 2006), underscoring the potential complexity of interactions between regulatory complexes that modulate gene expression.

In this chapter, I describe experiments which define a role for *let-765* in promoting vulval development. I have demonstrated that *let-765* function is required for RAS pathway activity during vulval induction and for the hyper-proliferation phenotype in a synMuv mutant background. I have gathered support for a similar function during RAS-dependent P12 cell fate specification. Finally, I have established that *let-765* promotes *lin-3* activity by positively regulating its expression.

4.2 Materials and methods

4.2.1 RNAi

RNAi was performed as in section 3.2.1.2.

4.2.2 Scoring VPC induction

Vulval induction was scored at the L4 stage using Nomarski optics as described (Sternberg and Horvitz, 1986). The number of VPCs that acquired a 1° or 2° fate was counted in each animal. The induction index was calculated by dividing the total number of 1° and 2° induced cells by the total number of animals scored. Statistical analysis was performed using a Mann Whitney test. Animals were scored as Muv if more than three VPCs were induced and Vul if one or more of P5.p – P7.p was not induced.

4.2.3 *egl-17:cfp* analysis

Wild type worms containing the *egl-17::cfp* reporter transgene (*arIs92*) were synchronized by hatching eggs in M9 buffer overnight. Larvae were plated on food and allowed to develop for about 24 hours until they reached mid-L2. Animals homozygous for *let-765*(*s2575*) and *arIs92* were picked at the L1 stage and left overnight at 20°C. Mutant animals were scored only if VPCs were present. Reporter expression was assayed using confocal microscopy (section 3.2.6). The level of CFP expression was compared between wild type and *let-765*(*s2575*) mutants.

4.2.4 Scoring suppression of synMuvB phenotypes

4.2.4.1 Assay for rescue of *mep-1* and *let-418* larval arrest

The *mep-1(q660)* allele is temperature sensitive; at 25°C nearly all homozygous progeny from heterozygous mothers arrest as L1 larvae. Heterozygous hermaphrodites, *mep-1(q660)*/*nT1(qIs51)*, were plated on bacteria expressing F20H11.2 dsRNA and allowed to lay eggs for 24 hours. Adults were removed and progeny allowed to develop at 25°C. Homozygous (non-GFP) larvae were scored for arrest three days later.

let-418(n3536) animals are viable at 20°C but exhibit early larval arrest at 25°C. Animals were raised at 25°C on plates expressing F20H11.2 dsRNA. Larval arrest was scored three days after eggs were laid.

4.2.4.2 Assay for germline transgene silencing

The strain PD7271 carries an extrachromosomal array of *let-858::gfp* that is expressed in most somatic cells, but is silenced in the germline. Hermaphrodites were

raised on F20H11.2 RNAi plates to test for suppression of germline silencing. The restoration of GFP expression in the germline was assayed in young adult F1 progeny.

4.2.4.3 Ectopic *lag-2::gfp* expression in the intestine

synMuv B mutants exhibit ectopic GFP expression of a *lag-2::gfp* reporter in the intestine. *lin-15B*(*n744*); *lag-2::gfp* animals were raised on F20H11.2 RNAi plates. The suppression of ectopic GFP expression in the intestine was scored in young adult F1 progeny.

4.2.5 *lin-3* qRT-PCR

Synchronized L1 larvae of the various genotypes were grown on *let-765*(RNAi) or empty vector control until early L3, estimated by the degree of gonad development. Worms were washed 3 – 5 times in M9 and frozen in liquid nitrogen. Total RNA was isolated using Trizol as in section 2.2.6.2 followed by treatment with DNaseI. DNase was removed by phenol/chloroform extraction and ethanol precipitation. cDNA was prepared from 1 µg of total RNA using a combination of oligo $dT_{(17)}$ and random hexamer primers and Superscript II reverse transcriptase (Invitrogen) as per manufacturer's instructions. Multiple biological replicates were collected and cDNA reactions pooled. Each qRT-PCR reaction contained 50 ng of RT products, 10 µL of 2× SYBR Green Supermix (Biorad), and 1 µM of each primer. qRT-PCR reactions were run in triplicate on a Biorad MyIQ Real-time thermocycler. Relative fold change was calculated using the ΔΔCt method. All primers were tested on serial dilutions and primer efficiency calculated. Data was normalized using *rpl-19*.

4.3 Results

4.3.1 *let-765/nsh-1* promotes vulval cell fates via the EGFR/RAS pathway

Because *let-765*(RNAi) animals exhibited hypo-induction of the VPCs and a protruding vulva phenotype, it raised the possibility of *let-765* being involved in promoting vulval development. To investigate this putative role, I used RNAi to assess the effect of *let-765(rf)* in animals with perturbed EGFR/RAS/MAPK pathway activity. Animals with gain-of-function (gf) mutations in EGFR/RAS/MAPK pathway genes exhibit a multivulva (Muv) phenotype where greater than three VPCs are induced; conversely reduction-of-function (rf) alleles lead to induction of less than three VPCs and a vulvaless (Vul) phenotype. I expected that if *let-765* promotes vulval induction, then a decrease in its activity would suppress a hyperactive pathway (gf) phenotype and would enhance a hypo-induced (rf) phenotype.

I first looked at the EGF-like ligand, LIN-3, which acts as the signal to activate RAS/MAPK signalling. A partial loss of function allele in *lin-3/egf* (*e1417*) has an incompletely penetrant Vul phenotype. In combination with *let-765*(RNAi), vulval induction was further reduced in *lin-3*(*e1417)* animals. Specifically, *lin-3*(*e1417*) animals treated with *let-765*(RNAi) exhibited a maximum of one cell induced (P6.p) compared to control animals where 10% of animals had three cells induced and developed a wild-type vulva. In contrast, a multicopy transgene that overexpresses LIN-3 (*syIs1*) (Hill and Sternberg, 1992) results in a strong Muv phenotype. Reducing *let-765* activity could not suppress the hyperactive phenotype in these animals, suggesting that *let-765* function is required upstream of *lin-3*. To support this further, a ligand-independent gain of function allele of *let-23*/*egfr* (*sa62gf*) (Katz et al., 1996) was only mildly affected by *let-*

765(RNAi). The fact that the receptor was not sensitive to a reduction in *let-765* activity implies that LET-765 must function upstream of LET-23, at or before the level of the LIN-3 ligand.

Additionally, *let-765*(RNAi) was able to suppress the Muv phenotype caused by a gain of function mutation in *let-60 ras* (*n1046*) (Figure 45) (Beitel et al., 1990; Chang et al., 2000), over expression of an inducible wild-type MAP kinase, *mpk-1,* in combination with activated *mek-2* (Lackner and Kim, 1998), or, to a lesser extent, a temperature-sensitive RAS mutation, *let-60*(*ga89 gf*) (Eisenmann and Kim, 1997) (Table 1). However, the gain of function phenotype of the *let-60*(*n1046*) allele and the *mapk*(+) transgene is partially dependent on *lin-3* expression from the gonadal anchor cell (Chang et al., 2000; Dutt et al., 2004). When the gonadal anchor cell is ablated in *let-60*(*n1046*) animals, vulval induction is reduced to below wild-type levels. (Chang et al., 2000; Yin et al., 2004) This implies that suppression of the Muv phenotype in *let-60*(*gf*) and *mapk*(+) animals can be attributed to a loss of pathway activation by LIN-3.

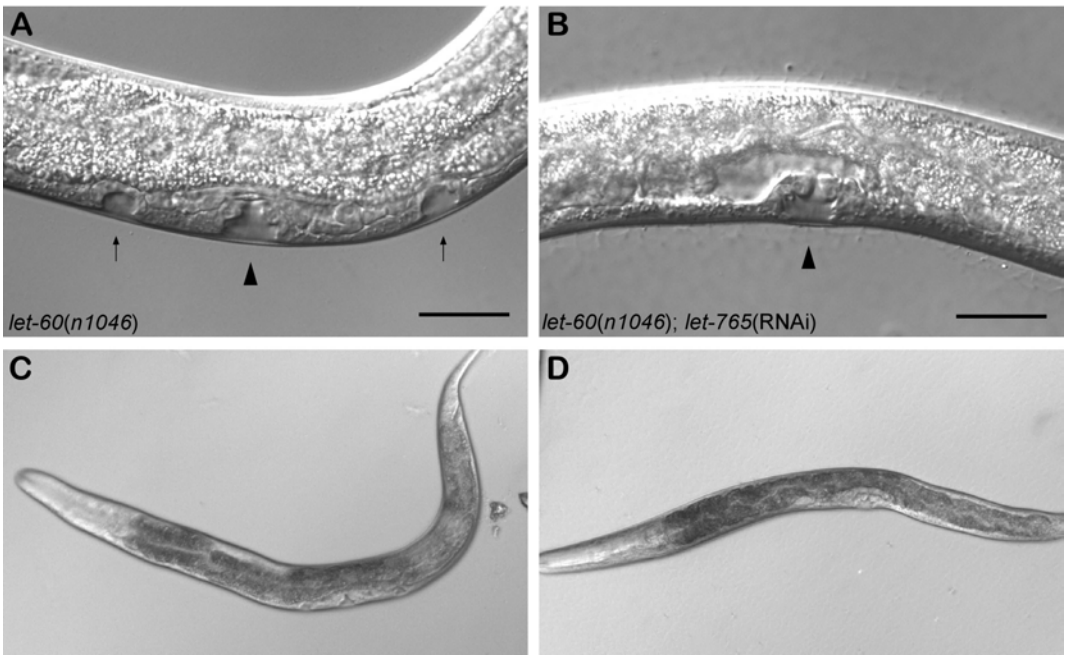

Figure 45. *let-765*(RNAi) suppresses the Muv phenotype in *let-60*/Ras gain of function animals.

An L4 stage *let-60(n1046)* animal **(A)** with a vulva (arrowhead) flanked by two pseudovulvae (arrows) and **(B)** after treatment with *let-765*(RNAi) exhibits wild type vulval development. Images in **(C-D)** are a lower magnification of the animals in **(A-B)**.

Table 1. *let-765* promotes vulval induction

Genotype	% muv[a]	% vul[b]	n	VPC induction[c] ± SE (n)
N2	0	0	>200	3.00 ± 0 (30)
rrf-3 (*pk1426*)	0	0	25	3.00 ± 0 (25)
rrf-3 (*pk1426*)*; let-765*(RNAi)	0	30	27	2.44 ± 0.17 (27) **
lin-3(*e1417*)	0	90	50	0.86 ± 0.12 (50)
lin-3(*e1417*); *let-765* (RNAi)	0	100	52	0.26 ± 0.06 (52) ***
syIs1[*lin-3*(+)]	100	0	50	5.20 ± 0.09 (20)
syIs1[*lin-3*(+)] *;let-765* (RNAi)	100	0	60	5.23 ± 0.11 (22)
let-23(*sa62*)	93	0	27	4.30 ± 0.12 (27)
let-23(*sa62*); *let-765* (RNAi)	89	7	27	3.85 ± 0.12 (27)
let-60(*n1046*)	98	0	91	4.29 ± 0.17 (28)
let-60(*n1046*); *let-765* (RNAi)	7	3	92	3.03 ± 0.13 (29) ***
let-60(*ga89*)	20	7	30	3.12 ± 0.09 (30)
let-60(*ga89*); *let-765* (RNAi)	3	12	41	2.90 ± 0.06 (41) *
[D*mek-2*(*gf*); hs-*mpk-1*] †	81	0	27	4.17 ± 0.14 (27)
[D*mek-2*(*gf*); hs-*mpk-1*]; *let-765* (RNAi) †	57	0	21	3.48 ± 0.13 (21) **

a % Muv indicates the percentage of animals with P(3, 4, or 8).p cell(s) induced.
b % Vul indicates the percentage of animals where P(5, 6, or 7).p are not induced.
c VPC induction was calculated as the average number of induced cells per animal.
n, number of animals scored.
SE, standard error.
† Animals were heat shocked at 33°C for 30minutes at early L2, transferred to 23°C and grown until L4.

** $0.01 < p < 0.001$, *** $p < 0.0001$; Data were compared with values from strains fed empty vector RNAi bacteria and statistical significance determined using a Mann-Whitney test.

Next I set out to examine potential interactions with downstream effectors of the pathway to identify additional effects of *let-765*(*rf*). RAS/MAPK signalling in the VPCs terminates with the transcription factors LIN-1/ETS and LIN-31. In the absence of MAPK phosphorylation activity, LIN-1 and LIN-31 form a dimer and inhibit vulval cell fates (Beitel et al., 1995; Tiensuu et al., 2005). Upon phosphorylation by MAPK, LIN-31 dissociates from LIN-1 and promotes vulval fates in the proximal VPCs (Miller et al., 2000; Tan et al., 1998). Thus, loss-of-function mutations in *lin-1* are Muv and *lin-31* null

mutants exhibit a mixed Muv/Vul phenotype (Miller et al., 2000). *let-765*(RNAi) had no effect on *lin-1* alleles but did reduce vulval induction in the *lin-31*(*n301*) and *lin-31*(*n1053*) animals. I observed that not only was the induction index reduced but there was a marked increase in the percentage of Vul animals (Table 2).

The Notch and Wnt pathways also promote vulval cell fates in parallel with RAS signalling. The Notch pathway acts to specify the 2° cell fate in P5.p and P7.p in response to a DSL signal from the neighbouring P6.p cell. In *lin-12*/*Notch(n137gf)* animals, no AC is formed and all VPCs adopt the 2° fate, resulting in a Muv phenotype (Sternberg and Horvitz, 1989, Wang, 2001 #28). This phenotype was not affected by *let-765*(RNAi), suggesting that *let-765* acts upstream of LIN-12/NOTCH activity, though there is still potential for an effect on the LIN-12 ligand(s) which would be concealed by the dominant *n137gf* mutation. A Wnt/β-catenin pathway promotes vulval cell fate specification in parallel to the EGFR/RAS/MAPK pathway. The Muv phenotype caused by over activation of the Wnt pathway by *pry-1*/axin was not affected by *let-765*(RNAi), nor was the hypo-induced (*rf*) phenotype of the *bar-1*/β-catenin allele (*ga80*) (Gleason et al., 2002).

In summary, these data provide evidence that *let-765* positively regulates the EGFR/RAS/MAPK pathway to promote vulval induction. LET-765 appears to function at or before the level of *lin-3/egf* since *let-765*(RNAi) cannot suppress the constitutive activity of the *let-23*(*gf*) allele, but can enhance a partial reduction in *lin-3* activity.

Table 2. Interactions with RAS, Notch, and Wnt pathway genes.

Genotype	% muv[a]	% vul[b]	n	VPC induction[c] ± SE (n)
lin-1(*e1777*)	100	1	55	4.36 ± 0.39 (11)
lin-1(*e1777*); *let-765* (RNAi)	100	0	40	4.47 ± 0.13 (15)
lin-31(n1053)	85	4	71	4.39 ± 0.12 (71)
lin-31(n1053); let-765 (RNAi)	58	20	71	3.51 ± 0.13 (71) ***
lin-31(*n301*)	60	5	36	3.75 ± 0.16 (36)
lin-31(*n301*); *let-765* (RNAi)	35	21	65	3.20 ± 0.11 (65) **
lin-12(*n137*)	100	0	45	6.00 ± 0 (18)
lin-12(*n137*); *let-765* (RNAi)	100	0	56	6.00 ± 0 (16)
bar-1(ga80)	0	64	14	1.90±0.27 (14)
bar-1(ga80); let-765(RNAi)	0	85	39	1.51±0.13(39)
pry-1(mu38)	21	11	19	3.11±0.13(19)
pry-1(mu38); let-765(RNAi)	0	33	15	2.53±0.22(15)

a % Muv indicates the percentage of animals with P(3, 4, or 8).p cell(s) induced.
b % Vul indicates the percentage of animals where P(5, 6, or 7).p are not induced.
c VPC induction was calculated as the average number of induced cells per animal.
n, number of animals scored.
SE, standard error.

** $0.01 < p < 0.001$, *** $p < 0.0001$; Data were compared with values from strains fed empty vector RNAi bacteria and statistical significance determined using a Mann-Whitney test.

4.3.2 The *s2575* mutation reduces *egl-17* expression in the vulval precursor cells

egl-17 acts as a reporter for *lin-3* activity as it is a primary transcriptional target of RAS signalling in the VPCs (Burdine et al., 1998). To obtain support for the genetic data, I examined how *let-765* affected the expression of *egl-17::cfp (arIs92)*. The reporter is expressed in the VPCs in mid L2 stage larvae, prior to the activation of LIN-12/NOTCH mediated lateral inhibition in L3(Yoo et al., 2004). The graded expression pattern is brightest in P6.p and lower in flanking Pn.P cells (Dutt et al., 2004). Since the *s2575* allele arrests during L2, I was able to examine reporter expression in a homozygous mutant background. Loss of LET-765 function mildly affected expression

in P6.p; however, in 90% of animals (n=39), the signal was reduced or eliminated in the remaining VPCs (Figure 46). *egl-17::cfp* expression was consistently visible in the M4 pharyngeal neuron, serving as a control for the presence of the reporter. Expression patterns were consistent, though less penetrant, using *let-765*(RNAi) as compared to *let-765*(*s2575*) animals. Overall, the loss of reporter expression in P5.p, P7,p and distal VPCs demonstrates that LET-765 is required for generating a wild-type pattern of *egl-17* expression. These results are consistent with the genetic data and in turn suggest that *let-765* is required for *lin-3* expression to reach a physiologically relevant level.

4.3.3 *let-765/nsh-1* is required for the synMuv phenotype

During vulval induction, the synMuv genes repress *lin-3* expression in the hyp7 hypodermal syncytium, thus restricting the action of the EGF signal and maintaining a wild-type pattern of cell fates (Cui et al., 2006). In synMuv mutant animals *lin-3* is derepressed, activating the RAS/MAPK pathway, and resulting in ectopic VPC induction; it follows that a reduction in *lin-3* activity in hyp7 leads to suppression of the synMuv phenotype. Since the results from the first set of experiments implied that *let-765* is functionally required at the level of *lin-3* expression to promote RAS signalling, I chose to examine the effect of *let-765*(*rf*) on the synMuv phenotype.

let-765(RNAi) completely suppressed the ectopic vulval induction conferred by the synMuv mutation *lin-15AB*(*n765*) (Clark et al., 1994; Huang et al., 1994), a complex locus that encodes both synMuv A and synMuv B activities (Table 3). To rule out specificity with the *lin-15* allele, we tested several other synMuv genotypes.

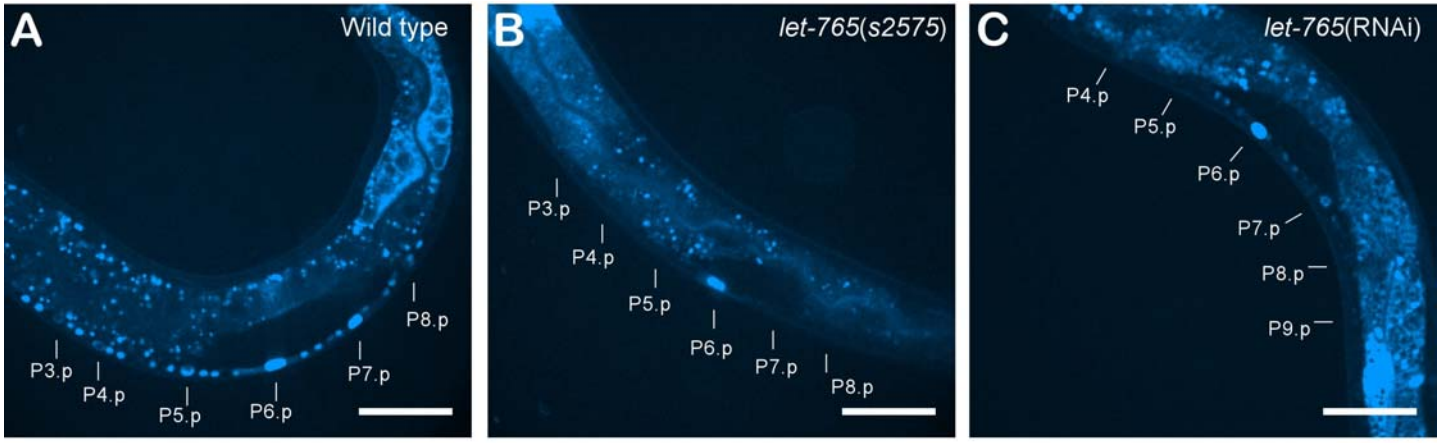

D Percentage of cells with wild-type expression

	P3.p	P4.p	P5.p	P6.p	P7.p	P8.p	
Wild type	100	100	88	100	94	100	n=16
let-765(*s2575*)	5	5	8	59	10	5	n=39

Figure 46. *egl-17::cfp* reporter expression is reduced in *let-765*(*s2575*) animals.

Images **(A-C)** show reporter expression in mid L2 hermaphrodites. **(A)** Wild-type expression is highest in P5.p, P6.p, and P7.p, with lesser expression in distal VPCs. In *let-765(s2575)* larvae **(B)**, reporter expression was usually reduced or eliminated in all VPCs except P6.p. **(C)** *let-765*(RNAi) led to a decrease in reporter expression in distal VPCs, but the effect was less penetrant than in *s2575* larvae. Scale bar 25 µm. **(D)** Summary of the percentage of animals that displayed a wild-type level of *egl-17::cfp* expression, in wild type and *let-765(s2575)* L2 stage larvae. n= number of animals scored

Table 3. The SynMuv phenotype requires *let-765* activity.

Genotype	% muv[a]	% vul[b]	n	VPC induction[c] ± SE (n)
lin-15(*n765*)‡	100	0	190	5.94 ± 0.03 (57)
lin-15(*n765*); *let-765*(RNAi)‡	0	37	59	2.36 ± 0.16 (59) ***
lin-36(*n766*); *lin-15A*(*n767*)	100	0	114	5.82 ± 0.08 (22)
lin-36(*n766*); *lin-15A*(*n767*); *let-765* (RNAi)	10	6	115	3.57 ± 0.23 (21) ***
lin-8(*n111*); *lin-15B*(*n374*)	100	0	151	5.65 ± 0.10 (23)
lin-8(*n111*); *lin-15B*(*n374*); *let-765* (RNAi)	22	0	72	3.04 ± 0.04 (26) ***
lin-8(*n111*); *lin-9*(*n112*)	100	0	105	5.87 ± 0.07 (23)
lin-8(*n111*); *lin-9*(*n112*); *let-765* (RNAi)	76	9	35	4.29 ± 0.19 (35) ***
lin-53(*n833*)*; lin-15A*(*n767*)	100	0	95	5.85 ± 0.06 (41)
lin-53(*n833*)*; lin-15A*(*n767*); *let-765* (RNAi)	100	0	86	5.74 ± 0.08 (42)
lin-35(*n745*); *lin-8*(*n111*)	98	0	43	5.72 ± 0.13 (43)
lin-35(*n745*); *lin-8*(*n111*); *let-765* (RNAi)	n/a	n/a	many	L1 arrest

a % Muv indicates the percentage of animals with P(3, 4, or 8).p cell(s) induced.
b % Vul indicates the percentage of animals where P(5, 6, or 7).p are not induced.
c VPC induction was calculated as the average number of VPCs induced per animal.
n, number of animals scored.
SE, standard error.
‡L4 animals were grown at 15°C until reaching the adult stage and were then transferred to 23°C.

*** $p < 0.0001$. Data were compared with values from strains fed empty vector RNAi bacteria and statistical significance determined using a Mann-Whitney test.

Reducing *let-765* activity had a significant effect on vulval induction in most of the strains. One notable exception was *lin-35*(*n745*); *lin-8*(*n111*) (Ferguson and Horvitz, 1989), in which *let-765*(RNAi) caused early larval arrest in all F1 animals. Experiments with other strains that carried *lin-8*(*n111*) resulted in synMuv suppression but no lethality. This indicates that *let-765* functions in a common process with *lin-35*/Rb that is

required for larval development and viability. In summary, *let-765* is genetically epistatic to synMuv mutations and appears to be required for the synMuv phenotype. These observations, together with the earlier finding that *let-765* affected EGFR/RAS/MAPK activity upstream of receptor activation, suggest that LET-765 affects production of the LIN-3 ligand.

4.3.4 synMuvB phenotypes are not suppressed by *let-765/nsh-1*

In addition to their repressor activity during vulval development, the synMuvB genes are required for transcriptional regulation during a number of other processes including cell division and proliferation (Boxem and van den Heuvel, 2001; Fay et al., 2002), germline versus somatic cell fate decisions (Kawasaki et al., 1998; Unhavaithaya et al., 2002), RNAi (Wang et al., 2005), and context-dependent transcriptional gene silencing (Tam phenotype)(Hsieh et al., 1999). A number of other genes with synMuv suppressor activity have been identified and although they are able to suppress both the ectopic vulval induction in synMuv double mutants as well as synMuvB phenotypes (Andersen et al., 2006; Cui et al., 2006), *let-765*(RNAi) did not affect synMuvB specific phenotypes.

mep-1 and *let-418*/Mi-2 both exhibit synMuvB activity and are required for restricting ectopic germ cell fates in the soma. Mutations in either gene result in a germline-like appearance of somatic cells and lethality (Unhavaithaya et al., 2002). Unlike other synMuv suppressor genes, *let-765*(RNAi) did not suppress the lethality of *mep-1*(*q660*) or *let-418*(*n3536*), or affect the cellular morphology. Furthermore, *let-765*(RNAi) did not cause de-silencing of a *let-858*:GFP transgene in the germline(Kelly and Fire, 1998) or affect ectopic expression of *lag-2*:GFP in the intestine (Poulin et al.,

2005). From these results, I propose that *let-765* does not promote the adoption of ectopic germ cell fates in the soma, nor is it required for repressing transgene expression in the germline, and extend this to propose that *let-765* does not antagonize synMuvB transcriptional targets in these processes.

4.3.5 *let-765* promotes RAS dependent P12 cell specification

The RAS pathway also controls the fate decision between the P11 and P12 ectodermal blast cells via LIN-3/EGF and LET-23/EGFR (Jiang and Sternberg, 1998). Normally, P11 and P12 divide to produce anterior neural blast cells (P11.a and P12.a) and two hypodermal cells P11.p and P12.pa, which can be identified by their distinct morphologies. Loss of function mutations in RAS pathway genes often leads to a loss of the P12.pa fate, resulting in two P11.p cells. Conversely, gain of function alleles exhibit a 0 P11.p phenotype. Since *let-765* positively regulates the EGFR/RAS pathway during vulval development, I suspected that it might play an analogous role in P12 fate specification.

The *lin-15(n765)* mutation causes a loss of the P11.p cell as a result of hyperactive RAS signalling. When *lin-15(n765)* animals were raised on control plates, 23% exhibited a 0 P11.p phenotype (n=48). However, when raised on *let-765*(RNAi) plates, 14% of animals were missing P11.p and 14% had 2 P11.p cells (n=14), demonstrating that *let-765(rf)* can suppress the gain of function phenotype. Further to this, that two P11.p cells are specified when *let-765* activity is reduced, suggests that LET-765 promotes specification of the RAS pathway-dependent P12.pa fate.

4.3.6 let-765/nsh-1 is required for efficient transcription of *lin-3* mRNA

Given the observation that *let-765* has a role in regulating *lin-3* expression and that *let-765* encodes a protein with homology to genes that are required for RNA metabolism and transcriptional regulation, I hypothesized that *let-765* may be involved in the regulation of *lin-3* transcription. Furthermore the repressive effect of synMuv gene function on *lin-3* transcription has been well demonstrated (Andersen and Horvitz, 2007; Andersen et al., 2008; Cui et al., 2006) and forms the basis of the synMuv phenotype. I analyzed two synMuv mutant genotypes that were strongly affected by *let-765*(RNAi), *lin-15AB*(*n765*) and *lin-36*(*n766*); *lin-15A*(*n767*), to determine whether suppression of their synMuv phenotype was a result of reduced *lin-3* transcription. qRT-PCR was used to measure the relative amount of *lin-3* mRNA present in control versus *let-765*(RNAi) treated strains, near the L2/L3 molt when induction occurs. In both synMuv genotypes tested, I found that the level of *lin-3* transcript decreased to approximately wild-type levels when *let-765* activity was reduced (Figure 47). In addition, in wild-type animals treated with *let-765*(RNAi), the level of *lin-3* mRNA decreased more than two fold. These results indicate that *let-765* function is required for efficient production of *lin-3* mRNA. It should be noted that mRNA levels of other RAS pathway components and of the examined synMuv genes were not significantly affected by *let-765*(RNAi). The suppression of the synMuv phenotype observed in RNAi treated animals likely results from a reduced levels of *lin-3* transcript and, as predicted by Andersen et al. (Andersen et al., 2008), the observed induction phenotype reflects the level of *lin-3* mRNA produced (*let-765* (RNAi) treated synMuv mutants exhibit nearly wild-type induction).

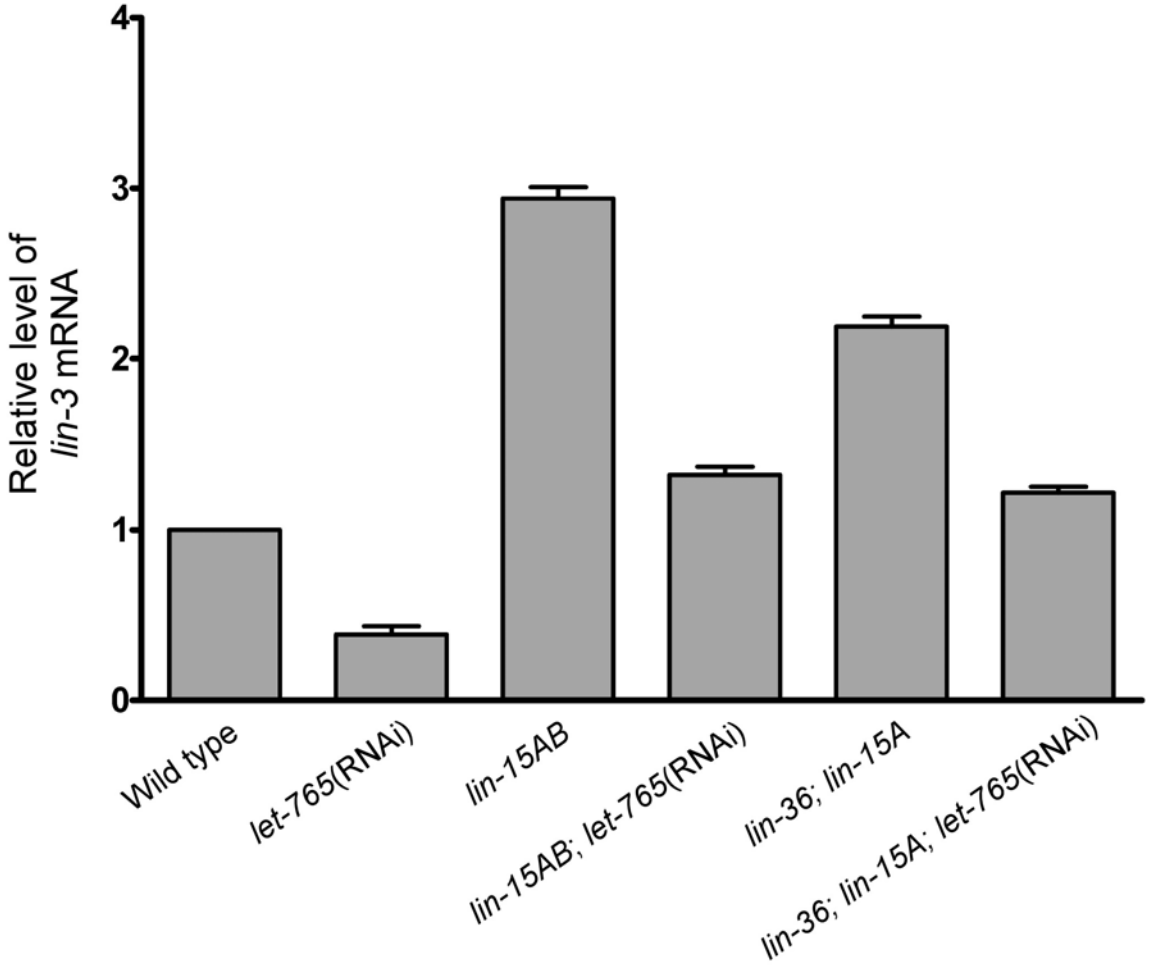

Figure 47. The level of *lin-3* transcripts is reduced in *let-765*(RNAi) treated animals.

Real-time RT-PCR was performed using RNA from early L3 staged animals of the indicated genotypes. *let-765*(RNAi) led to a reduction in the level of *lin-3* mRNA in wild type and synMuv mutant strains. *rpl-19* was used as an internal reference. Mean values and standard deviations of *lin-3*/*rpl-19* ratios from three replicates are shown.

CHAPTER 5: DISCUSSION

5.1 *let-765* encodes a DExD/H box helicase involved in transcriptional regulation

In this study, I have identified the essential gene, *let-765*, as F20H11.2/*nsh-1*, a DExD/H box helicase protein and characterized its expression and mutant phenotype during *C. elegans* development. Because the closest homolog is a gene known to be involved in the Notch signal transduction pathway in *Drosophila*, *let-765* was suggested to play a similar role during *C. elegans* development. The experimental data that I have collected indicate that this gene is ubiquitously expressed, consistent with a requirement for its activity during multiple developmental events. In particular, I have demonstrated that it functions to promote vulval induction by positively regulating expression of the epidermal growth factor, *lin-3*, to maintain physiologically relevant levels of the ligand.

Using transgenic rescue, I have shown that *let-765* is encoded by F20H11.2/*nsh-1* which translates to an 1866 amino acid protein with homology to *Drosophila strawberry notch*. Although similarity searches with the protein sequence revealed only a C-terminal helicase domain, I have confirmed that it contains all of the motifs common to the DExD/H box protein family and demonstrated that it possesses functional ATPase activity. Further to this, since hypodermal specific expression of the region denoted as F20H11.2 is sufficient to rescue larval lethality, this portion of the protein appears to contain the domains necessary for its enzymatic function.

The three alleles of *let-765* that were used in this study all result in premature termination of the protein; it is of interest that the mutation leading to the most severe

truncation, *s2575*, produces the weakest arrest phenotype. Furthermore, the mutation in the *s2630* allele is situated such that it eliminates only the C-terminal helicase domain, yet it consistently led to the least successful rescue –rescue to the adult stage was only obtained with the WRM0629dG03 fosmid clone. As DExD/H box family proteins are known to function as dimers or multimers (Fuller-Pace, 2006), the *s2630* allele may possess some dominant negative activity in this context. Further to this, since *s2630* and *ok2058* are putative null alleles and *s2575* exhibits a weaker phenotype, it appears that retaining part of the enzymatic domains is more detrimental to larval viability. It is possible that the truncated version of the protein may be acting as a sink for binding partners or co-factors.

There are several pieces of evidence that indicate the level of *let-765* expression to be tightly regulated. First, the transcriptional GFP reporter produces a low amount of signal in most tissues and further, the translational fosmid::GFP construct is expressed at an exceedingly low level. Secondly, the qRT-PCR results suggest that *let-765* expression is low during post-embryonic development. Thirdly, few expressed sequence tags (ESTs) have been identified for the gene and, furthermore, the proportion of SAGE tags present in embryonic libraries as well as in later developmental stages is low and, in some cases, undetectable (http://tock.bcgsc.bc.ca/cgi-bin/sage140). In addition, I noted that, for all three alleles, rescue with the fosmid transgene was more complete than with other constructs, including the F20H11 cosmid which covers essentially the same genomic content. This is likely due to the lower copy number present in the fosmid transgenes relative to the cosmid transgenes – 10-15ng/μL of cosmid DNA was used to generate the transgenic lines compared to only 2-3 ng/μL of fosmid DNA. Together with the lack of

success in producing a heat-shock inducible transgenic animal, these observations indicate that expression of this gene must be strictly controlled. Given that I have demonstrated a role for LET-765 in gene regulation, it is possible that adjusting its activity beyond an optimal level could lead to non-specific binding with cofactors or interaction partners, resulting in misexpression of target genes.

5.2 LET-765 is required for generating functional phasmid socket cells

The finding that *let-765* encodes a DExD/H box family protein implied that it is likely to possess a function related to RNA biogenesis or the regulation of gene expression. Furthermore, studies with the homologous proteins in Drosophila and mammals have established a role for strawberry notch proteins in transcriptional regulation. *Drosophila sno* acts downstream of Notch signalling in the wing disc to promote the expression of Notch target genes in cooperation with Su(H). Also, physical interactions between Sno and the transcription factors Su(H) and vg (*vestigial*) have been demonstrated, suggesting that Sno functions to regulate transcriptional activity (Majumdar et al., 1997; Nagel et al., 2001). In contrast, a mammalian strawberry notch protein, SBNO2, has been studied in the context of the anti-inflammatory response. SBNO2 is up-regulated by STAT3 dependent IL-10 signalling in macrophages and exhibits repressive activity for transcriptional targets of NF-κB (El Kasmi et al., 2007).

These studies predicted a possible transcriptional regulatory function for LET-765; however, the lack of gross morphological defects in *let-765* mutant animals did not immediately suggest potential targets. The prior identification of an asymmetry defect at the B cell division in males raised the possibility that LET-765 may promote the adoption of distinct fates at this division. The B cell divides during the L1 stage to produce a large

anterior daughter cell and smaller posterior cell that generate distinct lineages –neurons and associated support structures of the male spicules from the B.a cell and rectal epithelial cells from B.p (Chamberlin and Sternberg, 1993). The asymmetry of the first division of the B cell is regulated by LIN-17/Fz and the Wnt ligand LIN-44 (Herman and Horvitz, 1994; Sternberg and Horvitz, 1988). In *let-765*(*s2575)* animals, the B cell divides symmetrically, similar to *lin-17* mutants, but the daughter cells do not divide further. I elected to use the T cell division to investigate a potential role for *let-765* in regulating asymmetry since its polarity is also controlled by *lin-17*/*lin-44*. After examining *pop-1::gfp* expression and cellular morphology, as indicators of daughter-cell fates, a lineage defect was not apparent. However, *let-765* homozygotes exhibited a nearly fully penetrant phasmid dye fill defect even though the phasmid neurons and socket cells appeared to be present. From this, I conclude that LET-765 is required to promote the activity of components that contribute to the function or morphogenesis of the socket cells.

5.3 Development of a functional excretory duct requires *let-765* activity

An analysis of the expression of *let-765* in combination with phenotypes generated by a loss or reduction of function has provided further insight into the sites at which its activity is required and some of the processes to which it contributes. A *let-765* transcriptional GFP reporter (*sEx1800*) is strongly expressed in the excretory system, in the somatic gonad, and at lower levels in the hypodermis. Each of these expression patterns correlates with phenotypes observed when *let-765* activity is reduced. Although reporter expression was observed in neurons of the ventral cord and in many head neurons, I did not observe behaviour or phenotypes indicative of neuronal loss of

function. LET-765 may be involved in an aspect of neuronal function, which produces subtle phenotypes, or it may be redundantly required in these cells. On the other hand, LET-765 could be regulating the expression of a product that is acting non-cell autonomously in neuronal cells.

Animals homozygous for *let-765* mutations arrest at an early larval stage with an accumulation of fluid in the pseudocoelom and often exhibit a rod-like posture. This phenotype results from a failure in osmoregulation, usually due to defects in the excretory system, which provides renal function to the animal (Buechner, 2002; Buechner et al., 1999). The system is relatively simple, consisting of three cells that form unicellular tubes with a continuous lumen that is open to the external environment. The canals form two arms, which span the length of the animal and function to collect fluid and solutes, and transport it to the duct and pore cell, where it is expelled. The formation and maintenance of the canal lumen is controlled by apical membrane components and an associated cytoskeleton (Tong and Buechner, 2008). The canals join at the excretory cell body, where they connect to the duct cell and pore cell through apical junctions.

Mutations in core RAS pathway genes lead to a rod-like lethal phenotype which results from a failure to specify the duct cell (Sundaram, 2006). Since the morphology of *let-765* homozygotes closely resembles that of animals with loss of function mutations in the RAS pathway and it functions to promote transcription of *lin-3* during vulval development, I have proposed that LET-765 may also be required for duct cell specification. Although some *let-765* animals appear to posses a duct cell, this may result from partial rescue by maternally provided gene product. However, the aberrant morphology of the excretory system, including an apparent lack of duct-to-pore cell

connection, implies there are additional defects present and suggest a broader role for LET-765 in excretory function.

The development of the excretory canals requires guidance cues from the underlying basal lamina, and involves genes that are also used in neuronal outgrowth including α integrins, laminins, and UNC-6/Netrin and its receptor UNC-5 (Gettner et al., 1995; Hedgecock et al., 1987). Mutations in these genes produce shortened or misguided canals and may be the source of the branching phenotype in *let-765(ok2058)* animals In addition, the growth and maintenance of the apical membrane and lumen is supported by the β-spectrin SMA-1, whose expression is regulated by the ELAV homolog, EXC-7 (Fujita et al., 2003). Several other *exc* genes have been identified based on phenotypes involving defects in the excretory system, some of which encode ion channels, novel signalling components and the rho GEF EXC-5, which is involved in the synthesis and transport of components to the apical membrane (Suzuki et al., 2001). Conversely, other receptor proteins are expressed on the basal membrane, to communicate with components in the basal lamina of the hypodermis and affect the balance between apical and basal membrane growth (Buechner, 2002). Although *let-765* mutants exhibit unusual lumen characteristics, mutations in the *exc* genes result in cyst formation within the excretory canals or cell body that often appear as large bubbles, rather than overall fluid accumulation. LET-765 may be involved in an aspect of lumen function that results in a less severe phenotype.

Alternatively, a lipocalin-related gene, *lpr-1*, has been identified and functions to establish a lumenal connection between the duct and pore cell. LPR-1 is thought to bind small lipophilic molecules and transport them to receiving cells via receptor interactions

(Stone et al., 2009). There are several common features between the *lpr-1* mutants and *let-765*, aside from their phenotype. *lpr-1* is expressed in the excretory system and nearby hypodermal cells and, although *lpr-1* mutants possess an intact excretory system, they exhibit early larval arrest with excretory defects. The lethal phenotype can be rescued by hypodermal-specific expression of the *lpr-1* gene using a *dpy-7* promoter and, perhaps most interesting, *lpr-1* animals display a highly penetrant phasmid dye filling defect. Similar to the excretory system, the socket cells, or glia, of the amphid and phasmid neurons are made of unicellular tubes and it has been suggested that the formation and connectivity of the socket lumen also require intercellular signals (Shaham, 2006). Neuronal processes of the amphids and phasmids are supported by the socket cells, allowing them to contact the exterior of the body. The Patched-related protein, DAF-6, functions in the amphid glia and has been proposed to control endocytic versus exocytic vesicle trafficking. Together with an associated protein, CHE-14/Dispatched, it is required for lumen formation in the amphid glia and excretory canals – double mutants exhibit normal excretory canal length but an incomplete lumen and occasionally form intracellular cysts (Michaux et al., 2000; Perens and Shaham, 2005; Perkins et al., 1986).

As there appear to be many common features of tube formation in the socket glia and excretory system, it is interesting to speculate that LET-765 is involved in the production of signals or components that contribute to lumen formation or function in both the excretory system and the phasmid sockets. This could provide an explanation for the phasmid dye fill defect that is observed in *let-765* mutants. It is also notable that a protein that demonstrated a physical interaction with LET-765 in a yeast two hybrid

assay, encoded by T23G5.2 (see Appendix D), exhibits strong homology to the SEC-14 protein in humans. T23G5.2 contains a CRAL/TRIO domain, which is predicted to bind hydrophobic ligands and is found in proteins involved in intracellular transport and secretion (Finn et al., 2008). LET-765 may promote the expression and transport of small signalling molecules via an interaction with the T23G5.2 protein, and may function upstream of an intercellular transport protein such as *lpr-1*.

Given that excretory system performance is an essential requirement for larval viability, the severity and penetrance of the excretory defects in *let-765* animals suggest that they are likely a primary source of the lethal phenotype. In addition, the finding that the hypodermis, which is intimately associated with the excretory system, is an essential site of activity for LET-765 is consistent with this proposal. The formation of unicellular tubules is a process common to the generation of capillary beds of the brain and lung and the structure of the kidney nephron in mammals (Lubarsky and Krasnow, 2003). The excretory system of *C. elegans* provides a model for studying the development and function of tubular cells; further studies of a role for *let-765* in the excretory system may reveal additional regulatory mechanisms or components involved in this process.

5.4 LET-765 may be required for establishment of the vulval-uterine connection

let-765(RNAi)-treated *rrf-3* hermaphrodites exhibited a protruding vulva phenotype that was almost fully penetrant. It is unlikely that the phenotype is a result of the vulval induction defect, as the proportion of animals exhibiting hypo-induction was much lower. Given that *let-765* is expressed in the somatic gonad during the L3 and L4 stages, it may be required for vulval-uterine development, in addition to its role in vulval

induction. The cells of the somatic gonad generate the distal tip cells (DTCs), the spermatheca and sheath cells, and the uterus. By the L2 stage, the DTCs are specified and the remainder of the somatic gonad primordium consists of 9 blast cells (five that will produce uterine cells and four spermatheca and sheath precursors) and the anchor cell (AC). During the L3 stage, the dorsal (DU) and ventral uterine (VU) cells divide twice and remain situated adjacent to the site of the developing vulva (Figure 48).

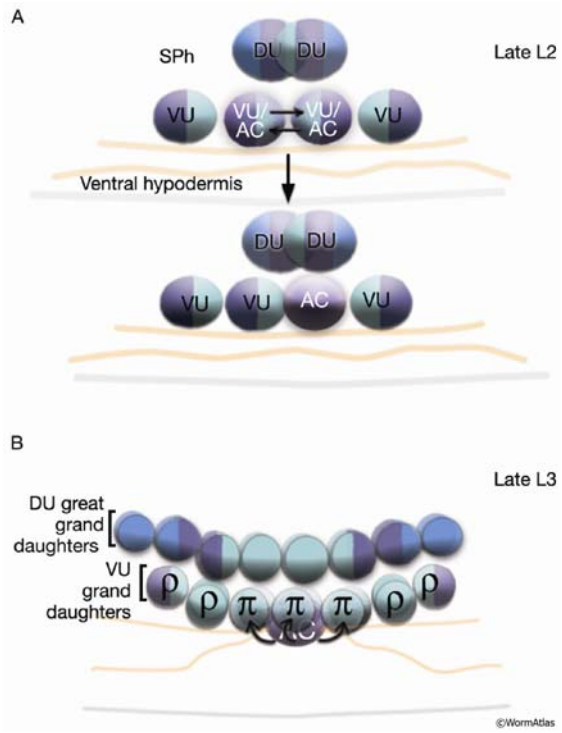

Image courtesy of WormAtlas (www.wormatlas.org)

Figure 48. Cell divisions of the somatic gonad.

Beginning in the L3 stage, *let-765p::gfp* is expressed in the uterine cells, including the anchor cell, with GFP appearing brightest in the VU progeny cells. This is consistent with its role in promoting vulval induction by regulating *lin-3* expression, however, it may also be required for patterning the uterus and the vulval-uterine connection.

As multiple concerted specification and migration events are required to form a functional connection, there are several possible sources of the Pvl phenotype observed in *let-765*(RNAi) animals. The most apparent is the disruption of the somatic gonad cells that is likely resulting from a failure in gonad arm extension and migration. It is possible that π cell fates, and possibly uv1 fates, are mis-specified due to improper positioning of the VU cells. Additionally, the uterine lumen does not form, suggesting that the requisite cell migrations have not taken place. The disorder amongst the somatic gonad and germline cells complicates the investigation of cell interactions making it difficult to discern which process(es) are most affected in the *rrf-3* animals. I have not determined the source of the gonad migration defect; however, given that some of the guidance cues that direct neuronal outgrowth and excretory canal extension are used for directing gonad migration, it is possible that the two phenotypes result from a deficiency in the underlying hypodermal cells.

Wild-type hermaphrodites raised on *let-765*(RNAi) also exhibit a Pvl phenotype, albeit at a lesser penetrance, and do not display the gonad migration defect. In these animals, π cell expression of a *lin-11* reporter was occasionally lost although VU progeny appear to form an intact utse. It is possible that LET-765 is required to generate another aspect of π cell function such that, in *let-765*(*rf*) animals, the vulval-uterine connection is structurally compromised.

A second potential source of the Pvl phenotype is a disruption in vulval morphogenesis. In *let-765*(RNAi) animals that exhibit wild-type levels of vulval induction, specification of all vulval progeny cell types appeared to occur, based on the expression of vulval-cell specific reporters. Furthermore, vulval morphogenesis

proceeded normally with invagination and separation of the primary vulval cells. From this, it appears that the Pvl phenotype is not likely to result from irregular morphogenesis. Since I have demonstrated a requirement for *let-765* in the regulation of *lin-3* expression, it is possible that the vulF cells are not expressing adequate levels to induce the uv1 fate. However, it is not clear whether this alone would result in the Pvl phenotype and I have not investigated it further at this point. Since a reduction of the level of *let-765* using RNAi may not be sufficient to identify subtle changes in reporter expression, further studies using tissue specific knockdown or a hypomorphic allele of *let-765* would better identify affected cells or tissues.

5.5 LET-765 promotes RAS dependent vulval induction

In this study, I have demonstrated a role for *let-765* in promoting vulval induction by positively regulating *lin-3/egf* expression to maintain physiologically relevant levels of the ligand. This may occur via direct interaction with transcriptional regulators of *lin-3*, or indirectly, by affecting the expression of an additional component that positively affects *lin-3* expression. Genetic analyses, using *let-765*(RNAi) in concert with mutations in RAS pathway components, substantiates the proposed function for *let-765* in promoting vulval induction and, furthermore, demonstrate that *let-765* is required for RAS dependent induction in all six VPCs and establish that LET-765 promotes induction even in the absence of a hyperactive RAS pathway.

let-765(RNAi) was found to suppress both the gonad-dependent (*let-60gf*) activity as well as the gonad-independent (synMuv) activity from hyp7. This is supported by a decreased induction of P(5, 6 or 7).p, leading to a vulvaless phenotype, observed when let-60(n1046) is treated with let-765(RNAi) (Table 1). In addition, lin-15(n765) also

exhibits reduced vulval induction in the proximal VPCs when fed let-765(RNAi) (Table 3). Therefore, it is highly likely that the protein has a role in promoting the expression of *lin-3* in both the somatic gonad anchor cell and hyp7. Nuclearly localized LET-765:GFP expression in these tissues at the time of induction is consistent with protein activity at these sites. Experments using qRT-PCR revealed that a reduction in *let-765* activity affects the level of *lin-3* mRNA in wild-type animals and in synMuv mutant animals. Together, the data supports a function for LET-765 in promoting vulval induction by positively regulating *lin-3*/*egf* expression. It is feasible that *let-765* acts to positively regulate *lin-3* transcription and, where appropriate, consequently antagonizes the activity of the synMuv genes (Figure 49). Since the Muv phenotype in *let-60*(*gf*) animals is suppressed in the presence of wild-type synMuv proteins, it is reasonable that LET-765 functions beyond simply blocking the repressive activity of synMuv genes. Instead I postulate that, in a synMuv mutant, *let-765* interacts with factors that promote *lin-3* activity while transcriptional repression is relieved.

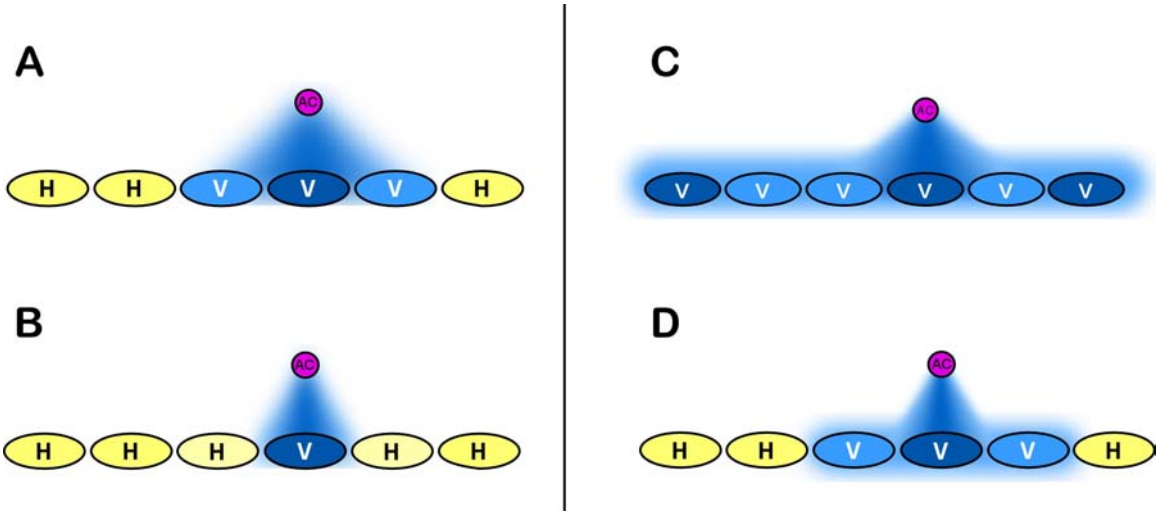

Figure 49. Proposed model for *let-765* mode of action.

In wild type animals, *lin-3* expression leads to induction of P(5, 6, and 7).p **(A)**. Upon exposure to *let-765*(RNAi), decreased levels of *lin-3* result in less than three cells being induced **(B)**. When RAS pathway activity is elevated (for example in synMuv mutant animals or *let-60*(gf) animals), more than three VPCs are induced **(C)**. In these same animals, reduction of *let-765* activity leads to reduced vulval induction **(D)** resulting from a reduction in *lin-3* expression.

The response to *let-765*(RNAi) in the examined synMuv strains reveals substantial variation in the interaction between *let-765*(*rf*) and some of the synMuv genotypes. For instance, synthetic lethality occurs when *let-765* levels are reduced in a *lin-35*(*n745*); *lin-8*(*n111*) mutant, which indicates that *let-765* and *lin-35* cooperate to promote larval development. *lin-35* is the *C. elegans* homolog of the mammalian tumour suppressor gene, Rb, which interacts with the E2F and DP heterodimeric transcription factors to repress E2F target-gene expression. *lin-35*/Rb exhibits synthetic lethality with several other genes that include *pha-1*/FOXO, *ubc-18* (Mani and Fay, 2009), *psa-1*/SWI3 (Cui et al., 2004), and *slr-2* (Kirienko et al., 2008), revealing a requirement for *lin-35* in cell cycle control, cell proliferation, organ development, and fertility. Thus, it appears

that LIN-35 operates redundantly in many processes, and as a result it is likely that, in *C. elegans*, the function of both LET-765 and LIN-35 converge on a common target in early development.

In contrast to *lin-35*, the failure of *let-765*(RNAi) to suppress ectopic vulval induction in *lin-53(n833)*; *lin-15A(n767)* indicates that derepression by the *lin-53* mutation does not rely on *let-765* activity. LIN-53 is the *C. elegans* homolog of the mammalian RbAp48 histone binding protein, which together with HDA-1/HDAC and LET-418/Mi-2 forms a Nucleosome Remodeling and Deacetylase (NuRD)-like complex. In *C. elegans,* LIN-53 has also been identified as part of the DRM complex, a multi-protein complex, which contains homologs of the *Drosophila* Myb-MuvB and DREAM complex components. The DRM and NuRD complexes are predicted to function separately to repress vulval induction, implying that LIN-53 may be required at multiple steps in *lin-3* repression. In addition, the *n833* mutation causes ectopic vulval induction even when heterozygous, demonstrating potential dominant negative activity (Lu and Horvitz, 1998). *lin-53*(*n833*) may lead to a chromatin state that can generate ectopic *lin-3* expression without the contribution of other activating factors. Alternatively, derepression of *lin-3* may occur at multiple sites, for example in the hypodermis and VPCs, and LET-765 may not be required for *lin-3* expression in all tissues.

The Notch signalling pathway is also a key player in promoting vulval cell fates. LIN-12/Notch specifies 2° cell fates in response to a signal from the 1° cell, P6.p. We have shown that *let-765* does not act downstream of LIN-12 during vulval development, but cannot rule out the possibility that the activity of the LIN-12 ligand(s) are affected in *let-765*(*rf*) animals. As the expression of LIN-12 ligands in P6.p is regulated by the LIN-

3/LET-23 inductive signal, a reduction in *lin-3* expression would result in reduced LIN-12 ligand expression in P6.p (Chen and Greenwald, 2004). *let-765*(*rf*) could directly affect transcription of the LIN-12 ligand(s), however, we cannot distinguish between these two potential outcomes when *lin-3* expression is compromised. During *Drosophila* eye development, EGFR expression in the R cells promotes the transcription of Delta, which activates Notch signalling in adjacent cells and promotes cone cell differentiation. Delta expression is activated by a disruption of a Su(H)-SMRTR repressor complex by Ebi and strawberry notch. Ebi/sno are thought to direct the nuclear export of SMRTR, leading to derepression by Su(H) (Tsuda et al., 2002). The specification of cone cell fates via sequential EGFR-Notch signalling pathways mirrors that seen in the specification of vulval cell fates in *C. elegans*. *let-765* may play a similar role in promoting DSL expression to promote 2° cell fates.

I observed that a reduction of function by RNAi lead to additional phenotypes that resemble those of RAS pathway mutants including the previously mentioned rod-like larval arrest phenotype, the observation that *let-765* can promote the P12 fate, and defects in male tail development. *let-765*(RNAi) leads to spicule defects, missing rays, and under-developed tails that may result from defective retraction of the hypodermal cells during morphogenesis. The development of the spicules is controlled in part by *lin-3* and the EGFR/RAS pathway that signals from the F and U cells to promote fates in the B.a progeny cells (Chamberlin and Sternberg, 1994). The fact that *let-765*(RNAi) causes spicule defects is consistent with an interaction with the RAS pathway; however, the significant variation in phenotypes implies that LET-765 is involved in the development of other cell types in the tail. The loss of V6-derived rays in some *let-765*(RNAi)

animals hints at a potential interaction with components regulating *pal-1*-dependent ray development (Zhang and Emmons, 2000; Zhang and Emmons, 2002). Overall, *let-765* appears to function in many RAS pathway regulated cell fate decisions, however, the nearly ubiquitous expression pattern and variety of phenotypes generated by a loss or reduction in *let-765* function is consistent with a global role for LET-765 in promoting expression of multiple targets.

5.6 Concluding remarks

The role of DExD/H box proteins in RNA processing and translation have been well established by studies both in vitro (Fairman et al., 2004; Jankowsky et al., 2001; Lai et al., 2008; Lee et al., 2008; Schwer, 2001) and from model systems (Johnstone and Lasko, 2004; Rajyaguru and Parker, 2009; Salinas et al., 2007; Tomancak et al., 1998). However, only recently are we starting to learn about their role in transcriptional regulation. Human RNA helicase A (RHA) is the homolog of the *Drosophila* gene *maleless* (*mle*), which is required for transcriptional repression and dosage compensation of the X chromosome(Lee et al., 1997). Human RHA has been shown to bind CREB binding protein (CBP) and RNA Pol II to activate CBP dependent transcription through a transactivation domain (MTAD) that has also been identified in *Drosophila mle* (Nakajima et al., 1997). Furthermore, the MLE protein can recruit RNA PolII to target genes via MTAD. Additionally, RHA has been shown to facilitate an interaction between the tumor suppressor BRCA1 and RNA Pol II, through a region of the protein distinct from that of MTAD (Anderson et al., 1998). The *C.elegans* homolog, *rha-1*, is required for transcriptional silencing in the germline, but an activator function is as of yet unidentified (Walstrom et al., 2005). Another well studied DEAD-box helicase, p68 and

its homolog p72, have been shown to possess both transcriptional activator and repressor functions. Both proteins interact with estrogen receptor α (ERα) and, like RHA, interact with CBP/p300 and RNA Pol II, suggesting a common 'bridging' function may exist for some DExD/H box proteins (Endoh et al., 1999; Rossow and Janknecht, 2003; Watanabe et al., 2001). Furthermore, upon activation by estrogen, p68 is recruited to the promoter of an ERα target gene, pS2, consistent with a role for p68 in transcription initiation (Metivier et al., 2003). More recently, p68/p72 have been shown to immunoprecipitate with HDAC1, and promoter specific transcriptional repressor activity has been demonstrated, highlighting the potential diversity of DExD/H box helicase function (Wilson et al., 2004).

The faithful reproduction of complex developmental programs relies on the precise spatio-temporal expression of intercellular signals, promoting or modifying the expression of downstream target genes. Often it is the action of sequence specific DNA binding proteins that directly regulate gene expression. However, a role for additional co-activator proteins in an interaction with the basal transcriptional machinery has been identified that enables the integration of diverse regulatory inputs at specific promoters. Subsequent to the establishment of an active chromatin structure by remodelling proteins that include SWI/SNF homologs and histone modification proteins, the recruitment of RNA PolII and general transcription factors commences in concert with the Mediator complex – a multi-subunit complex that integrates signals from activator/repressor cofactors and the basal transcriptional machinery (Emerson, 2002). It has been suggested that Mediator subunit composition, together with cofactor interactions and their substrate specificity, could lead to distinct activities at different promoters. The proposed role for

DExD/H box proteins, and more specifically *strawberry notch* homologs, in transcriptional regulation, together with our current data that demonstrates LET-765 positively regulates *lin-3* expression, suggests that LET-765 promotes transcriptional activity via an interaction with co-activator proteins or complexes. Futhermore, the identification of a physical interaction with T23G5.2, a protein with a predicted function in intracellular transport, suggests that LET-765 may assist in mRNA maturation or export. It is possible that LET-765 functions to promote and/or stabilize message during transcription and tethers a secretory protein to facilitate export.

The details surrounding the activation of *lin-3* expression in the anchor cell (AC) have not yet been fully realized; however several studies have allowed some insight into a potential mechanism. The LIN-12/Notch pathway is required for determining the AC fate at the L2 stage via a well studied lateral inhibitory process (Greenwald et al., 1983; Seydoux and Greenwald, 1989). Following specification, the *lag-2*/DSL ligand is expressed in the AC and functions to induce cells in the neighbouring somatic gonad to acquire the π cell fate (Newman et al., 2000). Thus, the AC expression of *lag-2* overlaps with that of *lin-3* and it has been suggested that LIN-12/Notch signalling may be involved in the establishment of *lin-3* expression in the AC, potentially through the action of the transcription factor, *hlh-2* (Hwang and Sternberg, 2004). *C. elegans* HLH-2 is a basic helix-loop-helix (bHLH) transcription factor and the E protein/Daughterless homolog. HLH-2 has been shown to bind E box enhancer elements in the *lin-3* promoter and its activity is required for anchor cell expression of *lin-3* (Hwang and Sternberg, 2004) and *lag-2* (Karp and Greenwald, 2003). bHLH proteins are known to function downstream of

Notch signalling during specification of cell fates in *Drosophila*; it follows that HLH-2 may provide a similar function during vulval development in *C. elegans*.

An overlapping requirement of *let-765* and *hlh-2* for *lin-3* expression during vulval induction suggests potential for collaboration in promoting *lin-3* transcription. Although *let-765*(RNAi) animals do not exhibit defects in specification of the AC or the distal tip cells, as is seen in *hlh-2*(RNAi) (Karp and Greenwald, 2004), the observed activity of Drosophila Sno downstream of Notch signalling raises the question of whether some conservation of function exists between LET-765 and Sno. Further studies on LET-765 should provide insight into the regulation of growth factor expression and of a potential connection between LIN-12/Notch signalling and the EGFR pathway in the AC. Moreover, identification of protein interactions with LET-765 will assist in elucidating additional components required for *lin-3* expression as well as other, yet undetermined, targets of *let-765* activity.

APPENDIX A

Strains used in this work

Strain	Genotype
AH142	*zhIs4(lip-1::gfp) III.*
BC4106	*dpy-17(e164) unc-32(e189) III*
BC4215	*sDp3(III;f); dpy-17(e164) let-765(s2575) unc-32(e189) III*
BC4270	*sDp3(III;f); dpy-17(e164) let-765(s2630) unc-32(e189) III*
BC4634	*sDp3(III;f); dpy-17(e164) sDf125(s2424) unc-32(e189) III*
BC4952	*sDp3(III;f); let-765(s2575) unc-36(e251) III; him-5(e1490) V*
BC6407	*dpy-5/dpy-5; sEX971*[*rCesF22E10.1-RFP+pCes361*] *(pgp-12:rfp)*
BC6455	*dpy-5/dpy-5; sEX996*[*pCes* CLS-K1+F22E10.4+GFP*+pCes361*]
BC6456	*let-765(s2575), unc-36(e251)III /hT2(qIs48)I; III; him-5 V*
BC6472	*dpy-5/dpy-5; sEX1018*[*pCes* CLS-X3+F22E10.4+GFP*+pCes361*]
BC6577	*rrf-3(pk1426)II; him-5(e1490)V*
BC6708	*dpy-5/dpy-5; sEx1153 (F20H11.3 subclone)*
BC6988	*dpy-5/dpy-5; sEX 1354* [*pCLS 78(hsp49.78-let-765),* F22E10.4::RFP]
BC6989	*dpy-5/dpy-5; sEX 1355* [*pCLS 78(hsp49.78-let-765);* F22E10.4::RFP]
BC6990	*dpy-5/dpy-5; sEX 1356* [*pCLS 83(hsp49.83-let-765);* F22E10.4::RFP]
BC6991	*dpy-5/dpy-5; sEX 1357* [*pCLS 83(hsp49.83-let-765);* F22E10.4::RFP]
BC7139	*let-765(s2575), unc-36(e251)III/hT2; qIs56 (lag-2::GFP)*
BC7161	*dpy-17(e164), unc-32(e189)III/let-765(s2630), unc-32(e189)III*
BC7162	*dpy-17(e164) sDf125(s2424) unc-32(e189) III/hT2[bli-4(e937) let-?(q782) qIs48] (I;III).*
BC7320	*dpy-5(e907)/dpy-5(e907) ; sEx157* [F20H11.2 (-376):GFP*+pCeh361*]
BC7494	*dpy-5/dpy-5; sIs 1578* [F20H11.2 (-376):GFP *(seg 1)*]

BC7496	*let-765(s2575), unc-36(e251)III/hT2; him-5/him-5; syIs78 (ajm-1:GFP)*
BC7548	+/+*; sEx 1595* [Fosmid WRM0629dG08:GFP*; pCeh361*]
BC7693	+/+*; sEx 1637* [Fosmid 629dG03 + F22E10.4:RFP*; pCeh361*]
BC7694	*sDp3(III,f) ; dpy-17(e164),let-765(s2575), unc-32(e189) III; sEx1637*
BC7695	*sDp3 (III, f); dpy-17(e164),let-765(s630), unc-32(e189) III; sEx1637*
BC7701	*dpy-5/dpy-5; sEx 1644* [F20H11.2 (-376) *pBluescript; myo-2:GFP; pCeh361*]
BC7726	*let-765(s2630), unc-32(e189) III/hT2* [*qIS48*]*(I;III)*
BC7727	*dpy-5/dpy-5; sEx1653* [*dpy-7p(-338 to -122):*GFP*, pCeh361*]
BC7739	+/+*; sIs 1637* [Fosmid WRM629dG03:GFP; F22E10.4:RFP*; pCeh361*]
BC7740	*unc-32 (e189) III; qIs74 (pop-1::gfp)X*
BC7808	*let-765(s2575), unc-32(e189) III / hT2* [*qIS48*]*(I;III); him-5 V*
BC7844	*unc-32(e189); mnIs7(lin-44::gfp)*
BC7846	*let-765(s2630), unc-32(e189) III / hT2 (I,III); mnIs7(lin-44::gfp)*
BC7852	*let-765(s2575), unc-32(e189) III / hT2 (I,III); mnIs7(lin-44::gfp)*
BC7864	*let-765(s2575), unc-32(e189) III / hT2 (I, III); qIs74(pop-1::gfp)*
BC7865	*let-765(s2630), unc-32(e189) III / hT2 (I, III); him-5 V; qIs74(pop-1::gfp)*
BC7868	*let-765(s2575), unc-32(e189) III/ hT2 (I, III); otIs45(unc-119::gfp)*
BC7880	*dpy-5/dpy-5; sEx 1739 (dpy-7p:F20H11.2, dpy-30:dsRED)*
BC7882	*nsh-1(ok2058) III/ hT2 (I, III); syIs78 (ajm-1:GFP)*
BC7893	*dpy-5/dpy-5; sEx1741* [WRM0632dE10*; myo-2:GFP, pCeh361*]
BC7894	*dpy-5/dpy-5; sEx1742* [WRM0639cE12*; myo-2:GFP, pCeh361*]
BC7957	*let-765(s2575), unc-32(e189) III/ hT2 (I, III); sIs1637*
BC7958	*let-765(s2630), unc-32(e189) III/ hT2 (I, III); sIs1637*
BC7959	*nsh-1(ok2058) III / hT2 (I, III); sIs1637*
BC8011	*nsh-1(ok2058) III/ hT2 (I, III); him-5 V*
BC8012	*nsh-1(ok2058) III/ hT2 (I, III); gmIs13(srb-6::gfp)*
BC8013	*dpy-5/dpy-5; sEx1800* [*F20H11.6p:GFP*]
BC8270	*nsh-1(ok2058) III/hT2(qIs48) I, III; saIs48*
BC8284	*nsh-1(ok2058) III/hT2(qIs48) I, III; qIs74 (pop-1::gfp)*

BC8866	*let-765(s2575), unc-32(e189) III/hT2(qIs48) I, III; arIs92 (egl-17::cfp)*
BC8868	*nsh-1(ok2058) III/hT2(qIs48) I, III; sEx971(pgp-12::rfp)*
CB1275	*lin-1(e1275) IV.*
CB1322	*lin-8(n111)II; lin-9(n112)III.*
CF491	*pry-1(mu38) I; him-5(e1490) V.*
CM119	*saIs14 (plin-48:GFP)*
EW15	*bar-1(ga80) X.*
GS3581	*unc-4(e120) II; arIs92(egl-17:cfp)*
JK2868	*qIs56 (lag-2::gfp)*
JK2906	*mep-1(q660) IV/nT1[qIs51] (IV;V).*
JK2945	*pop-1(q624) I/hT2[qIs48] (I;III).*
JR667	*unc-119(e2498::Tc1) III; wIs51 (scm::gfp).*
MT1001	*lin-1(e1777) IV*
MT10408	*lin-53(n833) I; unc-76(e911) V; lin-15A(n767) X*
MT14390	*let-418(n3536) V.*
MT1624	*lin-35(n745)I; lin-8(n111)II.*
MT1643	*lin-36(n766)III; lin-15A(n767)X.*
MT2131	*lin-31(n1053) II.*
MT301	*lin-31(n301)II.*
MT4051	*lin-44(n1792) I; him-5(e1490) V*
MT664	*lin-8(n111)II; lin-15B(n374)X.*
MT8189	*lin-15B(n765) X.*
NH2246	*ayIs4 I; dpy-20(e1282) IV (egl-17::gfp).*
NL4256	*rrf-3(pk1426)II*
OH441	*otIs45 V (unc-119::gfp).*
PD4251	*ccIs4251 I; dpy-20(e1282) IV.*
PD7271	*pha-1(e2123) III; ccEx7271 (let-858::gfp).*
PS1123	*unc-31(e169)? IV; syIs1 X (overexpresses lin-3).*
PS1839	*let-23(sa62) II.*

PS3239	*dpy-20(e1282) syIs49*[*pMH86(dpy-20(+) + pJB100(zmp-1::GFP)*]*IV.*
PS3504	*syIs54 II; unc-119(ed4) III (ceh-2::gfp).*
PS3528	*syIs51 V; syIs55 X (cdh-3::cfp, ceh-2::yfp).*
PS3745	*syIs51 (cdh-3::cfp)*
PS4198	*unc-119(ed4) III; syIs103 (lin-11::gfp).*
PS4308	*unc-119(ed4) III; syIs107 (lin-3::gfp).*
PS4657	*syIs78[ajm-1::GFP + unc-119(+)]; him-5(e1490) V*
PS524	*let-60(sy100)dn dpy-20(e1282) IV/nT1(IV); +/nT1(V)* [let on nT1]
SD418	*gaIs36(hs:mpk-1)*
SD551	*let-60(ga89) IV.*
SP1914	*mnIs7 (lin-44::gfp)*
SS104	*glp-4(bn2)I*
VC1622	*nsh-1(ok2058) III/hT2*[*bli-4(e937) let-?(q782) qIs48*] *I; III.*

APPENDIX B

Primer sequences

Primer name	Sequence	Experiment	Other
N-1	GACGCAGTACCTAAAAGCGT	Sequencing	
N-2	GGCGAATGGTGGACAAGGTA	Sequencing	
N-3	GGTGGATCTACAATGGTTCA	Sequencing	
N-4	GGAGGCCCAGCAAGAGTATT	Sequencing	
N-5	GCCACAGCCACTGACGAAAT	Sequencing	
N-6	GCAGTGTCTCACCTCCAGAC	Sequencing	
N-7	GATGCTGAACGTGATCTTCG	Sequencing	
N-8	CTGGACGAATGGTCTTAGAA	Sequencing	
N-9	GATGTACGATGCTGCGGTCA	Sequencing	
N-10	TCAGTCCACTGGAGAATCTG	Sequencing	
N-11	GGAAGAGTTGGAGATGGCGT	Sequencing	
N-12	GGTGGTAAAAGATGAGGATG	Sequencing	
N-13	AGAAGCGGCGGAGAGCTATT	Sequencing	
N-14	GAGAAGAAATGCGAATGCAG	Sequencing	
N-15	GTTGGCAGGAGAAAAACGAT	Sequencing	
N-16	GGTCTCCTCGCCAAGAACAA	Sequencing	
N-17	GGAAATTCACAAAATTGGAG	Sequencing	
N-18	GATGAAGCCAAGGAGGTTTG	Sequencing	
N-19	TCGTGTACGAACTGAACAGG	Sequencing	
N-20	GGTGCAGCAACTCGAAACAC	Sequencing	
N-21	GATATCGATCAGGGTTCAGT	Sequencing	
N-22	TCAGTAAGTGAAAAAGGCCG	Sequencing	
N-23	GTTGACACATGTTAGCAGCA	Sequencing	
N-24	ACATCATCGTTGCTGTGCTC	Sequencing	
N-25	GTTCAGCAACGATTTCCGAG	Sequencing	
N-26	GAACTGAGACAAATCACGAG	Sequencing	

N-27	GATTGCAATGAGATTCCAGA	Sequencing
N-28	GATGTCATCTTGTTCACCCG	Sequencing
N-29	GTGTGCCCATGGATCTGAAA	Sequencing
N-30	TCCATCAGAACTTTCACTGG	Sequencing
N-31	GGAAATGTTTGTCGATGAGA	Sequencing
N-32	GTCGAGCGTTCTTCTTCATC	Sequencing
N-33	GGAATGCTTGCCGTTCTCCC	Sequencing
N-34	GCGAAGTGTATGTGGCGAAC	Sequencing
N-35	AATGCAAGCGACAGTTCTTC	Sequencing
N-36	AGCCGAGATTTTCTTCCTGA	Sequencing
N-37	GACCAGCGTTGGTTGAAG	Sequencing
N-38	GAAAGCTGGTGACGATGTTG	Sequencing
N-39	GCTGAAACGACTTGGAACGA	Sequencing
N-40	GACCAATCGTTGATCCACCT	Sequencing
N-41	CGATTGTGAGTGTTTTTAATGTGA	Sequencing
N-42	CATGTGTTGTTTGTTTCCATTTTT	Sequencing
N-43	CATTGTTTCTCTTTCTTCTCATCA	Sequencing
N-44	CTTTCGATCACTTCCAGCAA	Sequencing
N-45	AAAGAGAGAATGTGTGGTATCTGC	Sequencing
N-46	CCCATCAAATTTTCCAGGTC	Sequencing
F20H11.2A	CAAACGAAAGACGGACTTCA	Sequencing
F20H11.2B	CAAATGTTGGTGGGAATTGA	Sequencing
3end-F	TGTTGGATTGGAGAAATTCAAA	Sequencing
3end-R	CGACAATTCCAAACAATTCG	Sequencing
T_{17}	TTTTTTTTTTTTTTTT	RT-PCR
SL1	GGTTTAATTACCCAAGTTTGAG	RT-PCR
SL2	GGTTTTAACCCAGTTACTCAAG	RT-PCR
SLa	ggttttaacccagttaaccaag	RT-PCR
SLb	ggttttaacccatataaccaag	RT-PCR
SL4	ggttttaacccaagttaaccaag	RT-PCR
F2-F	CAGTAGGAATGGCTGCTCGT	RT-PCR
F2-1	CGATTGGTCGTGGAGGTACT	RT-PCR
F2-3	CCACGGCCAACAAGATTTAC	RT-PCR
F2-4	CGTTGTTTCATGTCCATTGC	RT-PCR
F2-7	CGATTGGTCGTGGAGGTACT	RT-PCR

F2-3P	GGTGAAATTGATGGGAAGGA	RT-PCR	
F2-3est	CTCTTCCTCTTGTTCGTGCG	RT-PCR	
F2-100	TCCAGTAGGAATGGCTG	RT-PCR	
F2-101	CACAAATGTATCGAAAGGGAAA	RT-PCR	
F2-int8_9	TGTTGGATTGGAGAAATTCAAA	RT-PCR	
F2-ex8	GGAGTTGCACAAAGAGCACA	RT-PCR	
F2-ex10	CGACACTTGCCGTAGACGTA	RT-PCR	
F2-14	AACATCGTCACCAGCTTTCC	RT-PCR	
F2-16	CGGAGCTGGTGTAGGAAAAG	RT-PCR	
F2-20	GCGACAGTTCTTCCTTTTCCTA	RT-PCR	
F2-21	GTGAACTCCAAAGGAAAAATGG	RT-PCR	
F6A	GCCACTGTTTCACCTCACATAA	RT-PCR	
F6A*	CATACATCTTCACCAGCATCGT	RT-PCR	
F6-F	GCTGAGGCCATCTTGATTTT	RT-PCR	
F6-R	GCTTGGTGTCGGAGATGATT	RT-PCR	
F6-R2	AGTACCTCCACGACCAATCG	RT-PCR	
F6-ex3	GAAGTGTCACCGGAAGGTGT	RT-PCR	
F6-ex5	AGGTGACACCATCCTCTTGA	RT-PCR	
F20H11.2 A	CGATTGGTCGTGGAGGTACT	sIs16339	
F20H11.2 A*	CGATTGGTCGTGGAGGTACT	sIs16340	
F20H11.2B	AGTCGACCTGCAGGCATGCAAGCTGATTGTAGATCCACCAGTTCCA	sIs16341	
F2-B	TTTCTGAGCTCGGTACCCTCCAAGGGTGCGTGACGAGCAGCGATTCC	sEx1578	
765-N RT-F	CCACAACTAATGGAATGGTCATACAAGCCAAGACACCGGGGGCTGGC GTTtcgctgtcgagatatgacggtg	sIs1678 (recombineered fosmid)	
765-N RT-R	GGGCCTCCCGATGGGAAACTTTGTTGGGATTGCATATGTCTTGCCTGA ATgatgataagctgtcaaacatgag	sIs1678	
765-N gfp-F	CCACAACTAATGGAATGGTCATACAAGCCAAGACACCGGGGGCTGGC GTTatgagtaaaggagaagaacttttc	sIs1678	
765-N gfp-R	GGGCCTCCCGATGGGAAACTTTGTTGGGATTGCATATGTCTTGCCTGA ATtttgtatagttcatccatgccatgtg	sIs1678	
765-N FL-F	CATCATCAGCCACTCAATCG	sIs1678	
765-N FL-R	CGCTTTTTGTGATTTCGTCA	sIs1678	
F2-1B	AAAACTGCAGCGATTGGTCGTGGAGGTACT	sEx1644 (F2 rescue)	PstI
F2-3P	GCGGTACCGGTGAAATTGATGGGAAGGA	sEx1644 (F2 rescue)	KpnI
pD7-1	GGACTTAAGCTTCCACGATTTCTCGCAACACAT	sEx1653 (dpy-7 P)	HindIII
pD7-2	GGATTACTGCAGAAAAAGAACAGGGTGTGATAAATG	sEx1653 (dpy-7 P)	PstI
F2-100X	GATATCCCGGG TCCAGTAGGAATGGCTG	sEx1739 (pD7-765)	XmaI

F2-101S	GGTAGACTAGT CACAAATGTATCGAAAGGGAAA	sEx1739 (pD7-765)	SpeI
HSP-1	CGTAGGCTAGCTCCAGTAGGAATGGCTGCTC	sEx1354, sEX1355 (hsp)	NheI
HSP-2	GCTAGGTACCATTCTCAGCGGGAAAGATGA	sEx1356, sEx1357 (hsp)	KpnI
Fire-F	GCCTACATACCTCGCTCTGC	Fire vector backbone	
Fire-R	AGCTCACTCAAAGGCGGTAA	Fire vector backbone	
GFP-F	CCATGCCCGAAGGTTATGTA	GFP for seq	
GFP-R	AAAGGGCAGATTGTGTGGAC	GFP for seq	
CORE-F	CGTATCCCCGGGATCTGGAATGGCACATCCT	CORE_pGEX-6P1	SmaI
CORE-R	GCTATCCTCGAGGCCAAACGGAGAGAACAGAG	CORE_pGEX-6P2	XhoI
G_RNAi-F	ATTAACCCTCACTAAAGGGA GTGGACCGGAATATGTTGCT	Template for RNAi transcription	
G_RNAi-R	TAATACGACTCACTATAGGG CCTCGCTCAACTCCAATTTT	Template for RNAi transcription	
HP-Sal	CGGTCGAC-TGCGAATGCAGAAGTTTCAC	pD7-HP	SalI
HP-Bam	CGGGATCC-CGGTTCCAAGATCCATGATT	pD7-HP	BamHI
HP-Nco	GGCCATGG-CGGTTCCAAGATCCATGATT	pD7-HP	NcoI
HP-Xho	GGCTCGAG-TGCGAATGCAGAAGTTTCAC	pD7-HP	XhoI
RRF-3D	GGAAACAGTTGCGAAGACG	Genotyping	
RRF-3E	TCCTTCGATACCTTCAACAGG	Genotyping	
RRF-3F	TCCAAAAGTTGTTGCATTCG	Genotyping	
*ok2058*_Ex-F	CGGAGCTGGTGTAGGAAAAG	Genotyping	
*ok2058*_Int-F	TGCTGAACGTGATCTTCGAG	Genotyping	
*ok2058*_Ex-R	CAATCGTATTGCTGCTTCCA	Genotyping	

qRT-PCR Primers

Primer name	Sequence	Gene
CS1	CGTGGAAATTCACAAAATTGG	*let-765*
CS2	TCTTAGTGTTCGCTGTGTTGG	*let-765*
CS3	CCAGTCAAAGCATGATGGAA	*let-765*
CS4	CCAGTCAAAGCATGATGGAA	*let-765*
CS13	GAGGAGGAACCGGATCTGGAAT	tbb-2
CS14	GGCCTCGTTGTCAATGCAGTAG	tbb-2
CS19*	ACGGACTTATCATCCGCAAG	rpl-19
CS20*	GGGTCTTTTCTGGCATACGA	rpl-19

cs82	CAGTGCCACGTGTTGAAGTT	lin-3
cs83	CGGTGGTGGACATGTTACTG	lin-3
CS75	AATCATCTCCGACACCAAGC	F20H11.6
CS76	GGCCGACGATGAATGACTAT	F20H11.6
CS43	AAACGCTTCCAAAAACGAAA	lin-35
CS44	TCTCCAGACCGTTCCATAGC	lin-35
CS45	TCAGCTCCGAATGTTCTTCA	lin-45
CS46	GATTGTGGGGTTTTTGCAGT	lin-45
CS47	TCGAAATGCCTTCGAAAACT	mek-2
CS48	TCGTTCCCTTCACAAAAACC	mek-2
CS67	ATGCCTCCTCGACATATTGG	let-60
CS68	GCGAAAACCAACAGAAATCC	let-60
CS98	CTGAGGCGGACGAAGTCTAC	lin-8
CS99	CCACCGTACTGCTGTGAGAA	lin-8
CS100	TGGGATATCAACGCAAATCA	lin-53
CS101	TGCCAAGCAACATCTTCAAC	lin-53

APPENDIX C

ClustalW alignment of LET-765, *H. sapiens* SBNO1, and *Drosophila* sno.

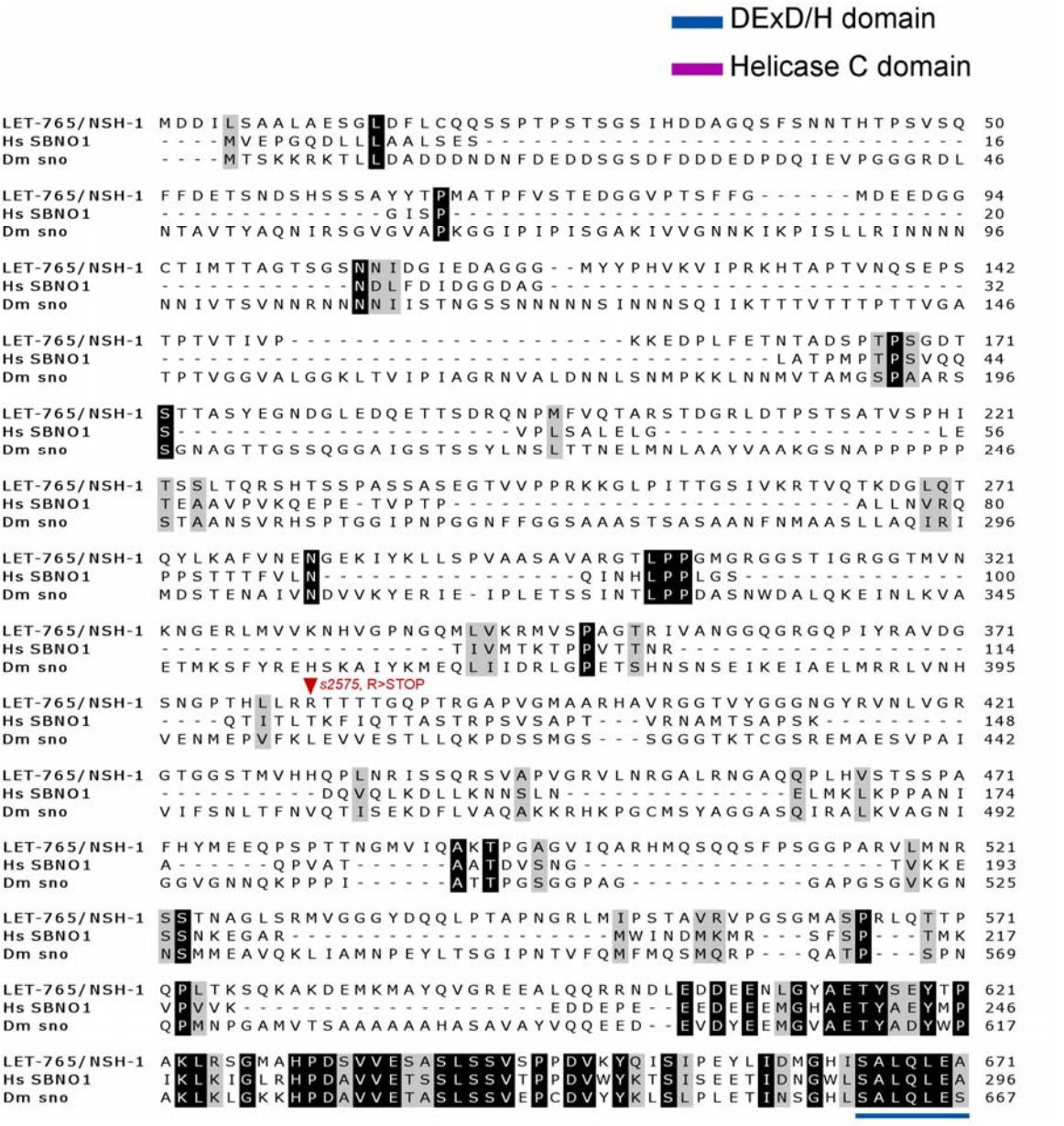

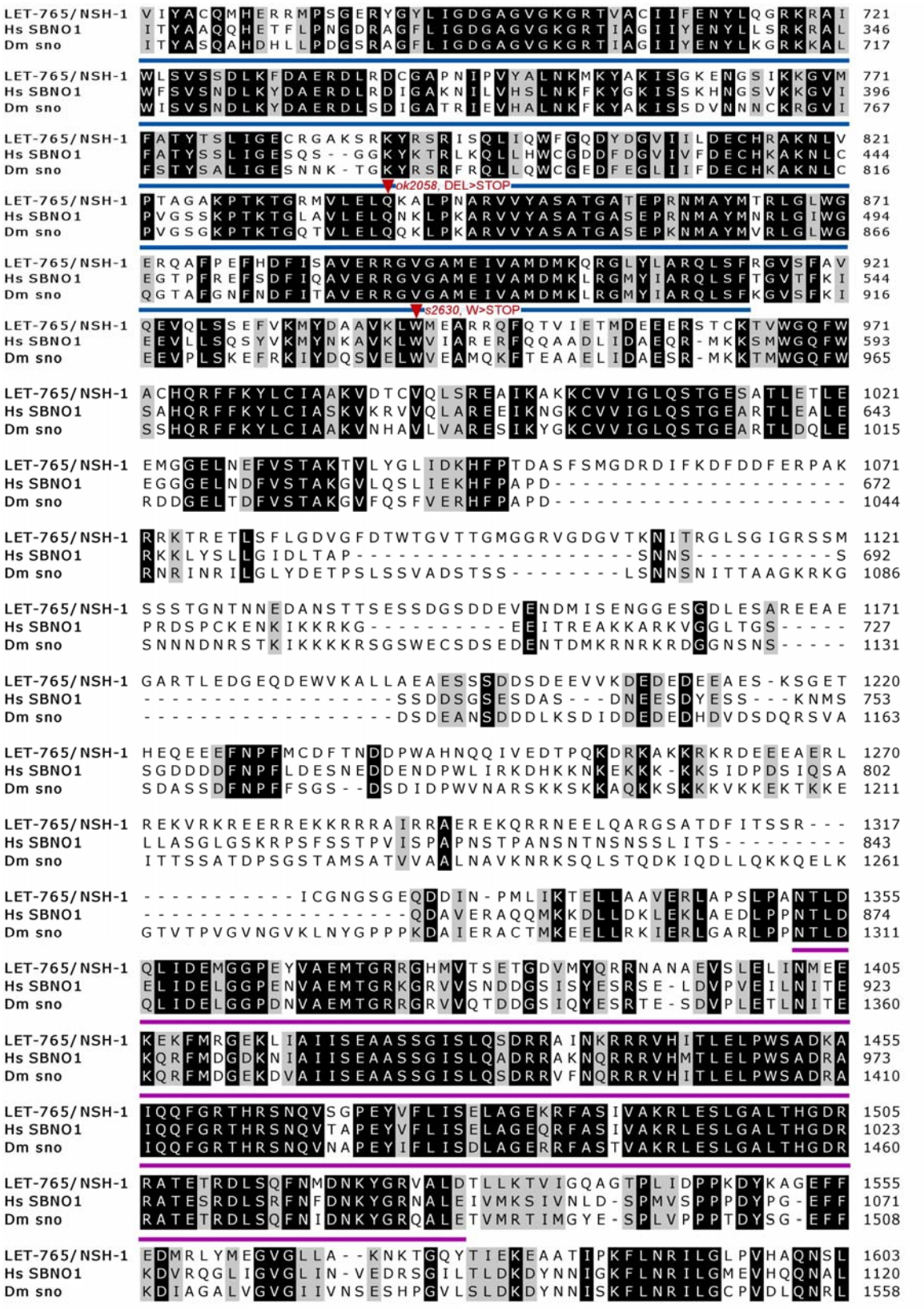
ok2058, DEL>STOP
s2630, W>STOP

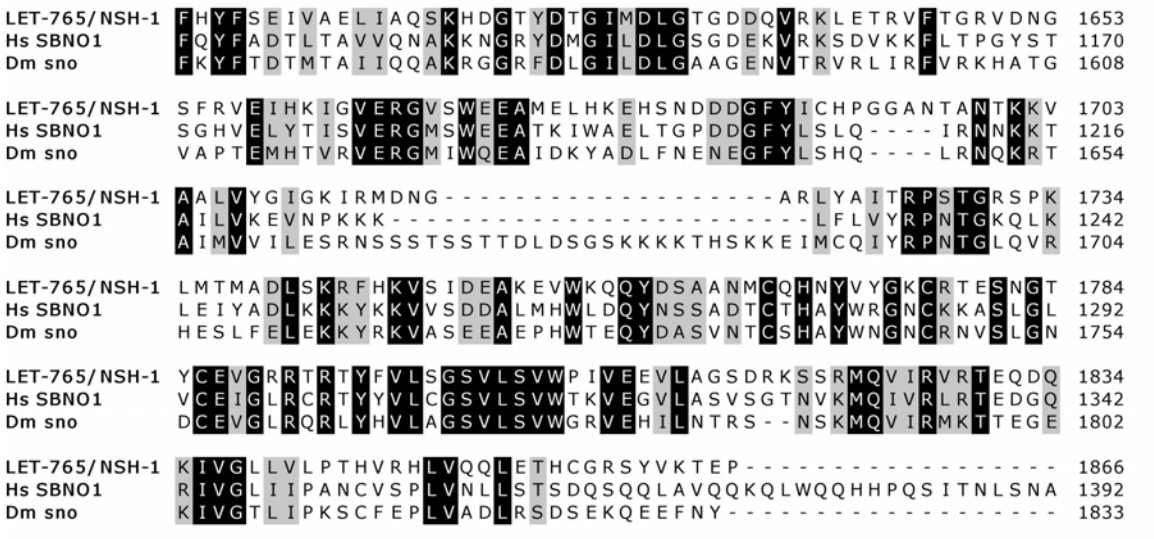
LET-765/NSH-1 FHYFSEIVAELIAQSKHDGTYDTGIMDLGTGDDQVRKLETRVFTGRVDNG 1653
Hs SBNO1 FQYFADTLTAVVQNAKKNGRYDMGILDLGSGDEKVRKSDVKKFLTPGYST 1170
Dm sno FKYFTDTMTAIIQQAKRGGRFDLGILDLGAAGENVTRVRLIRFVRKHATG 1608
LET-765/NSH-1 SFRVEIHKIGVERGVSWEEAMELHKEHSNDDDGFYICHPGGANTANTKKV 1703
Hs SBNO1 SGHVELYTISVERGMSWEEATKIWAELTGPDDGFYLSLQ----IRNNKKT 1216
Dm sno VAPTEMHTVRVERGMIWQEAIDKYADLFNENEGFYLSHQ----LRNQKRT 1654
LET-765/NSH-1 AALVYGIGKIRMDNG----------ARLYAITRPSTGRSPK 1734
Hs SBNO1 AILVKEVNPKKK----------LFLVYRPNTGKQLK 1242
Dm sno AIMVVILESRNSSSTSSTTDLDSGSKKKKTHSKKEIMCQIYRPNTGLQVR 1704
LET-765/NSH-1 LMTMADLSKRFHKVSIDEAKEVWKQQYDSAANMCQHNYVYGKCRTESNGT 1784
Hs SBNO1 LEIYADLKKKYKKVVSDDALMHWLDQYNSSADTCTHAYWRGNCKKASLGL 1292
Dm sno HESLFELEKKYRKVASEEAEPHWTEQYDASVNTCSHAYWNGNCRNVSLGN 1754
LET-765/NSH-1 YCEVGRRTRTYFVLSGSVLSVWPIVEEVLAGSDRKSSRMQVIRVRTEQDQ 1834
Hs SBNO1 VCEIGLRCRTYYVLCGSVLSVWTKVEGVLASVSGTNVKMQIVRLRTEDGQ 1342
Dm sno DCEVGLRQRLYHVLAGSVLSVWGRVEHILNTRS--NSKMQVIRMKTTEGE 1802
LET-765/NSH-1 KIVGLLVLPTHVRHLVQQLETHCGRSYVKTEP---------- 1866
Hs SBNO1 RIVGLIIPANCVSPLVNLLSTSDQSQQLAVQQKQLWQQHHPQSITNLSNA 1392
Dm sno KIVGTLIPKSCFEPLVADLRSDSEKQEEFNY---------- 1833

APPENDIX D

Data from Hybrigenics yeast two hybrid interaction screen

The bait fragment consisted of 1178 residues from Ile_498 to Asp_1676 of the LET-765 protein sequence that was fused to LexA at its N-terminus. 162.27 million clones were analyzed and 78 positive interactions selected. All interactions received high confidence scores. Of the three independent target genes identified, one was discarded as it produced only one interaction that was out of frame.

Gene Name	Seq type	Score	Start	Stop	Frame	Orientation
Celeg T23G5.2a	5p 3p	A	558	1983	IF	Sense
Celeg T23G5.2a	5p 3p	A	558	1983	IF	Sense
Celeg T23G5.2a	5p 3p	A	564	1979	IF	Sense
Celeg T23G5.2a	5p 3p	A	567	1969	IF	Sense
Celeg T23G5.2a	5p	A	615	No Data	IF	Sense
Celeg T23G5.2a	5p 3p	A	1533	1976	IF	Sense
Celeg nsh-1	3p	A	No Data	4854	??	Sense
Celeg nsh-1	5p 3p	A	3786	4455	IF	Sense
Celeg nsh-1	5p 3p	A	3786	4849	IF	Sense
Celeg nsh-1	5p 3p	A	3786	4849	IF	Sense
Celeg nsh-1	5p 3p	A	3786	No Data	IF	Sense
Celeg nsh-1	5p 3p	A	3786	4454	IF	Sense
Celeg nsh-1	5p 3p	A	3786	4849	IF	Sense
Celeg nsh-1	5p 3p	A	3786	No Data	IF	Sense
Celeg nsh-1	5p 3p	A	3786	No Data	IF	Sense
Celeg nsh-1	5p 3p	A	3786	No Data	IF	Sense
Celeg nsh-1	5p 3p	A	3786	4849	IF	Sense
Celeg nsh-1	5p	A	3786	No Data	IF	Sense
Celeg nsh-1	5p 3p	A	3786	4455	IF	Sense
Celeg nsh-1	5p 3p	A	3786	4455	IF	Sense
Celeg nsh-1	5p 3p	A	3786	4455	IF	Sense
Celeg nsh-1	5p 3p	A	3810	5132	IF	Sense
Celeg nsh-1	5p 3p	A	3810	5132	IF	Sense

Celeg nsh-1	5p 3p	A	3825	5035	IF	Sense
Celeg nsh-1	5p 3p	A	3825	5035	IF	Sense
Celeg nsh-1	5p 3p	A	3825	5035	IF	Sense
Celeg nsh-1	5p 3p	A	3825	5035	IF	Sense
Celeg nsh-1	5p 3p	A	3825	5035	IF	Sense
Celeg nsh-1	5p 3p	A	3834	5046	IF	Sense
Celeg nsh-1	5p 3p	A	3834	5046	IF	Sense
Celeg nsh-1	5p 3p	A	3837	4822	IF	Sense
Celeg nsh-1	5p 3p	A	3837	5039	IF	Sense
Celeg nsh-1	5p 3p	A	3837	4822	IF	Sense
Celeg nsh-1	5p 3p	A	3846	4497	IF	Sense
Celeg nsh-1	5p 3p	A	3846	4855	IF	Sense
Celeg nsh-1	5p 3p	A	3852	4840	IF	Sense
Celeg nsh-1	5p 3p	A	3852	4840	IF	Sense
Celeg nsh-1	5p 3p	A	3852	4840	IF	Sense
Celeg nsh-1	5p 3p	A	3852	5042	IF	Sense
Celeg nsh-1	5p 3p	A	3852	5041	IF	Sense
Celeg nsh-1	5p 3p	A	3852	4840	IF	Sense
Celeg nsh-1	5p 3p	A	3858	4849	IF	Sense
Celeg nsh-1	5p 3p	A	3861	5036	IF	Sense
Celeg nsh-1	5p 3p	A	3861	5036	IF	Sense
Celeg nsh-1	5p 3p	A	3861	5036	IF	Sense
Celeg nsh-1	5p 3p	A	3861	5036	IF	Sense
Celeg nsh-1	5p 3p	A	3861	5036	IF	Sense
Celeg nsh-1	5p 3p	A	3861	5036	IF	Sense
Celeg nsh-1	5p 3p	A	3861	5036	IF	Sense
Celeg nsh-1	5p 3p	A	3984	5039	IF	Sense
Celeg nsh-1	5p 3p	A	4011	5044	IF	Sense
Celeg nsh-1	5p 3p	A	4011	5044	IF	Sense
Celeg nsh-1	5p 3p	A	4014	4519	IF	Sense
Celeg nsh-1	5p 3p	A	4014	4742	IF	Sense
Celeg nsh-1	5p 3p	A	4047	5036	IF	Sense
Celeg nsh-1	5p 3p	A	4047	5036	IF	Sense
Celeg nsh-1	5p 3p	A	4047	5036	IF	Sense
Celeg nsh-1	5p 3p	A	4047	4741	IF	Sense
Celeg nsh-1	5p 3p	A	4047	5036	IF	Sense
Celeg nsh-1	5p 3p	A	4047	5036	IF	Sense
Celeg nsh-1	5p 3p	A	4047	5036	IF	Sense
Celeg nsh-1	5p 3p	A	4047	5036	IF	Sense
Celeg nsh-1	5p 3p	A	4047	5036	IF	Sense
Celeg nsh-1	5p	A	4057	No Data	OOF1	Sense
Celeg nsh-1	5p 3p	A	4059	5140	IF	Sense

Celeg nsh-1	5p 3p	A	4089	4750	IF	Sense
Celeg nsh-1	5p 3p	A	4089	4750	IF	Sense
Celeg nsh-1	5p 3p	A	4092	5007	IF	Sense
Celeg nsh-1	5p 3p	A	4092	5007	IF	Sense
Celeg nsh-1	5p 3p	A	4313	5007	OOF2	Sense
Celeg nsh-1	5p 3p	A	4313	5007	OOF2	Sense
Celeg nsh-1	5p 3p	A	4316	5007	OOF2	Sense
Celeg nsh-1	5p 3p	A	4319	5132	OOF2	Sense
Celeg nsh-1	5p 3p	N/A	4361	4809	OOF2	Sense
Celeg nsh-1	5p 3p	N/A	4394	4856	OOF2	Sense
Celeg nsh-1	5p 3p	N/A	4394	4856	OOF2	Sense
Celeg vit-5	5p 3p	N/A	3076	3398	OOF1	Sense

REFERENCES

Andersen, E. C., and Horvitz, H. R. (2007). Two C. elegans histone methyltransferases repress lin-3 EGF transcription to inhibit vulval development. Development *134*, 2991-2999.

Andersen, E. C., Lu, X., and Horvitz, H. R. (2006). C. elegans ISWI and NURF301 antagonize an Rb-like pathway in the determination of multiple cell fates. Development *133*, 2695-2704.

Andersen, E. C., Saffer, A. M., and Horvitz, H. R. (2008). Multiple levels of redundant processes inhibit Caenorhabditis elegans vulval cell fates. Genetics *179*, 2001-2012.

Anderson, S. F., Schlegel, B. P., Nakajima, T., Wolpin, E. S., and Parvin, J. D. (1998). BRCA1 protein is linked to the RNA polymerase II holoenzyme complex via RNA helicase A. Nat. Genet. *19*, 254-256.

Aroian, R. V., Koga, M., Mendel, J. E., Ohshima, Y., and Sternberg, P. W. (1990). The let-23 gene necessary for Caenorhabditis elegans vulval induction encodes a tyrosine kinase of the EGF receptor subfamily. Nature *348*, 693-699.

Aroian, R. V., and Sternberg, P. W. (1991). Multiple functions of let-23, a Caenorhabditis elegans receptor tyrosine kinase gene required for vulval induction. Genetics *128*, 251-267.

Austin, J., and Kimble, J. (1987). glp-1 is required in the germ line for regulation of the decision between mitosis and meiosis in C. elegans. Cell *51*, 589-599.

Austin, J., Maine, E. M., and Kimble, J. (1989). Genetics of intercellular signalling in C. elegans. Development *107 Supp.l*, 53-57.

Beitel, G. J., Clark, S. G., and Horvitz, H. R. (1990). Caenorhabditis elegans ras gene let-60 acts as a switch in the pathway of vulval induction. Nature *348*, 503-509.

Beitel, G. J., Tuck, S., Greenwald, I., and Horvitz, H. R. (1995). The Caenorhabditis elegans gene lin-1 encodes an ETS-domain protein and defines a branch of the vulval induction pathway. Genes Dev. *9*, 3149-3162.

Berset, T., Hoier, E. F., Battu, G., Canevascini, S., and Hajnal, A. (2001). Notch inhibition of RAS signaling through MAP kinase phosphatase LIP-1 during C. elegans vulval development. Science *291*, 1055-1058.

Bos, J. L. (1989). ras oncogenes in human cancer: a review. Cancer Res. *49*, 4682-4689.

Boxem, M., and van den Heuvel, S. (2001). lin-35 Rb and cki-1 Cip/Kip cooperate in developmental regulation of G1 progression in C. elegans. Development *128*, 4349-4359.

Brenner, S. (1974). The genetics of Caenorhabditis elegans. Genetics *77*, 71-94.

Buechner, M. (2002). Tubes and the single C. elegans excretory cell. Trends Cell Biol. *12*, 479-484.

Buechner, M., Hall, D. H., Bhatt, H., and Hedgecock, E. M. (1999). Cystic canal mutants in Caenorhabditis elegans are defective in the apical membrane domain of the renal (excretory) cell. Dev. Biol. *214*, 227-241.

Bulow, H. E., Boulin, T., and Hobert, O. (2004). Differential functions of the C. elegans FGF receptor in axon outgrowth and maintenance of axon position. Neuron *42*, 367-374.

Burdine, R. D., Branda, C. S., and Stern, M. J. (1998). EGL-17(FGF) expression coordinates the attraction of the migrating sex myoblasts with vulval induction in C. elegans. Development *125*, 1083-1093.

Cantin, G. T., Stevens, J. L., and Berk, A. J. (2003). Activation domain-mediator interactions promote transcription preinitiation complex assembly on promoter DNA. Proc. Natl. Acad. Sci. USA *100*, 12003-12008.

Casamassimi, A., and Napoli, C. (2007). Mediator complexes and eukaryotic transcription regulation: an overview. Biochimie *89*, 1439-1446.

Ceol, C. J., and Horvitz, H. R. (2001). dpl-1 DP and efl-1 E2F act with lin-35 Rb to antagonize Ras signaling in C. elegans vulval development. Mol. Cell *7*, 461-473.

Chalfie, M., Tu, Y., Euskirchen, G., Ward, W. W., and Prasher, D. C. (1994). Green fluorescent protein as a marker for gene expression. Science *263*, 802-805.

Chamberlin, H. M., Palmer, R. E., Newman, A. P., Sternberg, P. W., Baillie, D. L., and Thomas, J. H. (1997). The PAX gene egl-38 mediates developmental patterning in Caenorhabditis elegans. Development *124*, 3919-3928.

Chamberlin, H. M., and Sternberg, P. W. (1993). Multiple cell interactions are required for fate specification during male spicule development in Caenorhabditis elegans. Development *118*, 297-324.

Chamberlin, H. M., and Sternberg, P. W. (1994). The lin-3/let-23 pathway mediates inductive signalling during male spicule development in Caenorhabditis elegans. Development *120*, 2713-2721.

Chang, C., Hopper, N. A., and Sternberg, P. W. (2000). Caenorhabditis elegans SOS-1 is necessary for multiple RAS-mediated developmental signals. EMBO J. *19*, 3283-3294.

Chang, C., Newman, A. P., and Sternberg, P. W. (1999). Reciprocal EGF signaling back to the uterus from the induced C. elegans vulva coordinates morphogenesis of epithelia. Curr. Biol. *9*, 237-246.

Chen, N., and Greenwald, I. (2004). The lateral signal for LIN-12/Notch in C. elegans vulval development comprises redundant secreted and transmembrane DSL proteins. Dev. Cell *6*, 183-192.

Clandinin, T. R., DeModena, J. A., and Sternberg, P. W. (1998). Inositol trisphosphate mediates a RAS-independent response to LET-23 receptor tyrosine kinase activation in C. elegans. Cell *92*, 523-533.

Clandinin, T. R., Katz, W. S., and Sternberg, P. W. (1997). Caenorhabditis elegans HOM-C genes regulate the response of vulval precursor cells to inductive signal. Dev. Biol. *182*, 150-161.

Clark, S. G., Lu, X., and Horvitz, H. R. (1994). The Caenorhabditis elegans locus lin-15, a negative regulator of a tyrosine kinase signaling pathway, encodes two different proteins. Genetics *137*, 987-997.

Clark, S. G., Stern, M. J., and Horvitz, H. R. (1992). C. elegans cell-signalling gene sem-5 encodes a protein with SH2 and SH3 domains. Nature *356*, 340-344.

Cordin, O., Banroques, J., Tanner, N. K., and Linder, P. (2006). The DEAD-box protein family of RNA helicases. Gene *367*, 17-37.

Cordin, O., Tanner, N. K., Doere, M., Linder, P., and Banroques, J. (2004). The newly discovered Q motif of DEAD-box RNA helicases regulates RNA-binding and helicase activity. EMBO J. *23*, 2478-2487.

Cui, M., Chen, J., Myers, T. R., Hwang, B. J., Sternberg, P. W., Greenwald, I., and Han, M. (2006). SynMuv genes redundantly inhibit lin-3/EGF expression to prevent inappropriate vulval induction in C. elegans. Dev. Cell *10*, 667-672.

Cui, M., Fay, D. S., and Han, M. (2004). lin-35/Rb cooperates with the SWI/SNF complex to control Caenorhabditis elegans larval development. Genetics *167*, 1177-1185.

Cui, M., Kim, E. B., and Han, M. (2006). Diverse chromatin remodeling genes antagonize the Rb-involved SynMuv pathways in C. elegans. PLoS Genet. *2*, e74.

Davison, E. M., Harrison, M. M., Walhout, A. J., Vidal, M., and Horvitz, H. R. (2005). lin-8, which antagonizes Caenorhabditis elegans Ras-mediated vulval induction, encodes a novel nuclear protein that interacts with the LIN-35 Rb protein. Genetics *171*, 1017-1031.

Deshpande, R., Inoue, T., Priess, J. R., and Hill, R. J. (2005). lin-17/Frizzled and lin-18 regulate POP-1/TCF-1 localization and cell type specification during C. elegans vulval development. Dev. Biol. *278*, 118-129.

Dhillon, A. S., Hagan, S., Rath, O., and Kolch, W. (2007). MAP kinase signalling pathways in cancer. Oncogene *26*, 3279-3290.

Dolphin, C. T., and Hope, I. A. (2006). Caenorhabditis elegans reporter fusion genes generated by seamless modification of large genomic DNA clones. Nucleic Acids Res. *34*, e72.

Downward, J. (2003). Targeting RAS signalling pathways in cancer therapy. Nat. Rev. Cancer *3*, 11-22.

Dutt, A., Canevascini, S., Froehli-Hoier, E., and Hajnal, A. (2004). EGF signal propagation during C. elegans vulval development mediated by ROM-1 rhomboid. PLoS Biol. *2*, e334.

Edgley, M. L., Baillie, D. L., Riddle, D. L., and Rose, A. M. (2006). Genetic balancers. WormBook, 1-32.

Eisenmann, D. M., and Kim, S. K. (1997). Mechanism of activation of the Caenorhabditis elegans ras homologue let-60 by a novel, temperature-sensitive, gain-of-function mutation. Genetics *146*, 553-565.

Eisenmann, D. M., Maloof, J. N., Simske, J. S., Kenyon, C., and Kim, S. K. (1998). The beta-catenin homolog BAR-1 and LET-60 Ras coordinately regulate the Hox gene lin-39 during Caenorhabditis elegans vulval development. Development *125*, 3667-3680.

El Kasmi, K. C., Smith, A. M., Williams, L., Neale, G., Panopoulos, A. D., Watowich, S. S., Hacker, H., Foxwell, B. M., and Murray, P. J. (2007). Cutting edge: A transcriptional repressor and corepressor induced by the STAT3-regulated anti-inflammatory signaling pathway. J. Immunol. *179*, 7215-7219.

Emerson, B. M. (2002). Specificity of gene regulation. Cell *109*, 267-270.

Endoh, H., Maruyama, K., Masuhiro, Y., Kobayashi, Y., Goto, M., Tai, H., Yanagisawa, J., Metzger, D., Hashimoto, S., and Kato, S. (1999). Purification and identification of p68 RNA helicase acting as a transcriptional coactivator specific for the activation function 1 of human estrogen receptor alpha. Mol. Cell. Biol. *19*, 5363-5372.

Fairman, M. E., Maroney, P. A., Wang, W., Bowers, H. A., Gollnick, P., Nilsen, T. W., and Jankowsky, E. (2004). Protein displacement by DExH/D "RNA helicases" without duplex unwinding. Science *304*, 730-734.

Fay, D. S., Keenan, S., and Han, M. (2002). fzr-1 and lin-35/Rb function redundantly to control cell proliferation in C. elegans as revealed by a nonbiased synthetic screen. Genes Dev. *16*, 503-517.

Fay, D. S., and Yochem, J. (2007). The SynMuv genes of Caenorhabditis elegans in vulval development and beyond. Dev. Biol. *306*, 1-9.

Ferguson, E. L., and Horvitz, H. R. (1989). The multivulva phenotype of certain Caenorhabditis elegans mutants results from defects in two functionally redundant pathways. Genetics *123*, 109-121.

Finn, R. D., Tate, J., Mistry, J., Coggill, P. C., Sammut, S. J., Hotz, H. R., Ceric, G., Forslund, K., Eddy, S. R., Sonnhammer, E. L., and Bateman, A. (2008). The Pfam protein families database. Nucleic Acids Res. *36*, D281-288.

Fire, A., Xu, S., Montgomery, M. K., Kostas, S. A., Driver, S. E., and Mello, C. C. (1998). Potent and specific genetic interference by double-stranded RNA in Caenorhabditis elegans. Nature *391*, 806-811.

Freeman, M., and Gurdon, J. B. (2002). Regulatory principles of developmental signaling. Annu. Rev. Cell Dev. Biol. *18*, 515-539.

Fujita, M., Hawkinson, D., King, K. V., Hall, D. H., Sakamoto, H., and Buechner, M. (2003). The role of the ELAV homologue EXC-7 in the development of the Caenorhabditis elegans excretory canals. Dev. Biol. *256*, 290-301.

Fuller-Pace, F. V. (2006). DExD/H box RNA helicases: multifunctional proteins with important roles in transcriptional regulation. Nucleic Acids Res. *34*, 4206-4215.

Garvie, C. W., and Wolberger, C. (2001). Recognition of specific DNA sequences. Mol Cell *8*, 937-946.

Gettner, S. N., Kenyon, C., and Reichardt, L. F. (1995). Characterization of beta pat-3 heterodimers, a family of essential integrin receptors in C. elegans. J. Cell Biol. *129*, 1127-1141.

Gilleard, J. S., Barry, J. D., and Johnstone, I. L. (1997). cis regulatory requirements for hypodermal cell-specific expression of the Caenorhabditis elegans cuticle collagen gene dpy-7. Mol. Cell Biol. *17*, 2301-2311.

Gleason, J. E., Korswagen, H. C., and Eisenmann, D. M. (2002). Activation of Wnt signaling bypasses the requirement for RTK/Ras signaling during C. elegans vulval induction. Genes Dev. *16*, 1281-1290.

Gonczy, P., Echeverri, C., Oegema, K., Coulson, A., Jones, S. J., Copley, R. R., Duperon, J., Oegema, J., Brehm, M., Cassin, E*., et al.* (2000). Functional genomic analysis of cell division in C. elegans using RNAi of genes on chromosome III. Nature *408*, 331-336.

Greenwald, I. S., Sternberg, P. W., and Horvitz, H. R. (1983). The lin-12 locus specifies cell fates in Caenorhabditis elegans. Cell *34*, 435-444.

Gupta, B. P., and Sternberg, P. W. (2002). Tissue-specific regulation of the LIM homeobox gene lin-11 during development of the Caenorhabditis elegans egg-laying system. Dev. Biol. *247*, 102-115.

Hajnal, A., Whitfield, C. W., and Kim, S. K. (1997). Inhibition of Caenorhabditis elegans vulval induction by gap-1 and by let-23 receptor tyrosine kinase. Genes Dev. *11*, 2715-2728.

Han, M., Golden, A., Han, Y., and Sternberg, P. W. (1993). C. elegans lin-45 raf gene participates in let-60 ras-stimulated vulval differentiation. Nature *363*, 133-140.

Han, M., and Sternberg, P. W. (1990). let-60, a gene that specifies cell fates during C. elegans vulval induction, encodes a ras protein. Cell *63*, 921-931.

Harrison, M. M., Ceol, C. J., Lu, X., and Horvitz, H. R. (2006). Some C. elegans class B synthetic multivulva proteins encode a conserved LIN-35 Rb-containing complex distinct from a NuRD-like complex. Proc. Natl. Acad. Sci. USA *103*, 16782-16787.

Hedgecock, E. M., Culotti, J. G., Hall, D. H., and Stern, B. D. (1987). Genetics of cell and axon migrations in Caenorhabditis elegans. Development *100*, 365-382.

Herman, M. (2001). C. elegans POP-1/TCF functions in a canonical Wnt pathway that controls cell migration and in a noncanonical Wnt pathway that controls cell polarity. Development *128*, 581-590.

Herman, M. A., and Horvitz, H. R. (1994). The Caenorhabditis elegans gene lin-44 controls the polarity of asymmetric cell divisions. Development *120*, 1035-1047.

Herman, M. A., Vassilieva, L. L., Horvitz, H. R., Shaw, J. E., and Herman, R. K. (1995). The C. elegans gene lin-44, which controls the polarity of certain asymmetric cell divisions, encodes a Wnt protein and acts cell nonautonomously. Cell *83*, 101-110.

Hill, R. J., and Sternberg, P. W. (1992). The gene lin-3 encodes an inductive signal for vulval development in C. elegans. Nature *358*, 470-476.

Hobert, O. (2002). PCR fusion-based approach to create reporter gene constructs for expression analysis in transgenic C. elegans. Biotechniques *32*, 728-730.

Horvitz, H. R., and Sternberg, P. W. (1991). Multiple intercellular signalling systems control the development of the Caenorhabditis elegans vulva. Nature *351*, 535-541.

Hoskins, R., Hajnal, A. F., Harp, S. A., and Kim, S. K. (1996). The C. elegans vulval induction gene lin-2 encodes a member of the MAGUK family of cell junction proteins. Development *122*, 97-111.

Hsieh, J., Liu, J., Kostas, S. A., Chang, C., Sternberg, P. W., and Fire, A. (1999). The RING finger/B-box factor TAM-1 and a retinoblastoma-like protein LIN-35 modulate context-dependent gene silencing in Caenorhabditis elegans. Genes Dev. *13*, 2958-2970.

Huang, L. S., Tzou, P., and Sternberg, P. W. (1994). The lin-15 locus encodes two negative regulators of Caenorhabditis elegans vulval development. Mol. Biol. Cell *5*, 395-411.

Hubbard, S. R., and Miller, W. T. (2007). Receptor tyrosine kinases: mechanisms of activation and signaling. Curr. Opin. Cell Biol. *19*, 117-123.

Hwang, B. J., and Sternberg, P. W. (2004). A cell-specific enhancer that specifies lin-3 expression in the C. elegans anchor cell for vulval development. Development *131*, 143-151.

Inoue, T., Oz, H. S., Wiland, D., Gharib, S., Deshpande, R., Hill, R. J., Katz, W. S., and Sternberg, P. W. (2004). C. elegans LIN-18 is a Ryk ortholog and functions in parallel to LIN-17/Frizzled in Wnt signaling. Cell *118*, 795-806.

Inoue, T., Sherwood, D. R., Aspock, G., Butler, J. A., Gupta, B. P., Kirouac, M., Wang, M., Lee, P. Y., Kramer, J. M., Hope, I.*, et al.* (2002). Gene expression markers for Caenorhabditis elegans vulval cells. Mech. Dev. *119 Suppl 1*, S203-209.

Inoue, T., Wang, M., Ririe, T. O., Fernandes, J. S., and Sternberg, P. W. (2005). Transcriptional network underlying Caenorhabditis elegans vulval development. Proc. Natl. Acad. Sci. USA *102*, 4972-4977.

Janke, D. L., Schein, J. E., Ha, T., Franz, N. W., O'Neil, N. J., Vatcher, G. P., Stewart, H. I., Kuervers, L. M., Baillie, D. L., and Rose, A. M. (1997). Interpreting a sequenced genome: toward a cosmid transgenic library of Caenorhabditis elegans. Genome Res. *7*, 974-985.

Jankowsky, E., Gross, C. H., Shuman, S., and Pyle, A. M. (2001). Active disruption of an RNA-protein interaction by a DExH/D RNA helicase. Science *291*, 121-125.

Jansen, G., Hazendonk, E., Thijssen, K. L., and Plasterk, R. H. (1997). Reverse genetics by chemical mutagenesis in Caenorhabditis elegans. Nat. Genet. *17*, 119-121.

Jiang, L. I., and Sternberg, P. W. (1998). Interactions of EGF, Wnt and HOM-C genes specify the P12 neuroectoblast fate in C. elegans. Development *125*, 2337-2347.

Johnsen, R. C., Baillie, D. L. (1997). Mutation. In C. elegans II, D. L. Riddle, Blumenthal, T., Meyer, B.J., Priess, J. R. eds., ed. (Cold Spring Harbour Laboratory Press).

Johnson, A. D., Fitzsimmons, D., Hagman, J., and Chamberlin, H. M. (2001). EGL-38 Pax regulates the ovo-related gene lin-48 during Caenorhabditis elegans organ development. Development *128*, 2857-2865.

Johnstone, O., and Lasko, P. (2004). Interaction with eIF5B is essential for Vasa function during development. Development *131*, 4167-4178.

Jongeward, G. D., Clandinin, T. R., and Sternberg, P. W. (1995). sli-1, a negative regulator of let-23-mediated signaling in C. elegans. Genetics *139*, 1553-1566.

Kamath, R. S., Fraser, A. G., Dong, Y., Poulin, G., Durbin, R., Gotta, M., Kanapin, A., Le Bot, N., Moreno, S., Sohrmann, M.*, et al.* (2003). Systematic functional analysis of the Caenorhabditis elegans genome using RNAi. Nature *421*, 231-237.

Karp, X., and Greenwald, I. (2003). Post-transcriptional regulation of the E/Daughterless ortholog HLH-2, negative feedback, and birth order bias during the AC/VU decision in C. elegans. Genes Dev. *17*, 3100-3111.

Karp, X., and Greenwald, I. (2004). Multiple roles for the E/Daughterless ortholog HLH-2 during C. elegans gonadogenesis. Dev. Biol. *272*, 460-469.

Katz, W. S., Hill, R. J., Clandinin, T. R., and Sternberg, P. W. (1995). Different levels of the C. elegans growth factor LIN-3 promote distinct vulval precursor fates. Cell *82*, 297-307.

Katz, W. S., Lesa, G. M., Yannoukakos, D., Clandinin, T. R., Schlessinger, J., and Sternberg, P. W. (1996). A point mutation in the extracellular domain activates LET-23, the Caenorhabditis elegans epidermal growth factor receptor homolog. Mol. Cell Biol. *16*, 529-537.

Kawasaki, I., Shim, Y. H., Kirchner, J., Kaminker, J., Wood, W. B., and Strome, S. (1998). PGL-1, a predicted RNA-binding component of germ granules, is essential for fertility in C. elegans. Cell *94*, 635-645.

Kelly, W. G., and Fire, A. (1998). Chromatin silencing and the maintenance of a functional germline in Caenorhabditis elegans. Development *125*, 2451-2456.

Kelly, W. G., Xu, S., Montgomery, M. K., and Fire, A. (1997). Distinct requirements for somatic and germline expression of a generally expressed Caernorhabditis elegans gene. Genetics *146*, 227-238.

Kennedy, S., Wang, D., and Ruvkun, G. (2004). A conserved siRNA-degrading RNase negatively regulates RNA interference in C. elegans. Nature *427*, 645-649.

Kenyon, C. (1995). A perfect vulva every time: gradients and signaling cascades in C. elegans. Cell *82*, 171-174.

Kimble, J. (1981). Alterations in cell lineage following laser ablation of cells in the somatic gonad of Caenorhabditis elegans. Dev. Biol. *87*, 286-300.

Kimble, J., and Crittenden, S. L. (2005). Germline proliferation and its control. WormBook, 1-14.

Kirienko, N. V., McEnerney, J. D., and Fay, D. S. (2008). Coordinated regulation of intestinal functions in C. elegans by LIN-35/Rb and SLR-2. PLoS Genet. *4*, e1000059.

Kornberg, R. D. (2005). Mediator and the mechanism of transcriptional activation. Trends Biochem. Sci. *30*, 235-239.

Kornfeld, K., Hom, D. B., and Horvitz, H. R. (1995). The ksr-1 gene encodes a novel protein kinase involved in Ras-mediated signaling in C. elegans. Cell *83*, 903-913.

Kwon, J. Y., and Lee, J. (2001). Biological significance of a universally conserved transcription mediator in metazoan developmental signaling pathways. Development *128*, 3095-3104.

Kwon, J. Y., Park, J. M., Gim, B. S., Han, S. J., Lee, J., and Kim, Y. J. (1999). Caenorhabditis elegans mediator complexes are required for developmental-specific transcriptional activation. Proc. Natl. Acad. Sci. USA *96*, 14990-14995.

Kwong, A. D., Rao, B. G., and Jeang, K. T. (2005). Viral and cellular RNA helicases as antiviral targets. Nat. Rev. Drug Discov. *4*, 845-853.

Lackner, M. R., and Kim, S. K. (1998). Genetic analysis of the Caenorhabditis elegans MAP kinase gene mpk-1. Genetics *150*, 103-117.

Lackner, M. R., Kornfeld, K., Miller, L. M., Horvitz, H. R., and Kim, S. K. (1994). A MAP kinase homolog, mpk-1, is involved in ras-mediated induction of vulval cell fates in Caenorhabditis elegans. Genes Dev. *8*, 160-173.

Lai, M. C., Lee, Y. H., and Tarn, W. Y. (2008). The DEAD-box RNA helicase DDX3 associates with export messenger ribonucleoproteins as well as tip-associated protein and participates in translational control. Mol. Biol. Cell *19*, 3847-3858.

Lander, E. S., Linton, L. M., Birren, B., Nusbaum, C., Zody, M. C., Baldwin, J., Devon, K., Dewar, K., Doyle, M., FitzHugh, W.*, et al.* (2001). Initial sequencing and analysis of the human genome. Nature *409*, 860-921.

Lee, C. G., Chang, K. A., Kuroda, M. I., and Hurwitz, J. (1997). The NTPase/helicase activities of Drosophila maleless, an essential factor in dosage compensation. EMBO J. *16*, 2671-2681.

Lee, C. S., Dias, A. P., Jedrychowski, M., Patel, A. H., Hsu, J. L., and Reed, R. (2008). Human DDX3 functions in translation and interacts with the translation initiation factor eIF3. Nucleic Acids Res. *36*, 4708-4718.

Lu, X., and Horvitz, H. R. (1998). lin-35 and lin-53, two genes that antagonize a C. elegans Ras pathway, encode proteins similar to Rb and its binding protein RbAp48. Cell *95*, 981-991.

Lubarsky, B., and Krasnow, M. A. (2003). Tube morphogenesis: making and shaping biological tubes. Cell *112*, 19-28.

Mah, A. K., Armstrong, K. R., Chew, D. S., Chu, J. S., Tu, D. K., Johnsen, R. C., Chen, N., Chamberlin, H. M., and Baillie, D. L. (2007). Transcriptional regulation of AQP-8, a Caenorhabditis elegans aquaporin exclusively expressed in the excretory system, by the POU homeobox transcription factor CEH-6. J. Biol. Chem. *282*, 28074-28086.

Majumdar, A., Nagaraj, R., and Banerjee, U. (1997). strawberry notch encodes a conserved nuclear protein that functions downstream of Notch and regulates gene expression along the developing wing margin of Drosophila. Genes Dev. *11*, 1341-1353.

Maloof, J. N., and Kenyon, C. (1998). The Hox gene lin-39 is required during C. elegans vulval induction to select the outcome of Ras signaling. Development *125*, 181-190.

Mani, K., and Fay, D. S. (2009). A mechanistic basis for the coordinated regulation of pharyngeal morphogenesis in Caenorhabditis elegans by LIN-35/Rb and UBC-18-ARI-1. PLoS Genet. *5*, e1000510.

McCarter, J., Bartlett, B., Dang, T., and Schedl, T. (1999). On the control of oocyte meiotic maturation and ovulation in Caenorhabditis elegans. Dev. Biol. *205*, 111-128.

Mello, C. C., Kramer, J. M., Stinchcomb, D., and Ambros, V. (1991). Efficient gene transfer in C.elegans: extrachromosomal maintenance and integration of transforming sequences. EMBO J. *10*, 3959-3970.

Metivier, R., Penot, G., Hubner, M. R., Reid, G., Brand, H., Kos, M., and Gannon, F. (2003). Estrogen receptor-alpha directs ordered, cyclical, and combinatorial recruitment of cofactors on a natural target promoter. Cell *115*, 751-763.

Michaux, G., Gansmuller, A., Hindelang, C., and Labouesse, M. (2000). CHE-14, a protein with a sterol-sensing domain, is required for apical sorting in C. elegans ectodermal epithelial cells. Curr. Biol. *10*, 1098-1107.

Miller, L. M., Hess, H. A., Doroquez, D. B., and Andrews, N. M. (2000). Null mutations in the lin-31 gene indicate two functions during Caenorhabditis elegans vulval development. Genetics *156*, 1595-1602.

Moghal, N., and Sternberg, P. W. (2003). A component of the transcriptional mediator complex inhibits RAS-dependent vulval fate specification in C. elegans. Development *130*, 57-69.

Moghal, N., and Sternberg, P. W. (2003). The epidermal growth factor system in Caenorhabditis elegans. Exp. Cell Res. *284*, 150-159.

Mohler, W. A., Shemer, G., del Campo, J. J., Valansi, C., Opoku-Serebuoh, E., Scranton, V., Assaf, N., White, J. G., and Podbilewicz, B. (2002). The type I membrane protein EFF-1 is essential for developmental cell fusion. Dev. Cell *2*, 355-362.

Myers, L. C., and Kornberg, R. D. (2000). Mediator of transcriptional regulation. Annu. Rev. Biochem. *69*, 729-749.

Myers, T. R., and Greenwald, I. (2005). lin-35 Rb acts in the major hypodermis to oppose ras-mediated vulval induction in C. elegans. Dev. Cell *8*, 117-123.

Myers, T. R., and Greenwald, I. (2007). Wnt signal from multiple tissues and lin-3/EGF signal from the gonad maintain vulval precursor cell competence in Caenorhabditis elegans. Proc. Natl. Acad. Sci. USA *104*, 20368-20373.

Nagel, A. C., Wech, I., and Preiss, A. (2001). Scalloped and strawberry notch are target genes of Notch signaling in the context of wing margin formation in Drosophila. Mech. Dev. *109*, 241-251.

Nakajima, T., Uchida, C., Anderson, S. F., Lee, C. G., Hurwitz, J., Parvin, J. D., and Montminy, M. (1997). RNA helicase A mediates association of CBP with RNA polymerase II. Cell *90*, 1107-1112.

Newman, A. P., Acton, G. Z., Hartwieg, E., Horvitz, H. R., and Sternberg, P. W. (1999). The lin-11 LIM domain transcription factor is necessary for morphogenesis of C. elegans uterine cells. Development *126*, 5319-5326.

Newman, A. P., Inoue, T., Wang, M., and Sternberg, P. W. (2000). The Caenorhabditis elegans heterochronic gene lin-29 coordinates the vulval-uterine-epidermal connections. Curr. Biol. *10*, 1479-1488.

Newman, A. P., and Sternberg, P. W. (1996). Coordinated morphogenesis of epithelia during development of the Caenorhabditis elegans uterine-vulval connection. Proc. Natl. Acad. Sci. USA *93*, 9329-9333.

Newman, A. P., White, J. G., and Sternberg, P. W. (1995). The Caenorhabditis elegans lin-12 gene mediates induction of ventral uterine specialization by the anchor cell. Development *121*, 263-271.

Newman, A. P., White, J. G., and Sternberg, P. W. (1996). Morphogenesis of the C. elegans hermaphrodite uterus. Development *122*, 3617-3626.

Perens, E. A., and Shaham, S. (2005). C. elegans daf-6 encodes a patched-related protein required for lumen formation. Dev. Cell *8*, 893-906.

Perkins, L. A., Hedgecock, E. M., Thomson, J. N., and Culotti, J. G. (1986). Mutant sensory cilia in the nematode Caenorhabditis elegans. Dev. Biol. *117*, 456-487.

Poulin, G., Dong, Y., Fraser, A. G., Hopper, N. A., and Ahringer, J. (2005). Chromatin regulation and sumoylation in the inhibition of Ras-induced vulval development in Caenorhabditis elegans. EMBO J. *24*, 2613-2623.

Rajyaguru, P., and Parker, R. (2009). CGH-1 and the control of maternal mRNAs. Trends Cell Biol. *19*, 24-28.

Rocak, S., and Linder, P. (2004). DEAD-box proteins: the driving forces behind RNA metabolism. Nat. Rev. Mol. Cell Biol. *5*, 232-241.

Rocheleau, C. E., Ronnlund, A., Tuck, S., and Sundaram, M. V. (2005). Caenorhabditis elegans CNK-1 promotes Raf activation but is not essential for Ras/Raf signaling. Proc. Natl. Acad. Sci. USA *102*, 11757-11762.

Rogers, G. W., Jr., Komar, A. A., and Merrick, W. C. (2002). eIF4A: the godfather of the DEAD box helicases. Prog. Nucleic Acid Res. Mol. Biol. *72*, 307-331.

Rossow, K. L., and Janknecht, R. (2003). Synergism between p68 RNA helicase and the transcriptional coactivators CBP and p300. Oncogene *22*, 151-156.

Saha, A., Wittmeyer, J., and Cairns, B. R. (2006). Chromatin remodelling: the industrial revolution of DNA around histones. Nat. Rev. Mol. Cell Biol. *7*, 437-447.

Salinas, L. S., Maldonado, E., Macias-Silva, M., Blackwell, T. K., and Navarro, R. E. (2007). The DEAD box RNA helicase VBH-1 is required for germ cell function in C. elegans. Genesis *45*, 533-546.

Schultz, J., Copley, R. R., Doerks, T., Ponting, C. P., and Bork, P. (2000). SMART: a web-based tool for the study of genetically mobile domains. Nucleic Acids Res. *28*, 231-234.

Schwer, B. (2001). A new twist on RNA helicases: DExH/D box proteins as RNPases. Nat. Struct. Biol. *8*, 113-116.

Seydoux, G., and Greenwald, I. (1989). Cell autonomy of lin-12 function in a cell fate decision in C. elegans. Cell *57*, 1237-1245.

Shaham, S. (2006). Glia-neuron interactions in the nervous system of Caenorhabditis elegans. Curr. Opin. Neurobiol. *16*, 522-528.

Shaye, D. D., and Greenwald, I. (2002). Endocytosis-mediated downregulation of LIN-12/Notch upon Ras activation in Caenorhabditis elegans. Nature *420*, 686-690.

Shemer, G., and Podbilewicz, B. (2002). LIN-39/Hox triggers cell division and represses EFF-1/fusogen-dependent vulval cell fusion. Genes Dev. *16*, 3136-3141.

Shiratori, A., Shibata, T., Arisawa, M., Hanaoka, F., Murakami, Y., and Eki, T. (1999). Systematic identification, classification, and characterization of the open reading frames which encode novel helicase-related proteins in Saccharomyces cerevisiae by gene disruption and Northern analysis. Yeast *15*, 219-253.

Siegfried, K. R., and Kimble, J. (2002). POP-1 controls axis formation during early gonadogenesis in C. elegans. Development *129*, 443-453.

Simmer, F., Moorman, C., van der Linden, A. M., Kuijk, E., van den Berghe, P. V., Kamath, R. S., Fraser, A. G., Ahringer, J., and Plasterk, R. H. (2003). Genome-wide RNAi of C. elegans using the hypersensitive rrf-3 strain reveals novel gene functions. PLoS Biol. *1*, E12.

Simmer, F., Tijsterman, M., Parrish, S., Koushika, S. P., Nonet, M. L., Fire, A., Ahringer, J., and Plasterk, R. H. (2002). Loss of the putative RNA-directed RNA polymerase RRF-3 makes C. elegans hypersensitive to RNAi. Curr Biol. *12*, 1317-1319.

Simske, J. S., Kaech, S. M., Harp, S. A., and Kim, S. K. (1996). LET-23 receptor localization by the cell junction protein LIN-7 during C. elegans vulval induction. Cell *85*, 195-204.

Simske, J. S., and Kim, S. K. (1995). Sequential signalling during Caenorhabditis elegans vulval induction. Nature *375*, 142-146.

Singh, N., and Han, M. (1995). sur-2, a novel gene, functions late in the let-60 ras-mediated signaling pathway during Caenorhabditis elegans vulval induction. Genes Dev. *9*, 2251-2265.

Solari, F., and Ahringer, J. (2000). NURD-complex genes antagonise Ras-induced vulval development in Caenorhabditis elegans. Curr. Biol. *10*, 223-226.

Sonnichsen, B., Koski, L. B., Walsh, A., Marschall, P., Neumann, B., Brehm, M., Alleaume, A. M., Artelt, J., Bettencourt, P., Cassin, E.*, et al.* (2005). Full-genome RNAi profiling of early embryogenesis in Caenorhabditis elegans. Nature *434*, 462-469.

Sternberg, P. W. (2005). Vulval development. WormBook, 1-28.

Sternberg, P. W., and Han, M. (1998). Genetics of RAS signaling in C. elegans. Trends Genet. *14*, 466-472.

Sternberg, P. W., and Horvitz, H. R. (1986). Pattern formation during vulval development in C. elegans. Cell *44*, 761-772.

Sternberg, P. W., and Horvitz, H. R. (1988). lin-17 mutations of Caenorhabditis elegans disrupt certain asymmetric cell divisions. Dev. Biol. *130*, 67-73.

Sternberg, P. W., and Horvitz, H. R. (1989). The combined action of two intercellular signaling pathways specifies three cell fates during vulval induction in C. elegans. Cell *58*, 679-693.

Stetak, A., Gutierrez, P., and Hajnal, A. (2008). Tissue-specific functions of the Caenorhabditis elegans p120 Ras GTPase activating protein GAP-3. Dev. Biol. *323*, 166-176.

Stetak, A., Hoier, E. F., Croce, A., Cassata, G., Di Fiore, P. P., and Hajnal, A. (2006). Cell fate-specific regulation of EGF receptor trafficking during Caenorhabditis elegans vulval development. EMBO J. *25*, 2347-2357.

Stone, C. E., Hall, D. H., and Sundaram, M. V. (2009). Lipocalin signaling controls unicellular tube development in the Caenorhabditis elegans excretory system. Dev. Biol. *329*, 201-211.

Strahl, B. D., and Allis, C. D. (2000). The language of covalent histone modifications. Nature *403*, 41-45.

Sulston, J. E., Albertson, D. G., and Thomson, J. N. (1980). The Caenorhabditis elegans male: postembryonic development of nongonadal structures. Dev. Biol. *78*, 542-576.

Sulston, J. E., and Horvitz, H. R. (1977). Post-embryonic cell lineages of the nematode, Caenorhabditis elegans. Dev. Biol. *56*, 110-156.

Sulston, J. E., and White, J. G. (1980). Regulation and cell autonomy during postembryonic development of Caenorhabditis elegans. Dev. Biol. *78*, 577-597.

Sundaram, M., and Han, M. (1995). The C. elegans ksr-1 gene encodes a novel Raf-related kinase involved in Ras-mediated signal transduction. Cell *83*, 889-901.

Sundaram, M. V. (2006). RTK/Ras/MAPK signaling. WormBook, 1-19.

Suzuki, N., Buechner, M., Nishiwaki, K., Hall, D. H., Nakanishi, H., Takai, Y., Hisamoto, N., and Matsumoto, K. (2001). A putative GDP-GTP exchange factor is required for development of the excretory cell in Caenorhabditis elegans. EMBO Rep. *2*, 530-535.

Tabara, H., Grishok, A., and Mello, C. C. (1998). RNAi in C. elegans: soaking in the genome sequence. Science *282*, 430-431.

Takagi, Y., and Kornberg, R. D. (2006). Mediator as a general transcription factor. J. Biol. Chem. *281*, 80-89.

Tan, P. B., Lackner, M. R., and Kim, S. K. (1998). MAP kinase signaling specificity mediated by the LIN-1 Ets/LIN-31 WH transcription factor complex during C. elegans vulval induction. Cell *93*, 569-580.

Tanner, N. K., and Linder, P. (2001). DExD/H box RNA helicases: from generic motors to specific dissociation functions. Mol. Cell *8*, 251-262.

Thacker, C., Sheps, J. A., and Rose, A. M. (2006). Caenorhabditis elegans dpy-5 is a cuticle procollagen processed by a proprotein convertase. Cell Mol. Life Sci. *63*, 1193-1204.

Thein, M. C., McCormack, G., Winter, A. D., Johnstone, I. L., Shoemaker, C. B., and Page, A. P. (2003). Caenorhabditis elegans exoskeleton collagen COL-19: an adult-specific marker for collagen modification and assembly, and the analysis of organismal morphology. Dev. Dyn. *226*, 523-539.

Thomas, J. H., Ceol, C. J., Schwartz, H. T., and Horvitz, H. R. (2003). New genes that interact with lin-35 Rb to negatively regulate the let-60 ras pathway in Caenorhabditis elegans. Genetics *164*, 135-151.

Tiensuu, T., Larsen, M. K., Vernersson, E., and Tuck, S. (2005). lin-1 has both positive and negative functions in specifying multiple cell fates induced by Ras/MAP kinase signaling in C. elegans. Dev. Biol. *286*, 338-351.

Timmons, L., and Fire, A. (1998). Specific interference by ingested dsRNA. Nature *395*, 854.

Timmons, L., Tabara, H., Mello, C. C., and Fire, A. Z. (2003). Inducible systemic RNA silencing in Caenorhabditis elegans. Mol. Biol. Cell *14*, 2972-2983.

Tomancak, P., Guichet, A., Zavorszky, P., and Ephrussi, A. (1998). Oocyte polarity depends on regulation of gurken by Vasa. Development *125*, 1723-1732.

Tong, X., and Buechner, M. (2008). CRIP homologues maintain apical cytoskeleton to regulate tubule size in C. elegans. Dev. Biol. *317*, 225-233.

Tseng, S. S., Weaver, P. L., Liu, Y., Hitomi, M., Tartakoff, A. M., and Chang, T. H. (1998). Dbp5p, a cytosolic RNA helicase, is required for poly(A)+ RNA export. EMBO J. *17*, 2651-2662.

Tsu, C. A., Kossen, K., and Uhlenbeck, O. C. (2001). The Escherichia coli DEAD protein DbpA recognizes a small RNA hairpin in 23S rRNA. RNA *7*, 702-709.

Tsuda, L., Nagaraj, R., Zipursky, S. L., and Banerjee, U. (2002). An EGFR/Ebi/Sno pathway promotes delta expression by inactivating Su(H)/SMRTER repression during inductive notch signaling. Cell *110*, 625-637.

Unhavaithaya, Y., Shin, T. H., Miliaras, N., Lee, J., Oyama, T., and Mello, C. C. (2002). MEP-1 and a homolog of the NURD complex component Mi-2 act together to maintain germline-soma distinctions in C. elegans. Cell *111*, 991-1002.

Venter, J. C., Adams, M. D., Myers, E. W., Li, P. W., Mural, R. J., Sutton, G. G., Smith, H. O., Yandell, M., Evans, C. A., Holt, R. A.*, et al.* (2001). The sequence of the human genome. Science *291*, 1304-1351.

Vignali, M., Hassan, A. H., Neely, K. E., and Workman, J. L. (2000). ATP-dependent chromatin-remodeling complexes. Mol. Cell Biol. *20*, 1899-1910.

von Zelewsky, T., Palladino, F., Brunschwig, K., Tobler, H., Hajnal, A., and Muller, F. (2000). The C. elegans Mi-2 chromatin-remodelling proteins function in vulval cell fate determination. Development *127*, 5277-5284.

Walstrom, K. M., Schmidt, D., Bean, C. J., and Kelly, W. G. (2005). RNA helicase A is important for germline transcriptional control, proliferation, and meiosis in C. elegans. Mech. Dev. *122*, 707-720.

Wang, D., Kennedy, S., Conte, D., Jr., Kim, J. K., Gabel, H. W., Kamath, R. S., Mello, C. C., and Ruvkun, G. (2005). Somatic misexpression of germline P granules and enhanced RNA interference in retinoblastoma pathway mutants. Nature *436*, 593-597.

Watanabe, M., Yanagisawa, J., Kitagawa, H., Takeyama, K., Ogawa, S., Arao, Y., Suzawa, M., Kobayashi, Y., Yano, T., Yoshikawa, H.*, et al.* (2001). A subfamily of RNA-binding DEAD-box proteins acts as an estrogen receptor alpha coactivator through the N-terminal activation domain (AF-1) with an RNA coactivator, SRA. EMBO J. *20*, 1341-1352.

Wilson, B. J., Bates, G. J., Nicol, S. M., Gregory, D. J., Perkins, N. D., and Fuller-Pace, F. V. (2004). The p68 and p72 DEAD box RNA helicases interact with HDAC1 and repress transcription in a promoter-specific manner. BMC Mol. Biol. *5*, 11.

Woychik, N. A., and Hampsey, M. (2002). The RNA polymerase II machinery: structure illuminates function. Cell *108*, 453-463.

Wu, Y., and Han, M. (1994). Suppression of activated Let-60 ras protein defines a role of Caenorhabditis elegans Sur-1 MAP kinase in vulval differentiation. Genes Dev. *8*, 147-159.

Yin, X., Gower, N. J., Baylis, H. A., and Strange, K. (2004). Inositol 1,4,5-trisphosphate signaling regulates rhythmic contractile activity of myoepithelial sheath cells in Caenorhabditis elegans. Mol. Biol. Cell *15*, 3938-3949.

Yochem, J., Sundaram, M., and Han, M. (1997). Ras is required for a limited number of cell fates and not for general proliferation in Caenorhabditis elegans. Mol. Cell Biol. *17*, 2716-2722.

Yoda, A., Kouike, H., Okano, H., and Sawa, H. (2005). Components of the transcriptional Mediator complex are required for asymmetric cell division in C. elegans. Development *132*, 1885-1893.

Yoo, A. S., Bais, C., and Greenwald, I. (2004). Crosstalk between the EGFR and LIN-12/Notch pathways in C. elegans vulval development. Science *303*, 663-666.

Yoon, C. H., Lee, J., Jongeward, G. D., and Sternberg, P. W. (1995). Similarity of sli-1, a regulator of vulval development in C. elegans, to the mammalian proto-oncogene c-cbl. Science *269*, 1102-1105.

Zhang, H., and Emmons, S. W. (2000). A C. elegans mediator protein confers regulatory selectivity on lineage-specific expression of a transcription factor gene. Genes Dev. *14*, 2161-2172.

Zhang, H., and Emmons, S. W. (2002). Caenorhabditis elegans unc-37/groucho interacts genetically with components of the transcriptional mediator complex. Genetics *160*, 799-803.

Zhao, Z., Fang, L., Chen, N., Johnsen, R. C., Stein, L., and Baillie, D. L. (2005). Distinct regulatory elements mediate similar expression patterns in the excretory cell of Caenorhabditis elegans. J. Biol. Chem. *280*, 38787-38794.